Imaging of polarity during zygotic and somatic embryogenesis of carrot (*Daucus carota* L.)

Promotor : dr. M.T.M. Willemse
hoogleraar in de plantkunde

Co-promotor : dr. J.H.N. Schel
universitair hoofddocent plantencytologie en -morfologie

Imaging of polarity during zygotic and somatic embryogenesis of carrot (*Daucus carota* L.)

A.C.J. Timmers

Proefschrift
ter verkrijging van de graad van doctor
in de landbouw- en milieuwetenschappen
op gezag van de rector magnificus,
dr. H.C. van der Plas,
in het openbaar te verdedigen
op vrijdag 19 maart 1993
des namiddags te half twee in de Aula
van de Landbouwuniversiteit te Wageningen.

CIP-GEGEVENS KONINKLIJKE BIBLIOTHEEK, DEN HAAG

ISBN 90-5485-100-7

Cover photograph: Confocal scanning laser microscopical image of a somatic embryo of carrot.

Publication of this thesis was financially supported by Bio-Rad, Veenendaal.

STELLINGEN

1. Het gebruiken van alleen fluorescerende calmoduline bindende fenothiazines, zoals fluphenazine, voor de lokalisatie van calmoduline in planten en dieren, is ontoereikend en dient altijd vergezeld te gaan van andere lokaliseringsmethoden.

Haußer *et al.* (1984) Calmodulin in tip-growing plant cells, visualized by fluorescing calmodulin-binding phenothiazines. Planta 162:33-39.
Cotton G & Vanden Driessche T. (1987) Identification of calmodulin in *Acetabularia*: its distribution and physiological significance. J. Cell Sci. 87:337-437.
Dit proefschrift.

2. Aangezien het overbrengen van proembryogene massa's van de wilde peen vanuit medium met 2,4-D naar medium zonder 2,4-D slechts de continuering van een proces tot gevolg heeft, is het gebruik van de term inductie in dit geval niet juist.

Kiyosue T *et al.* (1991) Purification and immunohistochemical detection of an embryogenic cell protein in carrot. Plant Physiol. 95:1077-1083.
Dit proefschrift

3. Het gebruiken van somatische embryo's als modelsysteem voor bestudering van de fysiologie van de zygotische embryogenese is nauwelijks onderbouwd door empirisch wetenschappelijk onderzoek en berust voornamelijk op de onjuiste veronderstelling dat beide processen wel vergelijkbaar zullen zijn.

Choi JH, Sung ZR (1989) Induction, commitment, and progression of plant embryogenesis. In: Kung S-D, Arntzen CJ (eds) Plant Biotechnology. Butterworth, Boston, London, pp. 141-160
Dit proefschrift.

4. Aangezien de dissociatie-constante van calmoduline voor Ca^{2+} een waarde heeft in de orde van 10^{-6} tot 10^{-5} M is het toekennen van een rol voor extracellulair calmoduline in celwandvorming of -handhaving door Trewavas en Gilroy in strijd met de hoge Ca^{2+} concentratie (10^{-4} tot 10^{-3} M) die aanwezig is in de extracellulaire ruimte.

Trewavas A & Gilroy S (1991) Signal transduction in plant cells. Trends Genet. 7:356-361.

5. Het gebruik van osmiumtetroxide-kalium ferricyanide voor de bestudering van het endoplasmatisch reticulum in plantecellen op electronenmicroscopisch niveau is, ten gevolge van de grote variatie in de mate van contrastering daarvan, niet geschikt in kwantitatieve studies en kan derhalve beter worden vervangen door kaliumpermanganaat.

Hepler P (1981) The structure of the endoplasmic reticulum revealed by osmium tetroxide-potassium ferricyanide staining. Eur. J. Cell Biol. 26:102-110.

6. Het in de wetenschappelijke literatuur benoemen van zich ontwikkelende strukturen op calli van planten *in vitro* als scheut of embryo, respectievelijk aangeduid met de processen organogenese en somatische embryogenese, berust vaak slechts op waarnemingen van uitwendige vormverschillen en wordt ten onrechte bepaald door de op dat moment bestaande interesse van de desbetreffende onderzoeker in organogenese of somatische embryogenese.

Swedlund B & Locy RD (1988) Somatic embryogenesis and plant regeneration in two-year old cultures of *Zea diploperennis*. Plant Cell Reports 7:144-147.

7. Het beoefenen van sport als vrijetijdsbesteding verhoogt de levensvreugde en rechtvaardigt daarmee de kosten, onder andere als gevolg van blessure's, die het uitvoeren van sport met zich meebrengt.

8. De UNCED milieuconferentie in Rio de Janeiro in juni 1992 heeft laten zien dat voor de 'rijke' landen nog altijd geldt: 'verbeter de wereld begint bij je buurman'.

9. Bij de beoordeling van wetenschappelijke manuscripten door referenten ter plaatsing als artikel in een wetenschappelijk tijdschrift zou de objectiviteit van de beoordeling gewaarborgd moeten zijn door het onthouden van de auteursnamen van het artikel aan de referenten.

10. Het aantal citaties van een artikel is geen goede maat voor de kwaliteit van het betreffende artikel maar geeft aan hoeveel onderzoekers er werkzaam zijn in het veld van onderzoek waarop dit artikel betrekking heeft.

A.C.J. Timmers

Imaging of polarity during zygotic and somatic embryogenesis of carrot (*Daucus carota* L.)

19 maart 1993, Wageningen.

ABBREVIATIONS USED IN THE FIGURES

a	amyloplast
b	base
c	cotyledon
ca	calyptra
cc	central cilinder
ccvc	cell cluster of vacuolated cells
chl	chloroplast
ci	cotyledon initial
cu	cuticle
cw	cell wall
cx	cortex
d	dictyosome
em	embryo
ep	*epidermis*
er	endoplasmic reticulum
es	endosperm
fc	fruit coat
ge	globular embryo
h	hypocotyl
he	heart-shaped embryo
l	lipid droplet
m	mitochondrion
n	nucleus
nu	nucleolus
od	oil duct
oe	oblong embryo
p	plastid
pb	protein body
pd	plasmodesma
pem	proembryogenic mass
pes	peripheral endosperm
pr	protoderm
r	root(side)
ra	root apex
rc	root cortex
rhr	root hair region
sa	shoot apex
sc	seed coat
sm	shoot meristem
t	top
te	torpedo-shaped embryo
v	vacuole
vsc	vacuolated single cell
vi	vacuolar inclusion

ABBREVIATIONS USED IN THE TEXT

$[Ca^{2+}]$	concentration of ionized calcium
$[Ca^{2+}]_c$	concentration of free cytosolic Ca^{2+}
$[Ca^{2+}]_v$	concentration of free vacuolar Ca^{2+}
2,4-D	2,4-dichlorophenoxyacetic acid
ABA	abscisic acid
AM	acetoxy methyl
BP	band pass
CHAP	3-(cholamidopropyl) dimethylammonio-1-propanesulfonate
CSLM	confocal scanning laser microscopy
CTC	chlorotetracycline
d.a.i.	days after initiation
DIC	differential interference contrast
DM	dichroic mirror
DMSO	dimethylsulphoxide
EGTA	ethyleneglycol-bis-(ß-aminoethylether)-N,N,N',N'-tetraacetic acid
ER	endoplasmic reticulum
F	fluorescence
Fig(s).	figure(s)
FITC	fluorescein isothiocyanate
F_{max}	fluorescence at saturating Ca^{2+}
F_{min}	fluorescence in the absence of Ca^{2+}
GA_3	gibberellic acid 3
IAA	indole-3-acetic acid
K_d	dissociation constant
LP	long pass
M	molar
mg	milligram
min	minute(s)
mM	millimolar
NPN	N-phenyl-1-naphtylamine
PAGE	polyacrylamide-gel electrophoresis
PBS	phosphate buffered saline
PEG	polyethyleneglycol
PFA	paraformaldehyde
pH_c	cytosolic pH
pH_v	vacuolar pH
PIPES	1,4-piperazinediethanesulfonic acid
r.p.m.	revolutions per minute
SDS	sodium dodecyl sulfate
SER	smooth endoplasmic reticulum
UV	ultraviolet

CONTENTS

VOORWOORD

In het promotiereglement van de Landbouwuniversiteit is opgenomen dat op de titelpagina van een proefschrift uitsluitend de naam van de promovendus als auteur wordt vermeld. Echter, een proefschrift kan nooit het werk zijn van één persoon alleen en graag wil ik in dit voorwoord iedereen bedanken die op enigerlei wijze heeft bijgedragen aan de totstandkoming ervan.

Op de eerste plaats wil ik me richten tot Jan Schel, mijn co-promotor en begeleider. Van het begin tot het einde van mijn periode bij PCM heb je je uitstekend van je taak gekweten. Ik wil je speciaal bedanken voor het uiten van je vertrouwen in de wijze waarop ik het onderzoek aanpakte en de vele nuttige op- en aanmerkingen die je gaf tijdens de voorbereiding van artikelen en dit proefschrift. Als het al zo is dat AIO's in het algemeen slecht worden begeleid dan was dit zeker niet van toepassing op mijn situatie.

Professor Willemse, mijn promotor, u wil ik vooral bedanken voor het aanbrengen van de nodige verbeteringen in de algehele discussie van dit proefschrift en ook voor uw getoonde interesse in de resultaten van het onderzoek.

Siep Massalt, jouw vakmanschap en inzet waren onmisbaar tijdens het afdrukken van de vele foto's die dit schriftje sieren. Dank voor alle uren die je voor mij in het donker hebt doorgebracht.

Henk Kieft en Norbert de Ruijter, jullie wil ik graag in een adem noemen. Vooral tijdens de beginperiode van mijn onderzoek heb ik geprofiteerd van jullie kennis en kunde op het gebied van celbiologische technieken. Dank daarvoor.

Ook dank aan de andere leden van de celbiologie-groep, AnneMie Emons, André van Lammeren, Henk Mohamedjoenoes en Folbert Bronsema. Op een voor ieder van jullie kenmerkende manier zijn jullie van betekenis geweest voor mij.

Louis de Jong dank ik voor het zorgvuldig doornemen van het proefschrift en het aanbrengen van de nodige correcties zodat het engels ook echt engels is geworden.

Hans-Dieter Reiss, my colleague and friend from Heidelberg. Thank you very much for your kindness and hospitality. My stay in Heidelberg was a fruitful period and two chapters of this thesis have their origin in the work we performed together. I sincerely hope that our ways will cross again.

Professor Dudits, although our cooperation was less successful, for me it was an interesting experience to work at the Biological Research Centre in Szeged. Thank you for your interest in my work and the opportunity you have given me.

You, of all people I worked with, Beata Dedicova, are the most special one. Thank you for your invitation to visit your country and Nitra and the wonderful time I had there. I admire your courage and perseverance and wish you all the best for the future with your work and your nice husband and children. Also thanks to Anna Pretova and the other employees of the Institute of Genetics who all made my stay in Slowakia worthwhile.

I also want to thank P.P. Jablonsky and R.E. Williamson, from the Plant Cell Biology Group of the Australian National University at Canberra, for their generous gift of the monoclonal antibodies used in this study.

Naast de reeds genoemde personen zijn een groot aantal mensen van meer of minder belang geweest voor het succesvol verloop van mijn periode binnen PCM. Van hen verdienen zeker vermelding Sacco de Vries en Hilbert Booij van de vakgroep Moleculaire Biologie, Allex Haasdijk, Paul van Snippenburg, Joke Cobben, Truus van de Hoef-van Espelo, Regina van den Brink-de Jong, Adriaan van Aelst, Carmen Reinders, Juliette Janson, Kees Theunis, Paul Fransz, Clemens van de Wiel, Tom en Jan Brady, Gerrit van Geerenstein, Casper Pillen, Uday Tirlapur, de studenten Erwin van Florestein en Jeroen van Leeuwen, de overige niet bij name genoemde leden van PCM, El Bouw en Felix Thiel van de TFDL te Wageningen, Arnold Braaksma van het ATO te Wageningen en mijn vrienden van de turnvereniging Taxandria te Oisterwijk. Een ieder, ook degene die misschien ten onrechte niet is vermeld, bedankt voor zijn of haar bijdrage en interesse.

Niet wetenschappelijk, maar zeker zo belangrijk, ben ik ondersteund door jou, Els. Veel (ander) werk heb je mij uit handen genomen. Mijn oprechte dank daarvoor.

ABBREVIATIONS USED IN THE TEXT

$[Ca^{2+}]$	concentration of ionized calcium
$[Ca^{2+}]_c$	concentration of free cytosolic Ca^{2+}
$[Ca^{2+}]_v$	concentration of free vacuolar Ca^{2+}
2,4-D	2,4-dichlorophenoxyacetic acid
ABA	abscisic acid
AM	acetoxy methyl
BP	band pass
CHAP	3-(cholamidopropyl) dimethylammonio-1-propanesulfonate
CSLM	confocal scanning laser microscopy
CTC	chlorotetracycline
d.a.i.	days after initiation
DIC	differential interference contrast
DM	dichroic mirror
DMSO	dimethylsulphoxide
EGTA	ethyleneglycol-bis-(ß-aminoethylether)-N,N,N',N'-tetraacetic acid
ER	endoplasmic reticulum
F	fluorescence
Fig(s).	figure(s)
FITC	fluorescein isothiocyanate
F_{max}	fluorescence at saturating Ca^{2+}
F_{min}	fluorescence in the absence of Ca^{2+}
GA_3	gibberellic acid 3
IAA	indole-3-acetic acid
K_d	dissociation constant
LP	long pass
M	molar
mg	milligram
min	minute(s)
mM	millimolar
NPN	N-phenyl-1-naphtylamine
PAGE	polyacrylamide-gel electrophoresis
PBS	phosphate buffered saline
PEG	polyethyleneglycol
PFA	paraformaldehyde
pH_c	cytosolic pH
pH_v	vacuolar pH
PIPES	1,4-piperazinediethanesulfonic acid
r.p.m.	revolutions per minute
SDS	sodium dodecyl sulfate
SER	smooth endoplasmic reticulum
UV	ultraviolet

ABBREVIATIONS USED IN THE FIGURES

a	amyloplast
b	base
c	cotyledon
ca	calyptra
cc	central cilinder
ccvc	cell cluster of vacuolated cells
chl	chloroplast
ci	cotyledon initial
cu	cuticle
cw	cell wall
cx	cortex
d	dictyosome
em	embryo
ep	epidermis
er	endoplasmic reticulum
es	endosperm
fc	fruit coat
ge	globular embryo
h	hypocotyl
he	heart-shaped embryo
l	lipid droplet
m	mitochondrion
n	nucleus
nu	nucleolus
od	oil duct
oe	oblong embryo
p	plastid
pb	protein body
pd	plasmodesma
pem	proembryogenic mass
pes	peripheral endosperm
pr	protoderm
r	root(side)
ra	root apex
rc	root cortex
rhr	root hair region
sa	shoot apex
sc	seed coat
sm	shoot meristem
t	top
te	torpedo-shaped embryo
v	vacuole
vsc	vacuolated single cell
vi	vacuolar inclusion

CHAPTER 1

GENERAL INTRODUCTION

Seed plants are composed of roots, a stem, buds and leaves which all consist of several types of tissues and cells. The proper development of these plants depends on the accurate coordination of cell division, cell growth and cell differentiation. The ultimate shape of the organs is determined by the plane of subsequent cell divisions and the direction of cell elongation during the construction of these organs.

The function of the cells in an organ follows from their way of differentiation. Peripheral cells differentiate into epidermal cells which together form the epidermis, the cell layer which forms the border between the plant and its environment, giving mechanical protection and regulating transpiration and aeration. In the stem, subepidermal layers often acquire thick cell walls, thereby increasing the rigidity of the stem. Central cells can differentiate into xylem and phloem, together forming the vascular bundles, which are responsible for the main part of the longitudinal transport of solutes within the plant.

The whole sequence of plant development, from one cell, the zygote, to the germling, takes place during plant embryogenesis. In nearly all angiosperms, the zygote divides transversally into a basal and an apical cell. In most types of embryo development the small apical cell at the chalazal end is the commencement of the embryo, and the large basal cell at the micropylar end gives rise to the suspensor (Raghavan 1986). Further cell divisions and cell growth lead to the development of a globular-shaped embryo, demonstrating radial symmetry.

The first expression of tissue differentiation is the protoderm, produced by periclinal divisions in the upper part of the young globular-shaped embryo. In dicotyledons, bilateral symmetry is introduced by flattening of the embryo and the emergence of cotyledons. The embryo in this stage is described as heart-shaped. After elongation of the cotyledons and the then discernible hypocotyl the embryo reaches the torpedo-shaped stage, showing differentiation of apical meristems, procambium and radicle (see e.g. Esau 1977).

Embryogenesis involves two processes: induction of the embryogenic fate and expression of the embryogenic program (Choi & Sung 1989). According to Henshaw *et al.* (1982) embryo induction includes three steps: 1. the acquisition of a competent state, i.e. a state capable of receiving a developmental signal, 2. becoming determined, and 3. the loss of embryogenic potency as cells undergo differentiation. Embryogenic expression begins after fertilization and ends at dormancy. The start is a

consequence of changes due to fertilization events as well as activation of embryogenic events with a well-defined timing (Epel 1990).

Expression of the embryogenic program involves, besides coordinated cell division, cell growth and cell differentiation, the establishment of polarity. As pointed out by e.g. Kropf (1992) this establishment of polarity is indispensable for development and differentiation. At the macroscopical level, polarity is perceptible in the outline of an embryo with a clear root apex and shoot apex. At the microscopical level, polarity is perceptible in the distribution of organelles, especially the nucleus, vacuoles and plastids. Biochemically, polarity is, for example, perceptible in the distribution within a tissue of the intensity of DNA and RNA synthesis (Raghavan 1986).

Despite the large number of observations on embryogenesis, made in various plants, the molecular and cellular basis of this developmental pathway is still poorly understood. Increasing evidence is, however, available that the divalent cation Ca^{2+} participates in the initiation and maintenance of many plant processes (Table 1) from which several are also important during embryogenesis. Of special interest are the regulation of cell polarity, cell division, cell growth, cell volume, plant hormone action and distribution, and enzyme synthesis and activation (Timmers 1990). The principal targets of calcium signals in eukaryotes are members of a calcium-binding protein family known as the calcium-modulated proteins. Although many have been isolated from animal tissues, up to now only two, calmodulin and the calcium-dependent, calmodulin-independent protein kinase, are well-characterized from plant tissue (Roberts & Harmon 1992).

Studies on zygotic embryos are hampered by the presence of surrounding maternal tissue. Therefore, somatic embryos of carrot are often used as experimental substitutes for zygotic embryos, since the discovery of *in vitro* embryogenesis in cultures of *Daucus carota* (Reinert 1958, Steward *et al.* 1958). Carrot somatic embryos can be obtained, essentially free of surrounding tissue, just by transferring undifferentiated cell clusters from medium supplemented with the growth regulator 2,4-D to medium without 2,4-D. Embryogenesis can be controlled experimentally to achieve synchronized development and uniform embryogenic stages can be isolated in large amounts (Giuliano *et al.* 1983). Zygotic embryos can be obtained from flowers, which are very abundant in umbels of carrot plants, which can be cultivated easily. These features of carrot make this plant an ideal model system for the study of plant embryogenesis (see also Choi & Sung 1989).

In order to establish the role of Ca^{2+} in carrot embryogenesis it is necessary to determine if embryogenesis coincides with changes in the level or the distribution of Ca^{2+} or with changes in the level and distribution of calcium-modulated proteins. As a basis for the interpretation of the localization studies, a description of the development of zygotic and somatic embryos of carrot will be given in the following account. Basic information about the

Table 1. Published Ca^{2+}-linked processes in plants

Process	Reference
Gene expression	Guilfoyle 1989
Cell growth and proliferation	Poovaiah 1985, Hepler 1988
Cell polarity, polarized growth	Herth *et al.* 1990, Miller *et al.* 1992
Mitosis and cytokinesis	Hepler 1989
Organogenesis	Muto & Hirosawa 1987, Hush *et al.* 1991
Germination	Cocucci & Negrini 1991
Gravitropic responses	Poovaiah *et al.* 1987
Touch response	Braam 1992
Senescence	Ferguson & Drøbak 1988
Action of auxin	Ranjeva & Boudet 1987 Felle *et al.* 1992
IAA-induced leaflet opening	Bourbouloux *et al.* 1992
Polar transport and secretion of IAA	Dela Fuente 1984, Banuelos *et al.* 1987
Action of cytokinin	Kaminek 1992, Saunders 1992
Action of ABA	Owen 1988
Action of GA	Bush 1992
Phytochrome response	Roux *et al.* 1986
Cell wall synthesis	Brummel & Maclachlan 1989
Callose synthesis	Kauss 1987
Wound healing	Goddard & La Claire 1991
Secretion and activity of peroxidases	Penel *et al.* 1986
Carbohydrate metabolism	Brauer *et al.* 1990, Greger & Bertell 1992
Secretion and synthesis of α-amylase	Jones *et al.* 1986, Hayashi *et al.* 1989
Starch synthesis	Dreier *et al.* 1992
Calcium transport	Evans *et al.* 1991
Regulation of cell pH	Felle 1989
Phosphorylation of proteins	Poovaiah & Veluthambi 1986
Assembly and disassembly of microtubuli	Cyr 1991
Cytoplasmic streaming	Hepler & Wayne 1985
Exocytosis and endocytosis	Steer 1988
Photosynthesis	Brand & Becker 1984
Control of respiration	Owen *et al.* 1987
Closing of plasmodesmata	Tucker 1990
Volume regulation	Kauss 1987
Nastic movements	Satter & Galston 1981
Closing of stomata	Gilroy *et al.* 1991
Chloroplast movements	Russ *et al.* 1991

role of Ca^{2+} in living organisms has been reviewed extensively (Kauss 1987, Hepler 1988, Rasmussen 1989, Roberts & Harmon 1992) and the following section will therefore only give a summary of information which is essential in this study. Localization of Ca^{2+} and calmodulin requires the use of specific cell biological techniques which will be considered in a subsequent section of this Chapter.

EMBRYOGENESIS OF *DAUCUS CAROTA*

Zygotic embryogenesis

The formation of the macrogametophyte and embryo of carrot is described by Borthwick (1931). Development of the embryo begins after fertilization of the egg cell with an elongation of the zygote. The first transverse division results in an elongated basal cell and a small and round apical cell. Each of these cells divides transversely, giving rise to four cells that are arranged in a linear series. The distal cell of the 4-celled embryo produces the cotyledons and the upper part of the hypocotyl. The supra-median cell develops into the lower part of the hypocotyl, the root tip and the upper part of the suspensor. The infra-median and proximal cells are concerned only with the formation of the massive suspensor. From the 8-celled stage onwards the planes of division are less regular in orientation and consequently more than one way of development may occur. Through subsequent cell divisions the embryo reaches the globular-shaped stage. Periclinal divisions produce the protoderm, the outermost layer of cells, and vertical divisions shape out the procambium strands of the vascular cylinder, delimiting it from the ground meristem of the cortex. Subsequent changes involve the development of cotyledons and flattening of the embryo, introducing bilateral symmetry (see also Esau 1977).

In the globular-shaped stage the cells are isomorphic, with the exception of the protoderm with its smaller and tabular cells. In the heart-shaped stage the interior cells and the ground meristem become more vacuolated than the protoderm. Throughout the progression from zygote to torpedo-shaped embryo a decrease in size of the individual cells occurs.

Somatic embryogenesis

The ability of carrot cells to produce embryos *in vitro* was independently discovered in 1958 by Reinert and by Steward *et al.* Somatic embryos of carrot arise instantaneously by diluting a suspension culture and transferring a sieved fraction to 2,4-D omitted medium. In most cases, suspension cultures are derived from callus cultures of hypocotyl sections on solidified medium (e.g. Bhojwani & Razdan 1983). Alternatively, hypocotyl sections can be put directly into 2,4-D containing liquid medium (De Vries *et al.* 1988a).

Embryogenic suspension cultures are composed of small and cytoplasm-rich cells, capable to form embryos, occurring in clusters or clumps, and of vacuolated free cells

and small aggregates of such cells (Street & Withers 1974). The cell clusters which are able to form embryos have been termed proembryogenic masses by Halperin (1966).

The embryogenic potential of a culture is reflected by the number of proembryogenic masses present (De Vries *et al.* 1988a). The number of them in different embryogenic carrot suspension cultures varies between 0.1% and 5% of the total number of cells, whereas the remainder of the cells is present in larger aggregates and as single, highly vacuolated cells. Proembryogenic masses are derived from specific single cells (Nomura & Komamine 1985) and are composed of two distinctive cell types (Bhojwani & Razdan 1983). The central cells have a single large vacuole, a small and compact nucleus with a faintly staining nucleolus, a low population of ribosomes, very few endoplasmic reticulum profiles and normal mitochondria, just a few spherosome-like vesicles, low dehydrogenase activity, and a reduced number of amyloplasts. At the periphery of the proembryogenic mass, groups of highly meristematic cells are present. In contrast to the central cells, these are characterized by having several small vacuoles, a large diffusely staining nucleus with a single prominently staining nucleolus, a higher density of ribosomes, numerous profiles of rough endoplasmic reticulum, normal mitochondria, spherosome-like vesicles, higher dehydrogenase activity, and prominent amyloplasts. Upon transfer into 2,4-D omitted medium embryos are rapidly initiated from the exterior cells of the proembryogenic masses.

Somatic embryos most probably derive from a single cell (e.g. McWilliam *et al.* 1974). They progress through the successive stages of embryogenesis, i.e. globular, heart-shaped and torpedo-shaped, comparable with the development of zygotic embryos (Street & Withers 1974). Each stage displays a unique pattern of growth. The globular embryo undergoes isodiametric expansion to form a spherical mass of cells. The transition from the globular to the heart-shaped embryo is marked by the emergence of the cotyledons. Schiavone & Cooke (1985) distinguished an intermediate stage between the globular and heart-shaped embryo, characterized by considerable elongation of the longitudinal axis without any sign of cotyledon initiation, which they named the oblong embryo. Moreover, they also found that no morphological event, other than a general increase in overall size, marked the transition from heart-shaped to torpedo-shaped embryo. These authors propose, arbitrarily, an axial length of 400 μm as the transitional length between these two stages.

Differences between somatic and zygotic embryos of carrot have been described by Halperin (1966). He states that somatic embryos lack a clearly defined protoderm, may exhibit vascular differentiation earlier than zygotic embryos and have shorter cotyledons. Mature embryos *in vitro* also lack a period of dormancy like their counterparts *in ovulo* (Wetherell 1978). These differences, however, do not prevent somatic embryos from growing into normal, full-grown plantlets.

Ultrastructural changes accompanying carrot embryogenesis are described in detail by Halperin & Jensen (1967), Wochok (1973) and Street & Withers (1974). Most obvious are an increase in the free ribosomal content, differences in the number of ER profiles, the number and structure of Golgi bodies and mitochondria and a change in the orientation of microtubuli from a criss-cross organization to arranged in ordered parallel arrays.

Besides by structural changes, embryogenesis is also characterized by a number of metabolic changes. During the formation of globular embryos a high rate of DNA synthesis (Nomura & Komamine 1986b) and changes in protein (Racusen & Schiavone 1988, Slay *et al.* 1989) and polyamine (Fienberg *et al.* 1984) metabolism have been observed. For more information the reader is referred to Terzi *et al.* (1985).

Somatic embryogenesis is influenced by several exogenous factors (see Tazawa & Reinert 1969, Tisserat *et al.* 1979, Hari 1980, Bhojwani & Razdan 1983, Smith & Sung 1985, Michler & Lineberger 1987, De Vries *et al.* 1988b). In the culture medium 2,4-D, usually used in a concentration in the range of 0.5-1.0 $mg.l^{-1}$, is thought to be essential for the acquisition of embryogenic potential. However, Smith & Krikorian (1988) demonstrated that somatic embryos can be obtained from mericarps or zygotic embryos in hormone-free medium, if cultured at low pH. Embryogenesis itself is inhibited by exogenously supplied 2,4-D or IAA. Zeatin promotes, but other cytokinins inhibit embryogenesis. GA_3 or ABA do not affect the number of embryos formed in the globular and early heart-shaped stages but they cause a decrease in the number of embryos in the late heart-shaped and torpedo-shaped stages (Fujimura & Komamine 1975).

For normal cell proliferation in a carrot suspension culture at least a concentration of 30 μM $CaCl_2$ is essential. Between a $[Ca^{2+}]$ of 30 μM and 1.0 mM (the regular concentration in the medium), both the amount of somatic embryos and the cell density in proliferating cultures, i.e cultures with 2,4-D in the medium, augment with increasing $[Ca^{2+}]$. At concentrations over 1.0 mM there is a clear increase in the amount of somatic embryos which does not coincide with a simultaneous increase in cell proliferation (Jansen *et al.* 1990). High $[Ca^{2+}]$, i.e. more than 7.5 mM, are also promotive for the initiation of embryogenesis from single cells (Nomura 1987). From this it was, originally, concluded that Ca^{2+} influx promotes embryogenesis. Adding the Ca^{2+} ionophore A23187, however, inhibits embryogenesis in the presence of $[Ca^{2+}]$ higher than approximately 0.1 mM. Only at low $[Ca^{2+}]$ a promotive effect of an enlarged Ca^{2+} influx could be observed (Jansen *et al.* 1990). Experiments with embryogenic cells, pregrown at various $[Ca^{2+}]$ indicate that not the actual $[Ca^{2+}]$ is responsible for the increased amount of embryos but rather the rise of its concentration. The same increase of embryogenesis can be achieved when proembryogenic masses are transferred to medium with a tenfold higher $[Ca^{2+}]$, regardless of the initial concentration

(Jansen *et al.* 1990).

PROPERTIES OF CALCIUM AND CALMODULIN IN LIVING ORGANISMS

Calcium

Four principal roles of calcium in living organisms are distinguished (Ashley & Campbell 1979):

1. A structural role, including extracellular calcium precipitates, in plants, mainly calcium pectate of the middle lamella; also the binding to phospholipids, proteins and nucleic acids, which is required for the normal function of biological membranes and many intracellular structures.
2. A chemical role as a cofactor for enzymes.
3. An electrical role.
4. A regulatory role: changes in $[Ca^{2+}]$ are caused by a previous physiological stimulus (Fig. 1).

A number of properties of Ca^{2+} makes it suitable as a second messenger. Important is its low intracellular free concentration (about 0.1 μM) relative to the concentration outside the cell. At elevated levels, Ca^{2+} reacts with phosphate, forming an insoluble precipitate which would strongly inhibit the phosphate-based energy metabolism of cells (Kretsinger 1979). A low intracellular concentration of Ca^{2+} is, accordingly, a prerequisite for the normal functioning of a cell. Due to this steep gradient it is possible to raise the Ca^{2+} concentration very quickly which makes it suitable for rapid responses of cells to environmental stimuli mainly by opening Ca^{2+} channels (for review, see Schroeder & Thuleau 1991). A low internal Ca^{2+} concentration is maintained by actively pumping Ca^{2+} out of the cytoplasm (for review, see Evans *et al.* 1991). Ca^{2+} pumps are found in a variety of membranes such as in mitochondria, the tonoplast, the plasma membrane and rough ER. An important property of Ca^{2+} is its binding to a number of proteins in a reversible manner and thereby changing their activity (Fig. 1).

Much emphasis has been placed on free cytoplasmic Ca^{2+} as the determinant of physiological triggering. In plants, as in animals, the resting level of free cytosolic Ca^{2+} varies between 10^{-6} to 10^{-7} M and changes in response to a number of extracellular stimuli (Table 2).

Besides free, in the cytosol, Ca^{2+} is also present bound to membrane surfaces or intracellular chelating molecules, or is sequestered inside organelles where the concentration lies in the mM range (Poovaiah 1985, Bush 1992). Estimates of total calcium are therefore a sum of the free, bound and sequestered calcium and reflect only indirectly any changes in the concentration of free cytosolic calcium (Caswell 1979). For a more detailed description of the distribution of calcium in plant cells the reader is referred to Kauss (1987).

Calmodulin

Calmodulin is a small, acidic, heat-resistant Ca^{2+}-binding protein with an isoelectric point of 3.9, and it is

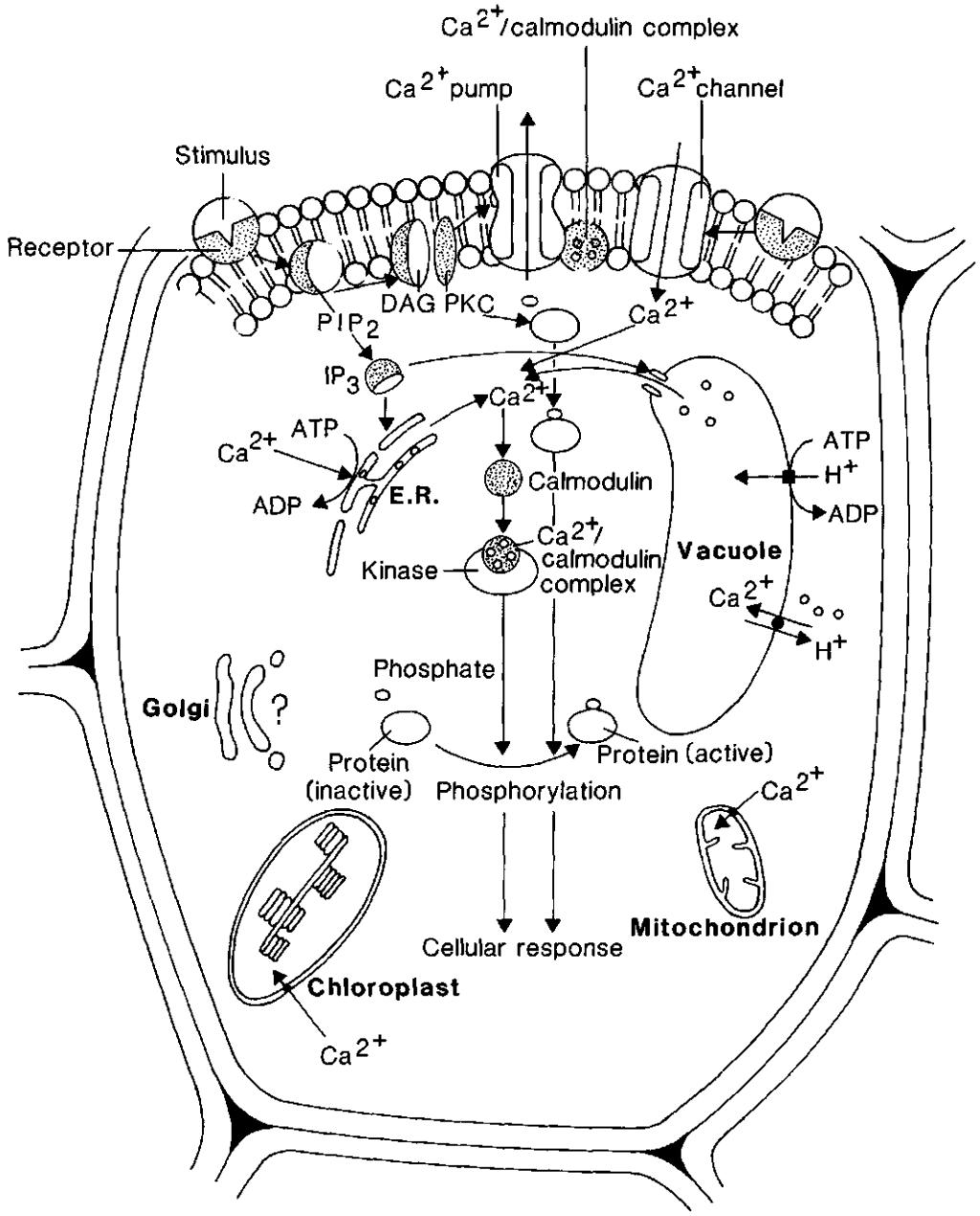
Ca2+/calmodulin complex
Ca2+ pump
Ca2+ channel
Stimulus
Receptor
DAG PKC
PIP2
Ca2+
IP3
Ca2+
Ca2+ ATP
ADP
E.R.
Calmodulin
ATP
H+
ADP
Ca2+/
calmodulin
complex
Kinase
Vacuole
Ca2+
H+
Phosphate
Golgi
?
Protein
(inactive)
Phosphorylation
Protein (active)
Ca2+
Mitochondrion
Cellular response
Chloroplast
Ca2+

Fig. 1. Schematic representation of the Ca^{2+} messenger system. An extracellular stimulus leads to an increase in $[Ca^{2+}]_c$ which eventually leads to a cellular response. The $[Ca^{2+}]_c$ can be either increased through direct action of the stimulus/receptor complex on Ca^{2+} channels in the plasma membrane (top right) or through the phosphatidyl-inositol (PI) signalling system (top left). In the latter, phosphodiesterase or phospholipase C is activated by the stimulus/receptor complex and causes hydrolysis of plasma membrane bound phosphatidyl inositol-4,5-biphosphate (PIP_2), producing inositol-1,4,5-triphosphate (IP_3) and diacylglycerol (DAG). DAG remains in the plasma membrane and activates the Ca^{2+}-requiring enzyme protein kinase C (PKC), thereby leading to the activation of proteins through phosphorylation. IP_3 moves to the cytosol and stimulates the release of Ca^{2+} from the endoplasmic reticulum (ER) and the vacuole. At elevated Ca^{2+} levels, Ca^{2+} binds to Ca^{2+}-binding proteins and activates them by a subsequent change of their conformation. Upon binding to calmodulin, a hydrophobic domain is exposed, which binds with Ca^{2+}/calmodulin dependent protein kinases, thereby increasing their activity. Ensuing protein phosphorylation, finally, results in a specific cellular response. The resting level of Ca^{2+} is restored by actively pumping Ca^{2+} out of the cytosol. Ca^{2+} ATPases are present in the plasma membrane, the endoplasmic reticulum and the envelopes of chloroplasts and mitochondria. Ca^{2+} transport at the tonoplast is achieved by H^+/Ca^{2+} antiport, driven by the electrochemical potential difference across the tonoplast. In these organelles the $[Ca^{2+}]$ can reach levels which are 1000 to 10,000 times the level in the cytosol. (Figure and text compiled of information from Poovaiah 1985, Rasmussen 1989, Evans *et al.* 1991 and Schroeder & Thuleau 1991).

present in all eukaryotic organisms investigated so far. It has been purified and characterized from a variety of higher plants (for review, see Roberts & Harmon 1992). It consists of a single polypeptide chain of 148 amino acid residues. Characteristic for all calmodulins is the presence of trimethyllysine at position 115, the lack of tryptophan and the high content of negatively charged amino acids. The molecular weight of calmodulin from plants is comparable to the molecular weight of animal calmodulin. On SDS-PAGE calmodulin shows a apparent molecular weight of 14,500 in the presence of Ca^{2+} and 17,000-19,000 in the absence of Ca^{2+} (Marmé & Dieter 1983). A comparison of sequences of calmodulins from various sources, including animals and higher plants, reveals a high degree of sequence identity and indicates that calmodulin may be one of the most highly conserved proteins known (Roberts *et al.* 1986). For example, spinach calmodulin differs from bovine calmodulin in only 12 amino acid residues. In contrast, calmodulins from phylogenetically earlier plant species markedly differ in amino acid sequence from higher plant calmodulins (Roberts *et al.* 1986). Antibodies directed against bovine calmodulin cross-react with calmodulin from higher plants (Schleicher *et al.* 1982). In addition, antisera against spinach calmodulin cross-react with pea, wheat and corn calmodulin but do not react with bovine brain calmodulin (Muto & Miyachi 1984).

Calmodulin contains four Ca^{2+} binding domains with an α-helix-loop-

Table 2. Cytosolic Ca^{2+} levels in plants

Plant species	Resting $[Ca^{2+}]_c$ nM	Elevated $[Ca^{2+}]_c$ nM	Stimulus	Reference
Commelina communis (guard cells)	100 - 200	500	$[Ca^{2+}]_c$ $[K^+]_c$ ABA	Gilroy et al. 1992
Dryopteris paleacea (spores)	50	500	$[Ca^{2+}]_c$	Scheurlein et al. 1991
Funaria hygrometrica (caulonema cells)	250	750	BAP	Saunders 1992
Hordeum vulgare (aleurone protoplasts)	200	350	GA_3	Bush & Jones 1988
Lilium longiflorum (pollen tubes)	170	490	-	Miller et al. 1992
Zea mays (coleoptiles)	119	oscillations	auxin	Felle 1988

α-helix repeat composed of 11,12 and 11 amino acid residues respectively. The Ca^{2+} binding domains are numbered I,II,III and IV, starting from the N-terminal side. Although many reports are available about the cooperativity of the Ca^{2+} binding sites and the order of Ca^{2+} binding to the four Ca^{2+} binding sites, data are conflicting. Most recent results of experiments on Ca^{2+} binding to calmodulin, however, can be explained by the assumption of four equivalent sites that bind Ca^{2+} and Mg^{2+} competitively (for discussion, see Cox *et al.* 1988). If one of the sites binds Ca^{2+} or Mg^{2+}, the association constant of the other sites for Ca^{2+} or Mg^{2+} increases (Iida & Potter 1986).

Ca^{2+} binding is affected by $[Ca^{2+}]$, $[Mg^{2+}]$, ionic strength, pH and temperature (Ogawa & Tanokura 1984). Over a pH range from 6.0 to 10.1 the affinity of calmodulin for Ca^{2+} increases with increasing pH (Iida & Potter 1986). At low pH (< 4.5), additional non-specific acid effects, such as massive protonation of all the carboxyl groups and precipitation of the protein, completely abolish the affinity of calmodulin for Ca^{2+} (Cox *et al.* 1988). For some calmodulin-dependent proteins, however, full Ca^{2+} occupancy is not required for either binding or activation, and binding to interacting proteins may

occur at even lower calcium concentrations than those needed for activation of calmodulin (Allan & Hepler 1989).

Calcium activates calmodulin by inducing a conformational change. On binding Ca^{2+}, the helicity of calmodulin increases from 40% to more than 50% (Dedman *et al.* 1977), and a hydrophobic domain is exposed. This exposed site interacts with a complimentary hydrophobic domain present on an inactive calmodulin-binding protein, resulting in a conformational shift and subsequent activation of the calmodulin-binding protein (Fig. 1). Phenothiazine antipsychotic drugs can also bind to this same hydrophobic domain, leading to the inactivation of calmodulin by obstructing its interaction with various calmodulin binding proteins (Brady *et al.* 1985).

The calmodulin content in plant tissue is not constant. The level has found to be high in growing tissues and leaves (Muto & Miyachi 1984). The yield of calmodulin from zucchini hypocotyls was found to be about 10 mg per kg of plant tissue, corresponding to a concentration of about 10^{-3}-10^{-2} $mol.m^{-3}$ in the cytoplasm (Marmé & Dieter 1983). In corn root sections calmodulin was mainly detected in the root cap cells. In terminal buds of spinach it was highly concentrated in the apical meristem and leaf primordia (Lin *et al.* 1986). Most of the calmodulin is localized, free or bound, in the cytoplasm whereas smaller fractions are associated with organelles. In pea seedlings calmodulin has been reported to be present in vacuoles and amyloplasts (Dauwalder *et al.* 1986). These immunocytochemical studies do not confirm the presence of calmodulin in the apoplast as found by radioimmunoassays (Biro *et al.* 1984). Furthermore, calmodulin is associated with cytoskeletal elements, which is very apparent in mitotic spindles (Lambert *et al.* 1983). Nucleoli seem to be devoid of calmodulin (Dauwalder *et al.* 1986). In animal cells a correlation between the calmodulin level and the cell cycle has been found (Means *et al.* 1982, Whitaker & Patel 1990). High calmodulin levels are present in late G_1 and early S phase. Also in yeast, calmodulin is required for the progression of the G_1 and M phase (Anraku *et al.* 1991). Similar findings for higher plant cells have not been reported.

LOCALIZATION OF CALCIUM AND CALMODULIN.

Calcium

Three types of intracellular calcium can be distinguished:

1. Cytosolic free Ca^{2+}.
2. Ca^{2+} bound to membrane surfaces or intracellular chelating molecules.
3. Ca^{2+} sequestered inside organelles.

Each type requires a different detection technique which have already been discussed in detail by various authors (e.g. Ashley & Campbell 1979, Caswell 1979, Borle & Snowdowne 1987, McCormack & Cobbold 1991, Read *et al.* 1992). Here it suffices to give information about

methods which are applicable with the study of the distribution of calcium during plant embryogenesis.

Total cellular calcium

Total amounts of calcium can be determined by atomic absorption spectrophotometry (Havelange 1989), which gives an indication of the calcium concentration of the whole tissue under investigation. However, more important is its subcellular distribution. This can be visualized by histochemical techniques (McGee-Russel 1958, Poenie & Epel 1987, Sobota *et al.* 1987), X-ray microanalysis (Somlyo 1985, Chaubal & Reger 1992), or autoradiography (Bednarska 1991). Especially X-ray microanalysis is promising for the study of the distribution of intracellular calcium. A major problem, however, with this technique is the preparation of the material without changing the amount and distribution of Ca^{2+}. The method always requires a fast freezing step, which is only possible with small specimens in order to avoid freezing-damage (Kaesser *et al.* 1989). Procedures include direct observation of frozen-hydrated or frozen-dried sections or sections of frozen-dried and resin embedded specimens, and the use of freeze substitution. Unfortunately, however, the biological calcium concentrations are very close to the detection limits of electron probe microanalysis of X-rays.

Free cytosolic Ca^{2+}

Methods of measuring the cytosolic free Ca^{2+} concentration include the use of photoproteins, Ca^{2+}-sensitive electrodes and dyes (Thomas 1986). Two photoproteins that have been successfully used to measure intracellular free Ca^{2+} are aequorin and obelin (Borle & Snowdowne 1987). In the presence of Ca^{2+} these proteins emit light in direct proportion to the $[Ca^{2+}]$. Aequorin is a very sensitive Ca^{2+} indicator with a limit of detection of 2.10^{-7} M (Gilroy *et al.* 1989). In animal cells, aequorin can be incorporated by the use of microinjection (Blinks *et al.* 1978), scrape-loading (Snowdowne & Borle 1985) or centrifugation-loading (Borle *et al.* 1986). In plant cells, microinjection has been used in cells of *Chara corallina* (Williamson & Ashley 1982). Very promising with regard to $[Ca^{2+}]_c$ measurements is the recently accomplished genetic transformation of *Escherichia coli* and *Nicotiana plumbaginifolia* with the aequorin gene (Knight *et al.* 1991).

The use of Ca^{2+} sensitive electrodes for the measurement of $[Ca^{2+}]$ in living plant systems is limited by the fact that only the concentration in one cell at a moment is measured. When used in a multicellular system it is very difficult to see in which cell or cell compartment the measurements take place.

A large number of dyes, specific for Ca^{2+}, is nowadays available (see e.g. Thomas & Delaville 1991, Read *et al.* 1992, Haugland 1992). These include the fluorescent indicators indo-1, fura-2 and fluo-3. They are all able to indicate low intracellular free Ca^{2+} levels. For a single-wavelength indicator, such as fluo-3, $[Ca^{2+}]$ can be calculated with the equation:

$$[Ca^{2+}] = K_d \times \frac{(F-F_{min})}{(F_{max}-F)}$$

where K_d is the dissociation constant, F_{min} is the fluorescence in the absence of Ca^{2+}, F_{max} is the fluorescence at saturating Ca^{2+} and F is the fluorescence at any known $[Ca^{2+}]$. The application of these dyes to whole plant tissues is, however, limited because of their cell impermeability and their tendency to sequester into intracellular membrane compartments (Hepler & Callaham 1987). In spite of this, the membrane permeable acetoxymethyl ester of the long wavelength Ca^{2+} indicator fluo-3 (Minta *et al.* 1987) is very useful for the study of the distribution of intracellular free Ca^{2+} in large plant tissue, especially in combination with the use of confocal scanning laser microscopy (Williams *et al.* 1990).

Changes in $[Ca^{2+}]$ can also be studied with the fluorescent indicator chlorotetracycline, which is cell permeable and loads easily into plant cells. This compound is, therefore, very suited for the visualization of Ca^{2+} in complete plant tissue. Nevertheless, in addition to high $[Ca^{2+}]$, the intensity of the fluorescence of CTC also rises with increasing hydrophobicity (Caswell 1979) and therefore CTC is used in plants as a marker for membrane-bound calcium. Dixon *et al.* (1984), however, state that CTC does not indicate membrane-bound Ca^{2+} as such, but that the Ca^{2+}-CTC complex must bind to the membrane before the Ca^{2+}-enhanced signal can be observed. It is not necessary to have a Ca^{2+} binding site on the membrane to see an enhancement of CTC fluorescence in response to elevations in $[Ca^{2+}]$. According to these authors the CTC fluorescence response is proportional to the free internal $[Ca^{2+}]$ and CTC is consequentially a faithful, nonperturbing indicator of the free Ca^{2+} concentration.

Calmodulin

Being a protein, properties of calmodulin can be studied by methods suitable for protein analysis. These include radioimmunoassays and immunocytochemistry (Wick & Duniec 1986). With these methods, total calmodulin levels and its distribution in plant tissue are indicated. The Ca^{2+}-calmodulin complex can be visualized by phenothiazines which bind rather specifically with activated calmodulin (Levin & Weiss 1975, 1977). They can be photooxidized to fluorescent derivatives and then become irreversibly bound to the Ca^{2+}-calmodulin complex (Prozialeck *et al.* 1981). The brightest fluorescence is produced by fluphenazine.2HCl (Haußer *et al.* 1984). This compound is cell permeable and therefore applicable to whole plant tissues.

SCOPE OF THE STUDY

Despite the large number of investigations on plant embryogenesis *in vivo* and *in vitro* the molecular and cellular basis of the regulation of plant embryogenesis is still poorly understood. Therefore, the main

objective of this study was to attain more fundamental knowledge about this process in relation to Ca^{2+} metabolism. As described above, Ca^{2+} and the Ca^{2+} binding protein calmodulin play a major role in the regulation of a number of physiological processes which are related with growth and development of plants. For that reason, localization of Ca^{2+} and calmodulin during embryogenesis was thought to be of paramount importance. Since carrot possesses a number of features which makes this plant an ideal object for the study of plant embryogenesis, this study was devoted to the localization of Ca^{2+} and calmodulin during embryogenesis of carrot.

The localization of Ca^{2+} is given in Chapters 2 and 5. Chlorotetracycline, a membrane permeable Ca^{2+} indicator which was used in Chapter 2, only gives a rough idea about the distribution of Ca^{2+} during carrot embryogenesis and cannot be used in combination with confocal laser scanning microscopy. More information can be gained with fluo-3, but this compound is membrane impermeable. Therefore, a method had to be developed to load this dye into plant cells, which is described in Chapter 4. Using this method the distribution of Ca^{2+} was studied during carrot somatic embryogenesis, as presented in Chapter 5.

The localization of calmodulin can be found in Chapters 2 and 3. In Chapter 2 the distribution of activated calmodulin is visualized by fluphenazine fluorescence. Chapter 3 describes the distribution of total calmodulin investigated by immunocytochemistry during somatic and zygotic embryogenesis and during zygotic embryo germination.

Changes in $[Ca^{2+}]$ are often associated with changes in pH (for review, see Kurkdjian & Guern 1989) and evidence is accumulating that cytoplasmic pH changes play a role as second messenger in animal systems (e.g. Frelin *et al.* 1988). The hypothesis that this is also true for plants, e.g. in the action of plant hormones, is still a subject of much controversy and needs further research. In Chapter 6 a beginning was made with the localization of changes in pH, and these changes were compared with the distribution of fluphenazine.

During this study obvious differences between somatic and zygotic embryos of carrot were observed in the distribution of signals from the various used indicators. These differences were linked with structural observations on somatic and zygotic embryos in Chapter 7.

CHAPTER 2

DISTRIBUTION OF MEMBRANE-BOUND CALCIUM AND ACTIVATED CALMODULIN DURING SOMATIC EMBRYOGENESIS OF *DAUCUS CAROTA* L.

A.C.J. TIMMERS[1], S.C. DE VRIES[2] & J.H.N. SCHEL[1]

[1]Department of Plant Cytology and Morphology, Agricultural University, Arboretumlaan 4, 6703 BD Wageningen, The Netherlands
[2]Department of Molecular Biology, Agricultural University, De Dreijen 11, 6703 BC Wageningen, The Netherlands

Reprinted, with permission, from *Protoplasma* 153:24-29 (1989)

SUMMARY

The distribution of membrane-bound calcium and activated calmodulin was visualized during carrot somatic embryogenesis by chlorotetracycline and fluphenazine fluorescence respectively. Somatic embryos of all stages possessed a higher CTC fluorescence in comparison with the signal from their precursors, the proembryogenic masses. The CTC fluorescence was evenly distributed in the somatic embryos. In contrast, fluphenazine fluorescence was observed in some regions of the proembryogenic masses only. In the globular, heart-shaped and early torpedo-shaped stage its fluorescence was restricted to the basal part of the embryo. In the older torpedo-shaped embryos also the shoot apex showed fluphenazine fluorescence. It is concluded that during carrot somatic embryogenesis a polarity in the distribution of the activated calmodulin already exists before this polarity is morphologically expressed.

INTRODUCTION

Carrot somatic embryogenesis is used extensively as a model system for early plant development (see reviews by Ammirato 1987, 1989, Nomura and Komamine 1986a). Somatic embryos of carrot usually develop from small clusters of cells, designated proembryogenic masses by Halperin (1966), after dilution and transfer of these masses from auxin containing to auxin free medium. Morphologically, somatic embryos resemble their zygotic counterparts when they progress through the successive stages of globular, heart-shaped and torpedo-shaped embryos. The phenomenon of differentiated

somatic cells, embarking on an embryogenic pathway, provides a superb opportunity for exploring fundamental questions of plant growth, differentiation and development (Cocking 1987). One approach is to identify biochemical markers that correlate with the process of embryogenesis, such as the expression of embryo-specific polypeptides (Sung and Okimoto 1981), changes in polyamine metabolism (Fienberg *et al.* 1984) or the inactivation of α-amanitin (Pitto *et al.* 1985). Another approach has been to study the morphological changes during early embryogenesis (see e.g. Van Lammeren *et al.* 1987).

The induction of polarity, as reviewed by Schnepf (1986), is considered to be an important control factor, not only during polar growth of unicellular organisms, but also during the development of multicellular systems. Morphological polarity during carrot somatic embryogenesis was observed earlier by Halperin and Jensen (1967). More recently, Nomura and Komamine (1986b) reported polarity of DNA-synthesis during somatic embryogenesis from single cell systems of carrot. There is increasing evidence that the divalent cation Ca^{2+} participates in the initiation and maintenance of this polarity in plant cells (Hepler and Wayne 1985, Hepler 1988). Nomura (1987) observed a polarized distribution of free Ca^{2+} in proembryogenic masses with the use of the fluorescent Ca^{2+}-indicator fura 2-AM. Furthermore, the frequency of somatic embryogenesis was enhanced by raising the Ca^{2+}-concentration of the basal medium (Jansen *et al.* 1990). In the light of these observations we have begun a more detailed study of the distribution of calcium during somatic embryogenesis of carrot, combining the data with the distribution of activated calmodulin because of its dominant role in the regulation of the calcium metabolism (Roberts *et al.* 1986, Marmé 1989).

The use of fura-2 for the localization of Ca^{2+} is not without difficulties (Borle and Snowdowne 1987). The acetoxymethyl ester form might be loaded into cellular membrane compartments before being cleaved by esterases and then becomes useless as a cytoplasmic indicator (Roe *et al.* 1987). Further, metallochromic and bioluminescent calcium indicators do not penetrate well into plant cells and can therefore only be used by means of microinjection, which is quite feasible for single cell systems such as stamen hair cells (Hepler and Callaham 1987), but rather complicated for multicellular plant embryos. These problems can be circumvented by the use of chlorotetracycline which has a good cell permeability and easily loads into plant cells (Caswell 1979, Blinks *et al.* 1982). For these reasons, CTC was used in this study in spite of the drawback that it is only indicative for membrane-bound calcium. Calmodulin can easily be detected, also in plant cells, by the use of fluphenazine.2HCl (Haußer *et al.* 1984) which binds specifically with activated calmodulin (Prozialeck *et al.* 1981). This compound was used to study the distribution of activated calmodulin during different developmental stages.

MATERIALS AND METHODS

Plant material and culture conditions

Embryogenic callus was obtained from hypocotyl sections of *Daucus carota* L. cv. Flakkese sg766 Trophy, on solid B5 medium with 2 μM 2,4-D. Embryogenic callus was transferred to liquid medium with 2 μM 2,4-D and was maintained on a rotary shaker at 100 r.p.m. under an 8 h light period at 25 °C on a 14 day subculture cycle. Embryogenesis was initiated essentially as described earlier (De Vries *et al.* 1988b) by size fractionation of suspension cells between 125 and 50 μm nylon meshes. The resulting purified proembryogenic masses were inoculated at a density of $2x10^4$ cells ml^{-1} in 2,4-D free B5 medium.

Localization of membrane-bound calcium and calmodulin

Membrane-bound calcium was visualized by CTC-fluorescence, while calmodulin was visualized by fluphenazine-fluorescence. CTC was added to the medium in a final concentration of 1.10^{-4} M. We found that an incubation time of 20 minutes was optimal. The fluorescence was observed with a Zeiss fluorescence microscope (BP355-425/DM 455/LP460). Fluphenazine.2HCl was added to the medium in a final concentration of 2.10^{-5} M. Also after 20 minutes the fluorescence was observed with a Nikon UV-fluorescence microscope (365/10/DM 400/LP420). With both fluorescent probes, observations were made immediately after the initiation of embryogenesis until 12 days after embryo initiation. Photographs were recorded on Kodak Ektachrome P800/1600 film with automatic exposure by the Nikon UFX system.

RESULTS

Distribution of membrane-bound calcium during embryo development

The fluorescence signal of CTC was very intense immediately after irradiation but decreased rapidly. Results were therefore recorded within ten seconds after irradiation. It was proved to be important to avoid damaging the embryos during incubation with CTC, because damaged cells were strongly fluorescent.

At the onset of embryogenesis (0 d.a.i.) the small cells in the embryogenic masses showed a faint diffuse fluorescence (Fig. 1a, large arrow.). In some cases, however, only the borderlines of these cells were fluorescent (Fig. 1a, small arrows). At 2 d.a.i. several regions with a more bright fluorescence were observed within the proembryogenic masses (Fig. 1b, large arrows). These regions represented the developing globular embryos as could be deduced from the number and orientation of their cells. These cells often also showed an increased fluorescence near their borders (Fig. 1b, small arrows). Dependent on the size of the proembryogenic masses the number of the globular embryos varied between one and ten. Later developmental stages, up to the torpedo-shaped embryo,

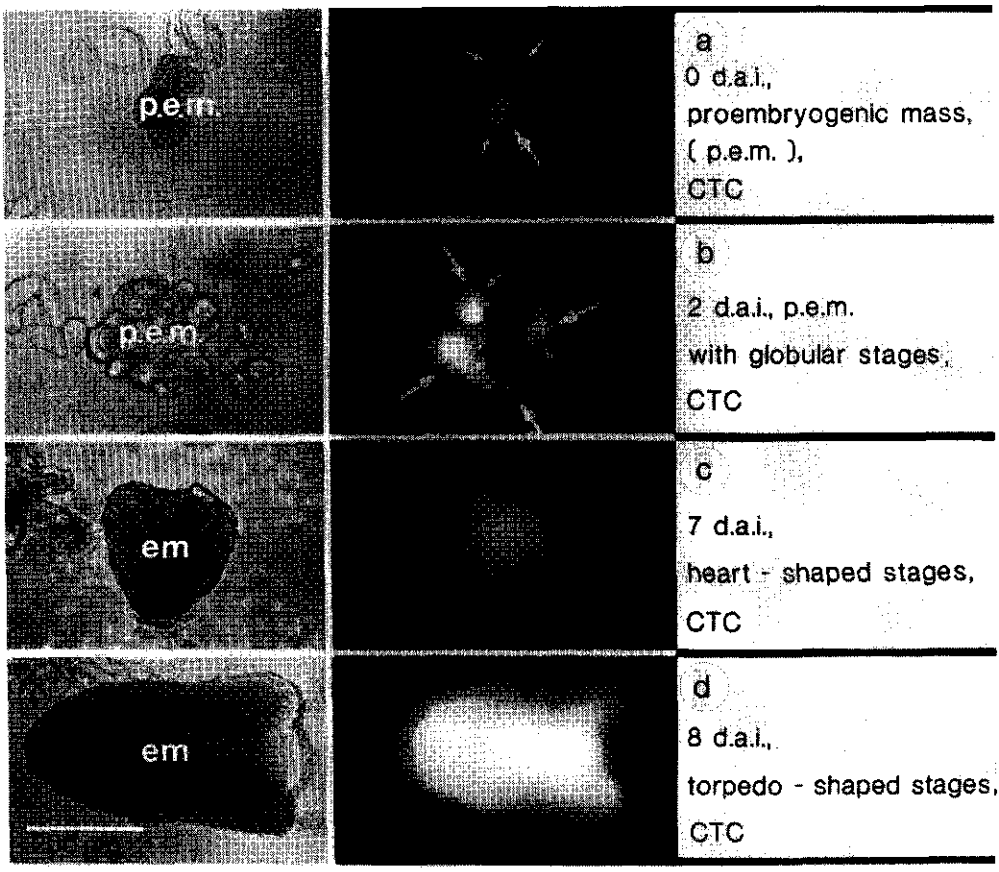

Figure 1. CTC fluorescence, indicating the presence of membrane-bound calcium during various stages of carrot somatic embryogenesis. **a.** 0 d.a.i. A faint fluorescence is present over some cells (large arrow); sometimes only the borderlines of the cells are fluorescent (small arrows). **b.** 2 d.a.i. Several regions with an increased fluorescence can be observed within the proembryogenic masses (large arrows); here also, in some cases only the borderlines are positive (small arrows). **c.** 7 d.a.i. A heart-shaped embryo with an uniform fluorescence. **d.** 8 d.a.i. A torpedo-shaped embryo, having also an uniform fluorescence.

Figure 2. Fluphenazine fluorescence, indicating the presence of activated calmodulin during various stages of carrot somatic embryogenesis. **a.** 0 d.a.i. A proembryogenic mass at the onset of embryogenesis; a diffuse fluorescence is present. **b.** The same stage, but now showing fluorescence in some regions of the proembryogenic mass (arrows). **c.** At 2 d.a.i. the outer region of the proembryogenic masses are clearly fluorescent (arrows). **d.** 5 d.a.i. A globular embryo, showing a distinct polarized distribution of activated calmodulin as indicated by the one-side orientation of the fluphenazine label (arrow). **e.** 6 d.a.i. A heart-shaped embryo with a strong fluorescence at the basal part (arrow). **f.** 12 d.a.i. In some torpedo-shaped embryos also the shoot apex is fluorescent (arrow).

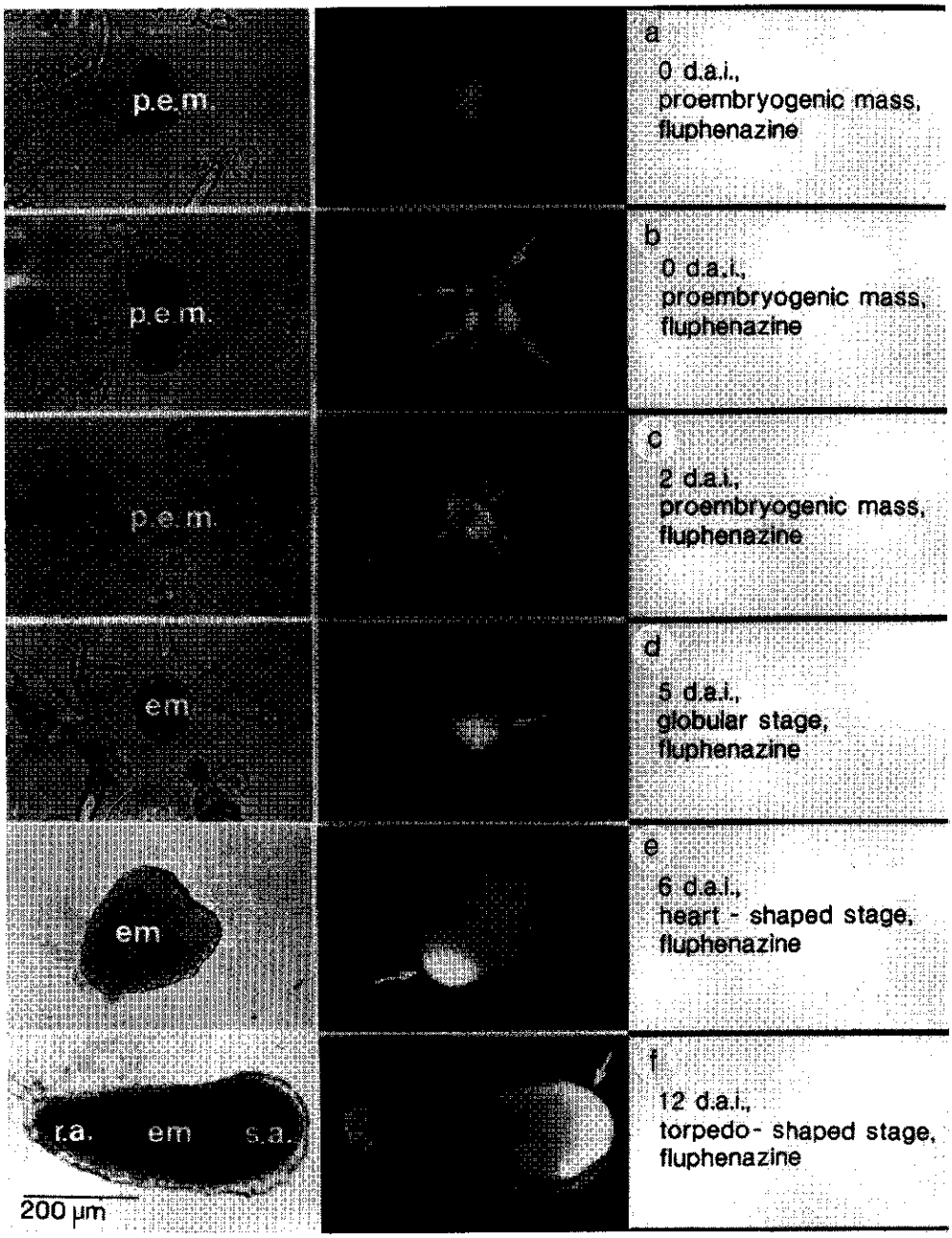
p.e.m.
p.e.m.
p.e.m.
em
em
r.a.
em
s.a.
200 µm
a
0 d.a.i.,
proembryogenic mass,
fluphenazine
b
0 d.a.i.,
proembryogenic mass,
fluphenazine
c
2 d.a.i.,
proembryogenic mass,
fluphenazine
d
5 d.a.i.,
globular stage,
fluphenazine
e
6 d.a.i.,
heart - shaped stage,
fluphenazine
f
12 d.a.i.,
torpedo- shaped stage,
fluphenazine

showed a diffuse and uniform fluorescence throughout the cells (Figs. 1c and 1d). It was found from higher magnifications that the fluorescence was evenly distributed over the cytoplasm, but not over the nucleus. In some cases, a punctate fluorescence was seen.

Distribution of activated calmodulin during embryo development

The fluphenazine fluorescence appeared shortly after UV-irradiation. The intensity increased during observation, but after a few minutes some fading could be detected. Therefore, photographs were made within 1 min after irradiation. Also here, a strong fluorescence of damaged cells was present.

Proembryogenic masses, present in high density suspension with 2,4-D, exhibited different fluorescence patterns. At the onset of embryogenesis (0 d.a.i.) some proembryogenic masses were nearly negative while in other cases a rather diffuse fluorescence was visible (Fig. 2a) Sometimes, the fluorescence was restricted to certain defined regions of the proembryogenic mass (Fig. 2b, arrows). Shortly after the onset of embryogenesis (2 d.a.i.) the strongest fluphenazine fluorescence was observed in cells of the outer layer of the proembryogenic masses (Fig. 2c, arrows).

At about 5 d.a.i., where embryos in the globular stage were present, the fluorescence was clearly located to one side of the developing embryo (Fig. 2d, arrow). At the time when the embryo was still attached to the proembryogenic mass from which it arose, then this part of the proembryogenic mass was also strongly fluorescent. From the heart-shaped stage up to the torpedo-shaped stage, the fluphenazine fluorescence was most prominent in the basal part of the embryo (Fig. 2e, arrow). In the late torpedo stage, however, around 12 d.a.i., fluorescence was present along the whole lower half of the embryo, by preference in the outer layer(s). In addition, the shoot apex now also became strongly fluorescent (Fig. 2f, arrow).

DISCUSSION

CTC and fluphenazine have been used extensively for the localization of calcium and calmodulin in unicellular organisms or organisms with cells that can easily be studied, free of surrounding tissue, such as pollen tubes and root hairs (Reiss & Herth 1979, Haußer *et al.* 1984). In this work we have shown that these fluorescent probes can also be used in more complex multicellular plant systems.

During the process of somatic embryogenesis we observed marked changes in the CTC and fluphenazine fluorescence, indicating an extensive increase of membrane-bound calcium and a local activation of calmodulin. Chlorotetracycline binds to divalent and trivalent cations in aqueous solution (Caswell 1979). The complexation of CTC with divalent cations causes a shift in the absorption spectrum and enhances the fluorescence of the compound. In less polar solvents the affinity for the cation is

higher, and the fluorescence of the complex is more intense. Therefore, increase of the CTC fluorescence may reflect an increase in the amount of membrane-bound calcium or indicate an increase in the amount of membranes. Street & Withers (1974) observed, by electron microscopy, an increase in the number of ER profiles in the outer cytoplasm-rich cells from carrot proembryogenic masses after transfer to 2,4-D depleted medium. The increased CTC signal could be in good correlation with these results and could represent a first light microscopical sign of such an increase. Possibly there is also a rise in the intracellular calcium concentration at the onset of embryogenesis but at present we cannot discriminate between both possibilities*.

From the uneven distribution of activated calmodulin in proembryogenic masses in cultures in the presence of 2,4-D, before the onset of embryogenesis, we conclude that obviously polarity is present in these proembryogenic masses. These masses are therefore not just clusters of undifferentiated suspension cells but already possess a high degree of organization. This view is supported by the fact that there is little difference between the protein pattern and gene-expression programs of proembryogenic masses with those of somatic embryos (Sung and Okimoto 1981, and Wilde *et al.* 1988). During the development of globular embryos to torpedo-shaped embryos most of the activated calmodulin was present in the basal part of the embryo. Only in mature embryos a signal could be observed in the shoot apex. A high calmodulin concentration was also reported for the root cap of several plant species (Lin *et al.* 1986) and for the apex of the embryonic axes of *Cicer arietinum* (Hernandez-Nistal *et al.* 1989). Previously, Jansen *et al.*(1990) and Goldberg *et al.* (1989 and ref. therein) did not detect such an evident redistribution or change in the expression of total calmodulin as described here. This implies that, although the total amount of calmodulin is similar during embryogenesis, its activation is strikingly regulated. Further, the results show no congruency of the calmodulin and the membrane-bound calcium distribution. Such a congruency was reported earlier by Cotton and Vanden Driessche (1987) for *Acetabularia*. There fore, we conclude that membrane-bound calcium is not exclusively bound to calmodulin as was also found by Haußer *et al.* (1984) for tip-growing plant cells. In spite of that, proembryogenic masses possessed a considerable variation in the distribution of activated calmodulin, which points to a change in the distribution of activated calmodulin during the growth of the proembryogenic mas ses in medium with 2,4-D.

In animal cells there seems to be a correlation between the calmodulin level and the cell cycle. High calmodulin levels are present in late G_1 and early S phase (Means *et al.* 1982,

*cf. chapter 5 and chapter 7; from these two chapters it is evident that embryogenesis coincides with a rise in the level of free cytosolic Ca^{2+} and not with an increase in the amount of ER profiles

You *et al.* 1988). The various alterations in fluorescence observed in the proembryogenic masses might therefore be related to cells that are in different phases of the cell cycle. An alternative explanation could be that the localized presence of activated calmodulin in only some surface cells of the proembryogenic masses is correlated with those cells that eventually lead to somatic embryos. If this hypothesis is true, the implications are that proembryogenic masses contain cells that are predetermined to give rise to somatic embryos, already during the seemingly unorganized suspension growth phase of an embryogenic culture.

CHAPTER 3

LOCALIZATION OF CALMODULIN DURING SOMATIC AND ZYGOTIC EMBRYOGENESIS AND DURING GERMINATION OF *DAUCUS CAROTA* L.

A.C.J. TIMMERS, H. KIEFT & J.H.N. SCHEL

Department of Plant Cytology and Morphology, Agricultural University, Arboretumlaan 4, 6703 BD Wageningen, The Netherlands

Partially published in : Nijkamp, H.J.J., van der Plas, L.H.W., van Aartrijk, J. (eds) *Progress in Plant Cellular and Molecular Biology*, Kluwer Academic Publishers, Dordrecht, pp. 443-448 (1990)

SUMMARY

The distribution of calmodulin was studied during somatic and zygotic embryogenesis and during germination of carrot. Total calmodulin levels were visualized by immunocytochemistry, using semithin sections of different developmental stages of embryogenesis. Activated calmodulin was visualized by fluphenazine fluorescence. In proembryogenic masses a great variety in the distribution of calmodulin was observed, ranging from a very low level in all cells to a higher level present in a group of cells in between cells with a lower amount. In all later stages of embryogenesis calmodulin was mainly found organelle-bound in the protoderm. Activated calmodulin was mainly found in the root side of the embryo with the highest amount present in the vacuoles of cells of the protoderm. Both by immunocytochemistry and by fluphenazine fluorescence, in zygotic embryos calmodulin was found to be evenly distributed over the entire embryo. A polarized distribution of calmodulin was again observed during germination of zygotic embryos. Anti-calmodulin was mainly found in the cytoplasm of the epidermis of the cotyledons and the hypocotyl, but was clearly organelle-bound in the root side of the germling. Differences between the localization of calmodulin with immunocytochemistry and fluphenazine fluorescence and possible roles for calmodulin during carrot embryogenesis and germination are discussed. It is concluded that obvious differences between somatic and zygotic embryogenesis exist and that somatic embryogenesis shows resemblances with zygotic embryo germination.

INTRODUCTION

In a suspension culture of carrot somatic embryos develop from proembryogenic masses after transfer from 2,4-D containing to 2,4-D free medium. The carrot system can be used as a model system to study fundamental problems of the regulation of *in vitro* plant growth, differentiation and development (Cocking 1987).

Modulation of the intracellular Ca^{2+} concentration has proved to be important in the initiation and coordination of a variety of cellular mechanisms involved in developmental processes (e.g. Hepler 1988, Timmers 1990). A key regulatory protein in a number of Ca^{2+}-linked processes is calmodulin (e.g. Roberts & Harmon 1992). In Chapter 2 it has been described that activated calmodulin, visualized by fluphenazine fluorescence, is irregularly distributed in proembryogenic masses of carrot, but that an obvious polar distribution is present in later embryogenic stages. Since the distribution of activated and total calmodulin is not necessarily identical, we examined the distribution of total calmodulin by immunocytochemical techniques. The observations on fluphenazine fluorescence were extended with high magnification images which revealed the cellular distribution of the signal.

Although carrot somatic embryos are used extensively as substitutes for zygotic embryos, comparative studies between somatic and zygotic embryogenesis are rare. Carrot somatic embryos grow under artificial conditions which may lead to changes in metabolism or cell composition. An obvious difference between somatic and zygotic embryos is the absence of dormancy, prior to germination, in somatic embryos. Calmodulin has been reported to be present in high amounts during germination of a number of plant species (e.g. Cocucci & Negrini 1991) and comparison of the distribution during zygotic embryo germination with the distribution during somatic embryogenesis may give insight in the mechanism of seed dormancy. Therefore, we also examined the distribution of calmodulin in immature seeds of carrot, which contained heart-shaped to torpedo-shaped embryos, and during zygotic embryo germination to compare the distribution of calmodulin during somatic embryogenesis with the distribution during zygotic embryogenesis and zygotic embryo germination.

MATERIALS AND METHODS

Plant material and culture conditions

The carrot (*Daucus carota* L.) cultivar Trophy was used. Embryo cultures were maintained in liquid B5 medium (Gamborg *et al.* 1968) with 2μM 2,4-D, and initiation of embryogenesis was as described previously (De Vries *et al.* 1988b) by transferring the fraction of 50μm to 125 μm, which contains many proembryogenic masses, to 2,4-D free B5 medium. Flowers of carrot at different stages of development were kindly provided by Zaadunie B.V. (Enkhuizen, The Netherlands). To obtain germinated

zygotic embryos, mature seeds were placed in Petri dishes, on filter paper wetted with tapwater, and incubated in the dark at 25°C. Seeds germinated after two to three days.

Specimen preparation for immunolabelling

Cell aggregates and somatic embryos were harvested directly after initiation of embryogenesis and during subsequent stages of embryo development. Immature mericarps of carrot were harvested at a size of approximately 3 to 6 mm, divided into two parts by a tangential cut and de-aerated to improve uptake of the fixative. Germinated zygotic embryos were harvested 3 days after the induction of germination, separated from the mericarp and put into the fixative.

Originally, specimens were fixed in 3% paraformaldehyde in culture medium for one hour and rinsed in phosphate buffered saline (135 mM NaCl, 2.7 mM KCl, 1.5 mM KH_2PO_4, 8 mM Na_2HPO_4, pH 7.4). Alternatively, a fixation protocol, described to be optimal for the localization of calmodulin in plant cells, using 3.7% PFA in 50 mM phosphate buffer at pH 10, was employed (Wick and Duniec 1986). The specimens were either dehydrated with ethanol (30%, 50%, 70%, 90%, each step taking 10 minutes, and 3 times 10 minutes 100%) and embedded in polyethyleneglycol (mixture of 1500 and 4000, 3:2) or stepwise infiltrated to a final concentration of 2.3 M sucrose in PBS (0.1 M, 4 hours; 1.0 M, overnight; 2.3 M, 4 hours), quickly frozen in liquid propane and stored under liquid nitrogen.

Semithin (3-5 μm) PEG sections were made with a Leitz Wetzlar microtome equipped with a steel knife. Ribbons were broken into small pieces, picked up with a drop of 40% PEG 6000 and tipped onto poly-L-lysine (Sigma, M 70,000, 0.1% w/v in distilled water) coated slides. Semithin (2-5 μm) cryosections were made with a Reichert Ultracut E ultramicrotome with the FC 4D chamber at -80°C, specimen temperature at -20°C and knife temperature at -35°C. Sections were picked up with a drop of 2.3 M sucrose in PBS, thawed and tipped onto poly-L-lysine coated slides.

Antisera

We used a commercial polyclonal antiserum directed against bovine calmodulin (Calbiochem) and a monoclonal antibody (designated FF7) directed against pea calmodulin (a generous gift of drs. P. Jablonski and R. Williamson, Canberra). The specificity and properties of this antibody are described by Jablonsky *et al.* (1991). The fluorochrome conjugated antisera were respectively rabbit-anti-sheep-FITC and rabbit-anti-mouse-IgM-FITC (Nordic).

Immunolabelling and immunofluorescence

Slides, covered with sections, were rinsed in PBS to remove PEG or sucrose, incubated for 5 minutes in 0.1 M NH_4Cl, rinsed again in PBS and incubated with the first antibody. The polyclonal antiserum was diluted 50 or 100 times, the monoclonal

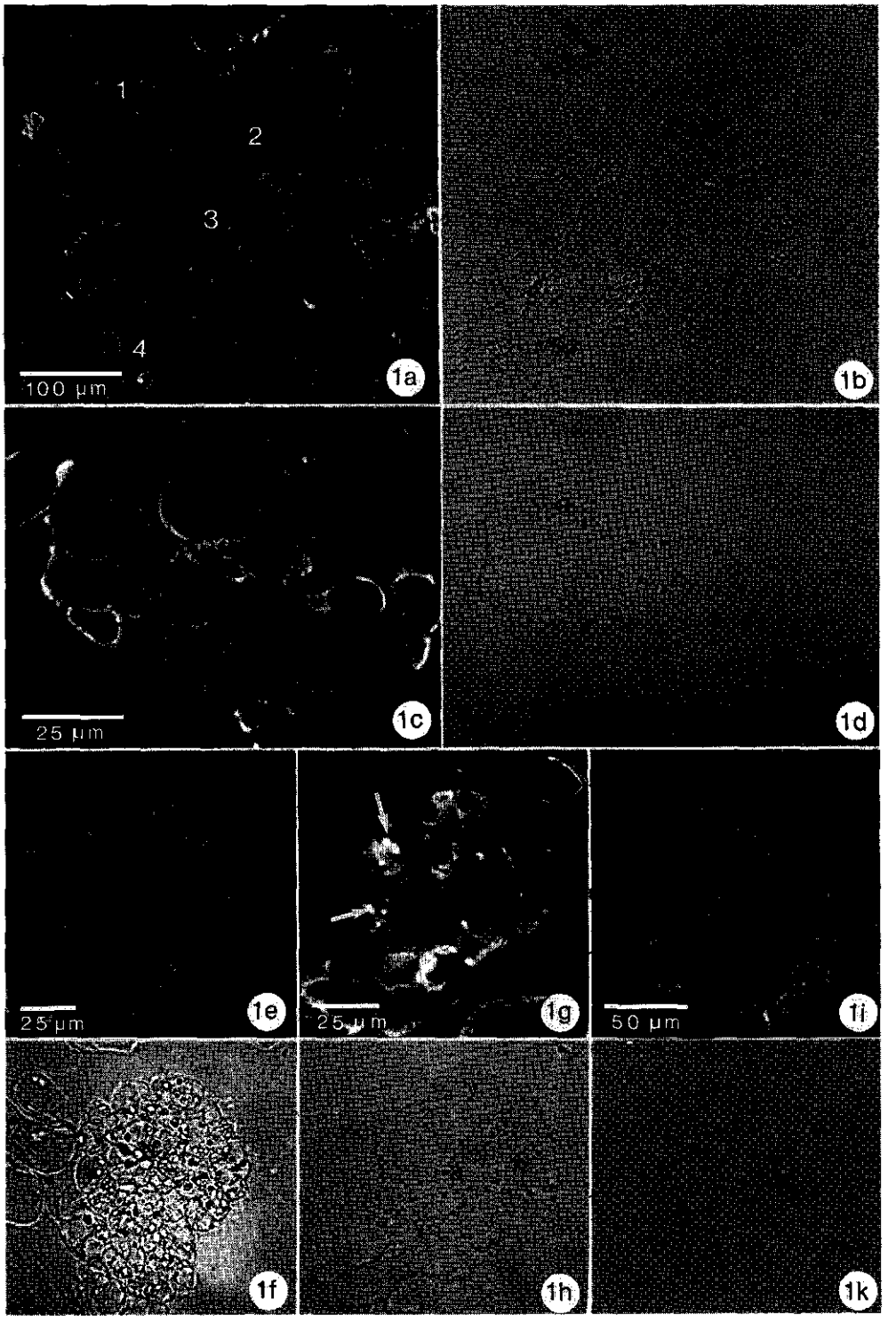
1
2
3
4
100 µm
1a
1b
25 µm
1c
1d
25 µm
1e
25 µm
1g
50 µm
1i
1f
1h
1k

antibodies were diluted 5 times. After another rinsing in PBS the slides were incubated with the appropriate FITC-conjugated antiserum and afterwards rinsed again in PBS. All incubations were done at room temperature for 45 minutes. Finally, sections were embedded in saturated Mowiol 4-88 in Citifluor (Citifluor Ltd, London).

As controls, for aspecific labelling of respectively the second and the first antibody, sections were incubated either with only the second antiserum or with normal mouse serum in stead of the anti-calmodulin antibody. Also as a control, sections of mericarps were incubated in antiserum treated with an excess of calmodulin isolated from spinach (Sigma).

Observations were made with a Nikon Labophot, using Nikon Fluor 20x/0.75, Leitz Fluor 50x/1.00 water and Nikon Plan 100x/1.25 oil objectives, or a Nikon Microphot-FXA, using Nikon Fluor 20x/0.75, Fluor 40x/0.85, PlanApo 60x/1.40 oil and PlanApo 100x/1.40 oil objectives, with automatic exposure using the Nikon UFX system. Data were recorded on Kodak Ektachrome P800/1600.

Localization of activated calmodulin

Activated calmodulin was visualized by fluphenazine fluorescence. Fluphenazine.2HCl (Serva) was added to the growth medium for carrot somatic embryos, or to tapwater for germinated zygotic embryos, in a final concentration of 2.10^{-5} M. After a minimum incubation time of 20 minutes fluorescence was observed with a Nikon Labophot UV-fluorescence microscope (BP 365/10, DM 400, LP 420, equipped with a 100 W mercury lamp) and recorded as described above.

Figure 1. Distribution of anti-calmodulin in cryosections of a carrot suspension culture before the initiation of embryogenesis. a. An overview at low magnification of the various distribution patterns indicated by the numbers 1 to 4. **b.** The bright field image of a. **c.** The distribution in a cell cluster consisting of highly vacuolated cells, comparable with number 4 in a. **d.** The bright field image of c. **e.** A proembryogenic mass with the highest signal confined to the most outer cell layer, comparable with number 1 in a. **f.** The bright field image of e. **g.** A proembryogenic mass with cells varying substantially in fluorescence intensity, comparable with number 3 in a. Note also the organelle bound presence of the signal (arrows). **h.** The bright field image of g. **i.** A proembryogenic mass with uniformly distributed fluorescence, low in intensity, over all cells, comparable with number 2 in a. **k.** The bright field image of i. All sections were incubated with the monoclonal antibody FF7.

RESULTS

Anti-calmodulin distribution during somatic embryogenesis

The development of carrot somatic embryos from proembryogenic masses to torpedo-shaped embryos was characterized by a conspicuous distribution of anti-calmodulin. In 2,4-D containing medium four patterns, differing in intensity and distribution of the fluorescent signal, were observed (Figs. 1a, 1b, numbers 1 to 4). In clusters of cells, consisting of large, vacuolated cells, all cells showed a fine punctate labelling which was scattered over the cytoplasm of the whole cell (Figs. 1c, 1d and 1a, number 4). The intensity of the signal was not consistent and varied between the cells with sometimes a strong fluorescence confined to the peripheral cells (Figs. 1e, 1f and 1a, number 1). In some proembryogenic masses differences in the intensity of labelling of the cytoplasm were present and some cells showed an organelle-bound fluorescence (Figs. 1g, arrows, 1h and 1a, number 3). Usually, however, proembryogenic masses had a weak and uniform signal (Figs. 1i, 1k and 1a, number 2).

In 2,4-D free medium the overall image of the distribution of the signal was more consistent. Shortly after the initiation of embryogenesis, proembryogenic masses with only one cell (Figs. 2a, 2b) or a few cells (Figs. 2c, 2d) with an organelle-bound fluorescence (arrows) were observed. Occasionally, the clusters with large vacuolated cells had a strong peripheral fluorescence (Figs. 2e, 2f). From the globular to the torpedo-shaped embryo, anti-calmodulin was most obviously present in the outer layer, the protoderm, of the embryo (Figs. 2g, 2h, 2i, 2k). It was typical that at this stage also the cells of the proembryogenic mass showed the organellebound fluorescence (Fig. 2l).

Higher magnifications revealed that

Figure 2. Distribution of anti-calmodulin in cryosections of a carrot suspension culture after the initiation of embryogenesis. **a.** A proembryogenic mass 1 d.a.i. Only one cell shows an organelle bound fluorescence (arrow), while the other cells are only weakly and uniformly labelled. **b.** The bright field image of a. **c.** A proembryogenic mass 2 d.a.i. A number of cells at the periphery of the proembryogenic mass contain the fluorescent organelles (arrows). **d.** The bright field image of c. **e.** A cluster consisting of highly vacuolated cells 2 d.a.i. with a cytoplasmic fluorescence restricted to the peripheral cells. **f.** The bright field image of e. **g.** A globular embryo showing the typical distribution of anti-calmodulin in somatic embryos. The highest fluorescence is present in organelles surrounding the nucleus of protoderm cells (arrow). At the base of the embryo two to three cell layers contain the signal. **h.** The bright field image of g. **i.** A heart-shaped embryo with anti-calmodulin labelling present in all cells of the protoderm. **k.** The bright field image of i. **l.** A globular embryo with the proembryogenic mass still attached to it. The fluorescent organelles are also present in the cells of the proembryogenic mass. All sections were incubated with the monoclonal antibody FF7.

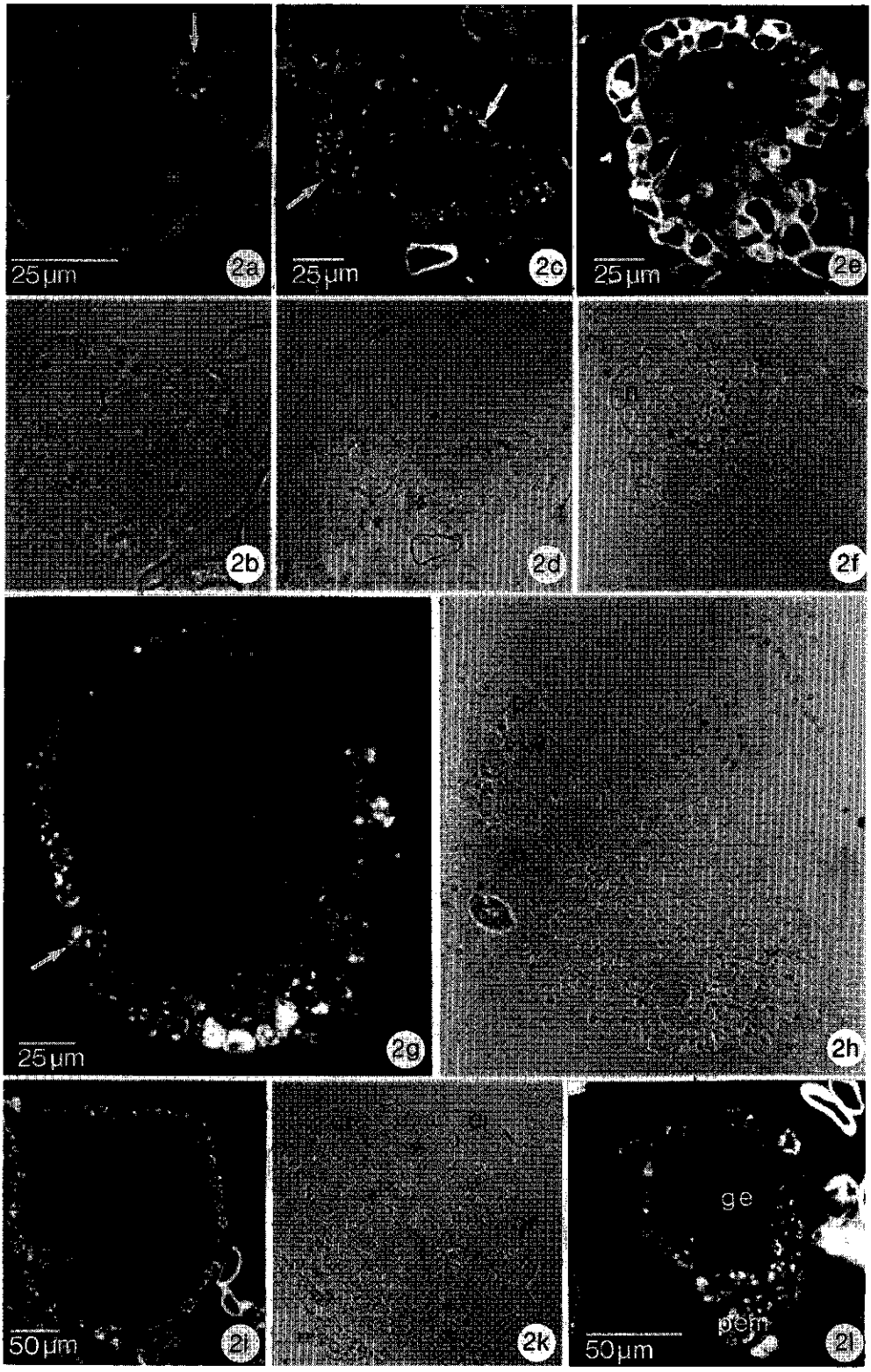
25 µm
2a
25 µm
2c
25 µm
2e
2b
2d
2f
25 µm
2g
2h
50 µm
2i
2k
ge
pem
50 µm
2l

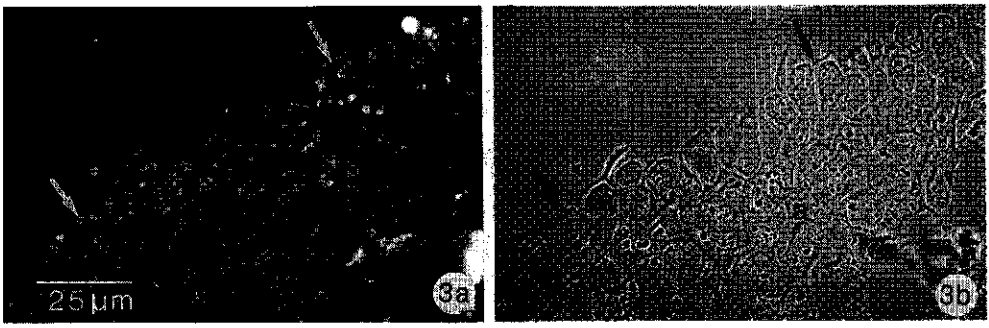

Figure 3. A high magnification image of the peripheral cell layers of a cryosection through a torpedo-shaped somatic embryo incubated with the polyclonal anti-calmodulin serum. **a.** Fluorescence image: the label is present prominently in amyloplasts in the protoderm. **b.** The bright field image of a. Arrows point to corresponding positions on both images.

Figure 4. Distribution of anti-calmodulin in immature seeds of carrot. **a.** A torpedo-shaped zygotic embryo showing the typical distribution of anti-calmodulin in zygotic embryos. No obvious differences are visible between different cell layers. **b.** The DIC image of a. **c.** A high magnification image of the hypocotyl of a torpedo-shaped zygotic embryo. Note the punctate fluorescence and the low intensity of fluorescence in the region of the future shoot meristem. Occasionally, the label was observed in nuclei but excluding the nucleolus (arrow) **d.** The DIC image of c. **e.** The distribution of anti-calmodulin in a cotyledon of a torpedo-shaped zygotic embryo. Note the absence of label in the nuclei (arrows) **f.** The bright field image of e. **g.** A longitudinal section through the middle of the concave side of an immature seed of carrot, showing the distribution of anti-calmodulin in the endosperm and seed coat. **h.** A longitudinal section through the top of an immature seed of carrot, showing the presence of a highly fluorescent, immature, seed coat, directly adjacent to the endosperm at the convex side of the seed. **i.** A high magnification image of the outer cell layer of the endosperm with label present in the cytoplasm and organelle-bound. **k.** The distribution of anti-calmodulin at high magnification in a cell of the middle of the endosperm (see the area outlined in the box in m). In this cell protein bodies are negative (arrowheads). **l.** The bright field image of k. The arrow in k and l points to a corresponding position in the two images. **m.** A longitudinal section through the middle of the convex side of the immature seed with a group of cells showing punctate presence of anti-calmodulin between less intensively labelled cells. The area outlined in the box is magnified in k. **n.** A longitudinal section through the base of the immature seed showing the presence of label within two to three cell layers at the periphery of the endosperm (arrows). **o.** Endosperm cells at high magnification showing annular fluorescence of protein bodies within the cells. **p.** The DIC image of o. **q.** High magnification of the threadlike distribution of fluorescence in the immature seed coat. Figures g, h, i, k, l and m are made of PEG sections, the others of cryosections. All sections were incubated with the monoclonal antibody FF7.

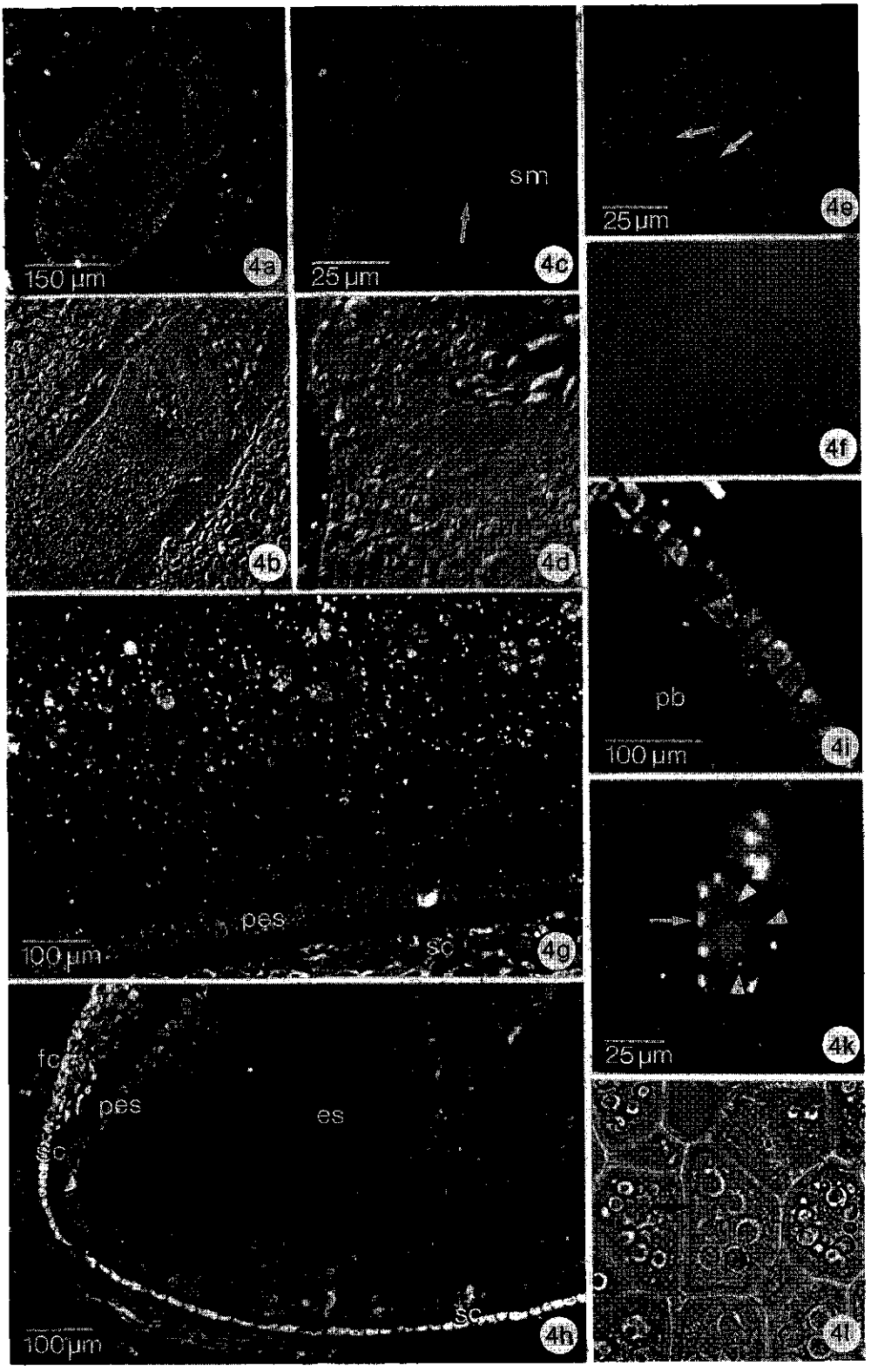
150 µm
4a
sm
25 µm
4c
25 µm
4e
4b
4d
4f
pb
100 µm
4l
pes
100 µm
sc
4g
25 µm
4k
fc
pes
es
sc
100 µm
4h
4l

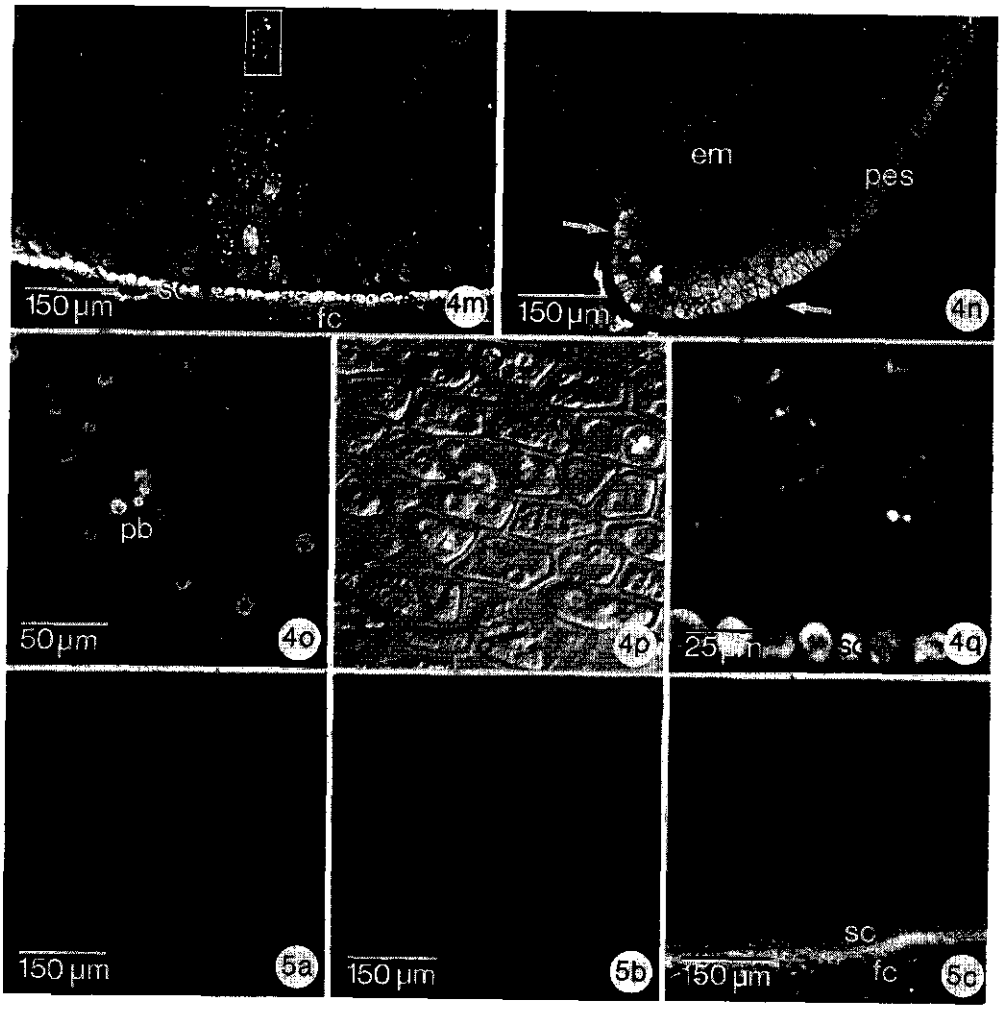

Figure 5. Control sections. Cryosections were made from the convex side of an immature seed of carrot and treated as indicated. **a.** First antibody replaced with PBS. **b.** First antibody replaced with normal mouse serum. **c.** First antibody incubated with an excess of calmodulin from spinach before applying to the section.

the strong signal in the protoderm cells came from the amyloplasts and proplastids surrounding the nucleus (Figs. 3a, 3b, arrows). The nature of the fluorescent organelle was, however, not always clear because, even at the highest magnification, it was not possible to discriminate between small vacuoles, which are current in these cells, and small plastids. Therefore, the presence of label also in these small vacuoles can not be excluded.

The intensity of the signal was improved by a fixation at high pH, but also a fixation at pH 7 gave acceptable results. Cryosections were, in most cases, superior to sections of

PEG embedded material if one compared the general preservation of cellular structure. Both methods, however, showed no difference in distribution nor intensity of the fluorescent signal. No striking differences were observed after immunolabelling with the polyclonal antiserum, directed against bovine calmodulin, or with the monoclonal antibody, directed against pea calmodulin.

In control sections proembryogenic masses and embryos were usually negative, although sometimes a weak signal was present. After using only the second antiserum no signal was observed in proembryogenic masses or embryos (results not shown). Replacing the first antibody with normal mouse serum resulted in embryos with a granular fluorescence in vacuoles of the future cortex of the embryo, among a weak signal from the other cells. The large vacuolated cells showed an organelle-bound or cytoplasmic fluorescence in both controls. The typical organelle-bound fluorescence of the protoderm, characteristic for somatic embryos, was never observed in control sections.

Anti-calmodulin distribution in immature seeds

The distribution of anti-calmodulin was observed in mericarps of about 3 to 6 mm with a well-developed cellular endosperm and an embryo of approximately 400 to 1000 μm in length.

In the zygotic embryo the fluorescent signal was distributed uniformly over the embryo with no obvious differences between the protoderm and other cell layers of the embryo (Figs. 4a, 4b). Higher magnification images revealed a punctate labelling in the cytoplasm, surrounding the nucleus or scattered over the cytoplasm (Figs. 4c, 4d and 4e, 4f). Nuclei were negative (Fig. 4e, arrows) or slightly positive with a negative nucleolus (Fig. 4c, arrow).

In contrast with the uniform distribution of the signal in the embryo, the distribution in the endosperm was eminently variable. In the mid region of the endosperm the outmost cell layer, in cereals often described as the aleurone layer, showed a strong fluorescence in comparison with the other cells of the endosperm. Five to six cell layers more inside the endosperm, almost without any signal, were followed by cells with a conspicuous, punctate fluorescence (Fig. 4g). In most cases the strong fluorescence of the outmost layer was restricted to one side of the endosperm. Another strongly fluorescent layer, directly adjacent to the endosperm, could be observed (Fig. 4h). This layer, the immature seed coat, forms the outer layer of the integuments between the two linked mericarps, but lies directly against the endosperm at the opposite side. Also the remnants of the integuments were strongly fluorescent.

At higher magnifications the differences between the various tissues became more clear. The strong signal of the outmost endosperm layer was localized in the cytoplasm. The nuclei were only faintly fluorescent, while nucleoli were negative. The peripheral, punctate fluorescence was also found in these cells (Fig. 4i). In the

centre of the endosperm the signal was most obvious in particles at the cell edge (Figs. 4k, 4l, arrow). The cytoplasm was only weakly stained. In the cell shown in figure 4k, large, round organelles, which, from their appearance and abundance were judged to be protein bodies (Jacobsen *et al.* 1976), were negative (Figs. 4k, arrowheads).

Occasionally, cells with the punctate fluorescence were found as a group, 2 to 3 cell layers wide and 8 to 9 cells long, oriented from the edge of the endosperm to the centre of it (Fig. 4m). At the micropylar region the strong fluorescence of the endosperm was present in 2 to 3 cell layers (Fig. 4n, arrows). In some, irregularly dispersed, parts of the endosperm the protein bodies had a strong annular fluorescence (Figs. 4o, 4p). If present, large vacuoles were always negative. The strong fluorescence of the immature seed coat had a threadlike appearance and was almost uniform in intensity (Fig. 4q).

Control sections were always much weaker in intensity than sections treated with anti-calmodulin serum. Sections treated with only the second antibody (Fig. 5a) or treated with normal mouse serum instead of the anti-calmodulin serum (Fig. 5b) were totally negative. Sections treated with anti-calmodulin serum pretreated with an excess of spinach calmodulin (Fig. 5c) showed a very reduced signal. Since in control sections through the pericarp a signal was always present in this part of the immature seed (Fig. 5c), we take this for non-specific labelling.

Anti-calmodulin distribution in germinated zygotic embryos

The distribution of anti-calmodulin in germinated zygotic embryos was strikingly different from the distribution during zygotic embryo development. From cotyledons to root tip most of the signal was present in the epidermis, especially in the region below the cotyledons (Figs. 6a, 6b). The shoot meristem did not show any noticeable fluorescence. In the cortex of the hypocotyl many nuclei were positive and a scattered punc-

Figure 6. Distribution of anti-calmodulin in cryosections of germinated zygotic embryos of carrot. **a.** Median longitudinal section of a seedling showing the distribution of anti-calmodulin in the cotyledons and hypocotyl. The highest signal is present in the epidermis. **b.** The DIC image of a. **c.** A high magnification of the hypocotyl. **d.** High magnification of an oblique sagittal section through the region just above the root tip, showing prominent labelling of the cytoplasm and vacuolar borders (arrows) of the epidermal cells. **e.** The DIC image of d. **f.** Oblique cross-section through the root tip. Note the organelle-bound fluorescence of the peripheral cell layers. **g.** The DIC image of d. **h.** Higher magnification of the area outlined in the box in f. Most of the signal is present in amyloplasts of the peripheral cell layers (arrows). **i.** The bright field image of h. All sections were incubated with the monoclonal antibody FF7.

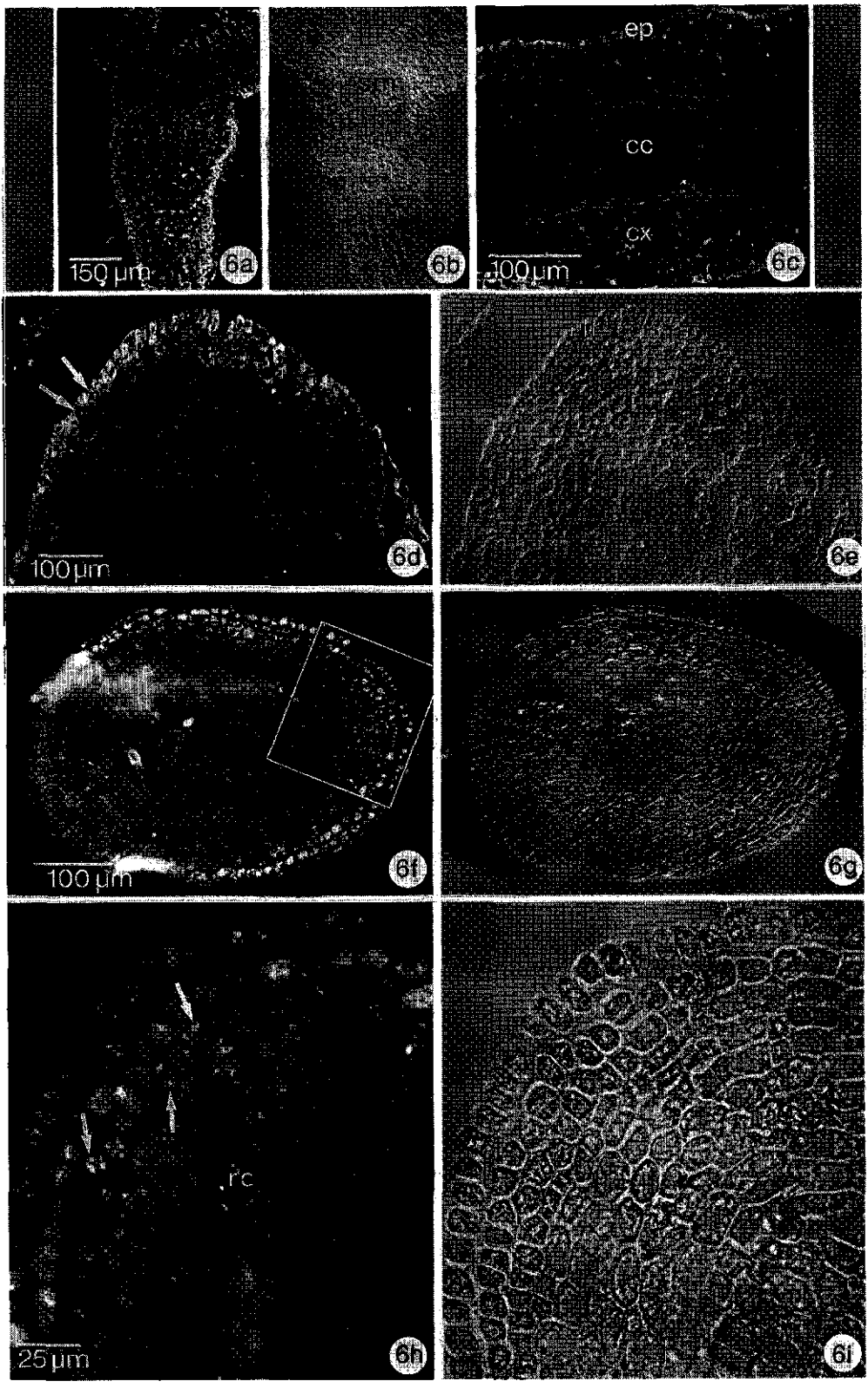
150 µm
6a
6b
ep
cc
cx
100 µm
6c
100 µm
6d
6e
100 µm
6f
6g
rc
25 µm
6h
6i

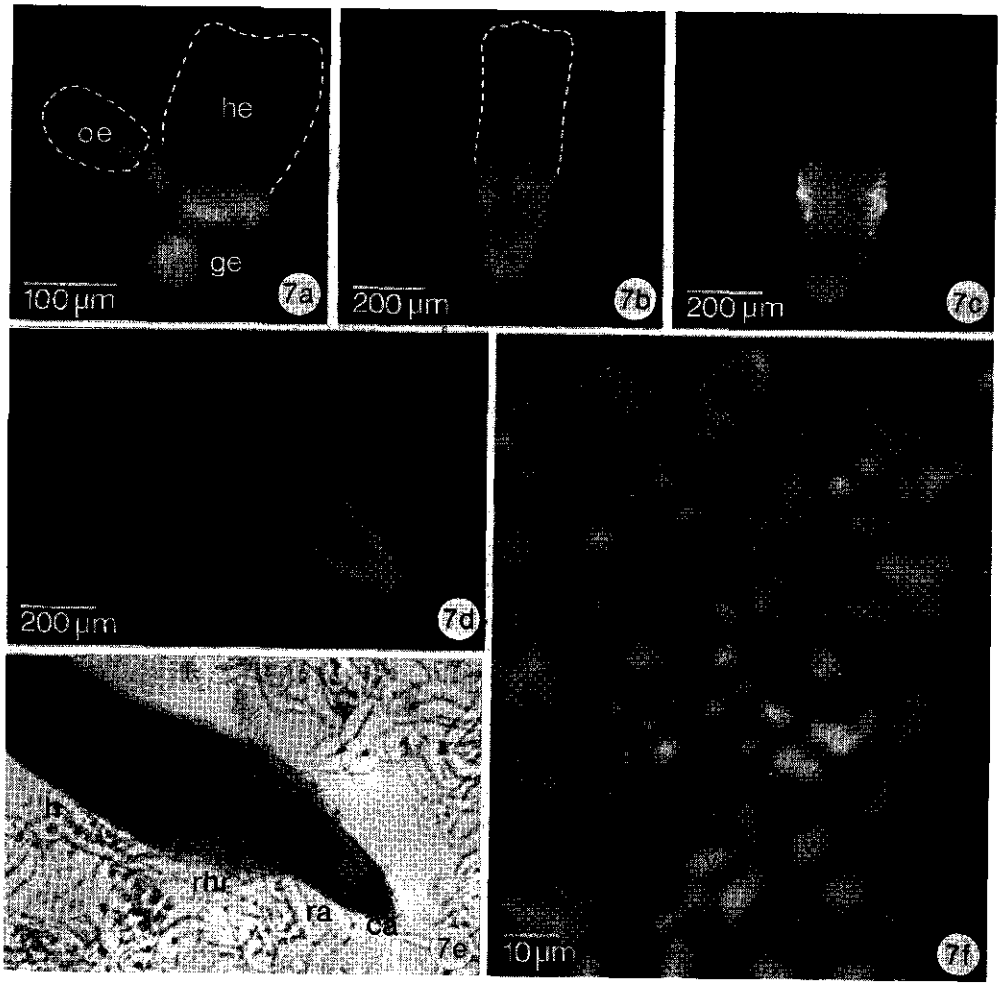

Figure 7. The distribution of activated calmodulin in somatic embryos of carrot visualized by fluphenazine fluorescence. **a.** The signal in a globular, oblong and heart-shaped somatic embryo. Note the change from overall present to a restricted presence in the root side. **b.** A torpedo-shaped embryo with a nearly uniformly fluorescent lower half. **c.** A torpedo-shaped embryo with a fluorescent lower part interrupted by a weakly fluorescent portion. **d.** The signal in the root of a germinated somatic embryo. Only the extreme root tip is fluorescent. **e.** Bright field image of d. **f.** A high magnification image of the signal present in the lower part of torpedo-shaped somatic embryos. The distribution suggest a presence of the fluorescence both in plastids and in vacuoles.

tate fluorescence was observed in these cells. Besides a stronger fluorescence of the epidermis no obvious signal was present in median sections of germinated embryos (Fig. 6c). The fluorescence of the epidermis was mainly localized in the cytoplasm, but had also a vacuolar portion (Fig. 6d, arrows).

The distribution of the signal in root sections through germinated embryos, with already a root length of a few millimetres, was very characteristic. Two to three peripheral cell layers were strongly fluorescent and the three to four adjacent cell layers showed an organelle-bound fluorescence (Figs. 6f, 6g). The more inner cells were not conspicuous in fluorescence. At a higher magnification it was observed that most peripheral cells possessed three to four organelles with a strong signal (Fig. 6h, arrows). From their appearance and location these organelles were judged to be proplastids or small amyloplasts (Figs. 6h, 6i).

Distribution of activated calmodulin during somatic embryogenesis

The overall distribution of activated calmodulin, visualized by fluphenazine fluorescence, has already been described in Chapter 2. Here we will mainly focus on the cellular localization. During the development of somatic embryos the localization of the signal changed from uniform in globular embryos to clearly polarized in oblong, heart-shaped and torpedo-shaped embryos (Fig. 7a). The size of the fluorescent region of torpedo-shaped embryos could be as large as the half of the embryo and could contain intervening regions with a less intense fluorescence (Figs. 7b, 7c). In germinated somatic embryos the signal was restricted to the root tip below the root hair region (Figs. 7d, 7e). Two cellular localizations were distinguished (Fig. 7f). The first was granular, in size comparable with plastids. These particles could be found scattered through the cell or organized around the nucleus. The second was larger, more comparable to vacuoles, and could be found as a single spot or as two to three spots linked by thin strands. Well-developed cotyledons of germinated somatic embryos possessed a strong, granular fluorescence (not shown).

Distribution of activated calmodulin in zygotic embryos

In contrast to the distinct polarized localization of fluphenazine fluorescence in torpedo-shaped somatic embryos, the signal from torpedo-shaped zygotic embryos was strikingly uniform (Figs. 8a, 8b). The fluorescence was localized in the cytoplasm and was not specifically organelle-bound.

Distribution of activated calmodulin in germinated zygotic embryos

The distribution of the fluphenazine fluorescence changed dramatically during the germination of zygotic embryos. The signal from zygotic embryos one day after incubation in water, to induce germination, closely resembled the signal from developing somatic embryos in the torpedo-shaped stage (Fig. 9a). From two days after the induction of germina-

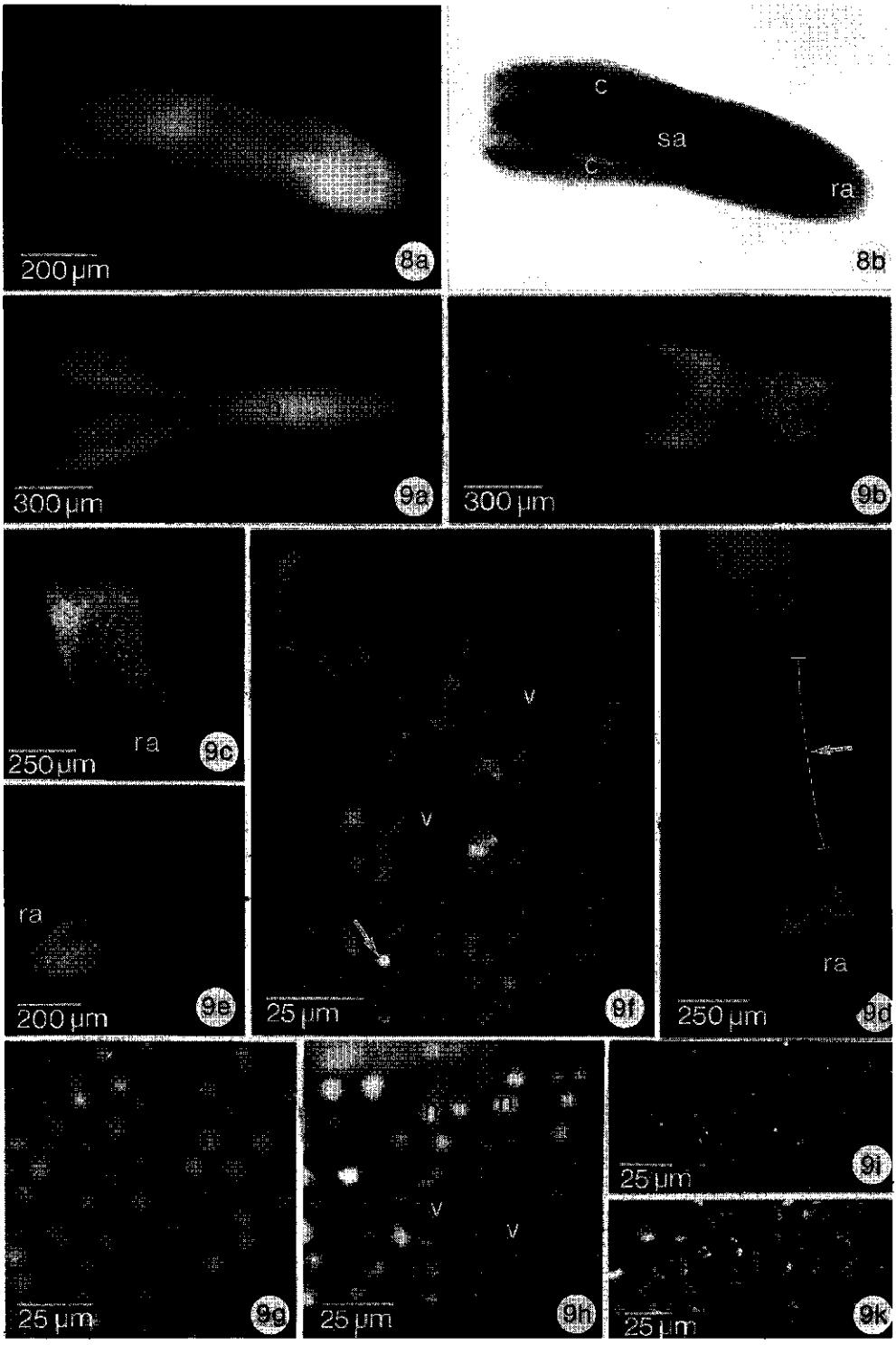
200 µm
8a
c
sa
c
ra
8b
300 µm
9a
300 µm
9b
ra
250 µm
9c
ra
200 µm
9e
v
v
25 µm
9f
ra
250 µm
9d
25 µm
9g
v
v
25 µm
9h
25 µm
9i
25 µm
9k

tion a distinctly polarized, organelle-bound fluphenazine fluorescence became visible. The strongest signal was present in the root tip, bordered by a small, faintly fluorescent region. This was followed by a hypocotyl and cotyledon region with a faint, cytoplasmic fluorescence (Fig. 9b). The size and the location of the strongly and faintly fluorescent regions of germinated zygotic embryos varied between the various specimens observed. The extreme tip of the root was sometimes very faint (Fig. 9c) and the non-fluorescent region could reach a significant size (Fig. 9d, arrow). In the hypocotyl region of these embryos a granular fluorescence appeared. In germlings, about five days after induction of germination, the fluphenazine fluorescence was restricted to the extreme root tip (Fig. 9e).

At the cellular level four different patterns, each characteristic for a defined region of the germinated embryo, were observed. In the root tip the fluorescent organelles were localized around the nucleus and had the size of plastids (Fig. 9f, arrow) or small vacuoles (Fig. 9f). In some cells the fluorescent spots appeared to be linked by thin strands. The region directly adjacent to the root tip was characterized by large, strongly fluorescent, spherical organelles, most probably the nuclei (Fig. 9g). The transition between these two regions was gradual (Fig. 9h). A few small spherical fluorescent granules were observed in the cells of the very faintly fluorescent region adjacent to the brightly fluorescent root tip (Fig. 9i). In the fluorescent region of the hypocotyl larger strongly fluorescent particles were observed (Fig. 9k).

Figure 8. The distribution of activated calmodulin in isolated zygotic embryos visualized by fluphenazine fluorescence. **a.** Fluorescence image. Note its uniform distribution. **b.** Bright field image of a.

Figure 9. The distribution of activated calmodulin in germinated zygotic embryos visualized by fluphenazine fluorescence. **a.** Shortly, 1 day, after the induction of germination. The signal is low and uniformly present. **b.** Two days after the induction of germination. The highest signal is present in the lower part of the embryo, with a weaker root tip. **c.** The lower part of a germinated zygotic embryo with fluorescent regions sharply delineated from the bordering negative regions. **d.** The lower part of a germinated zygotic embryo with a very large non-fluorescent region (arrow) between two regions with a high fluorescence. **e.** The root tip of a seedling some five days after induction of germination. Only the extreme root tip is fluorescent. **f.** High magnification of the signal present in the root tip of germinated zygotic embryos. The distribution suggests a presence of the fluorescence both in plastids (arrow) and in vacuoles. Compare with Fig. 7f. **g.** High magnification of the part of the root just above the part shown in f. The signal is confined to nuclei. **h.** High magnification of the border between the regions shown in Fig. f and Fig. g. **i.** High magnification of the weakly stained region between two highly fluorescent regions as shown in Fig. d. A weakly punctate fluorescence is present. **k.** Hypocotyl of a germinated zygotic embryo, some days after induction of germination, with a granular fluorescence.

DISCUSSION

The overall distribution of calmodulin in somatic embryos of carrot differs strikingly from the overall distribution in zygotic embryos of carrot. Immunolocalization of calmodulin revealed a high concentration of calmodulin located in the protoderm of somatic embryos. In zygotic embryos calmodulin was found to be evenly distributed over all cell layers. In germinated zygotic embryos, however, a specific localization of calmodulin was again observed with a higher amount of calmodulin in the peripheral layers of the young seedling. At the cellular level, calmodulin was found predominantly in plastids in somatic embryos. In zygotic embryos, calmodulin was present in the cytoplasm at a low, evenly distributed, level with higher amounts in small organelles, which were found scattered over the cytoplasm. In germinated zygotic embryos, calmodulin was present in the highest amount in amyloplasts in the peripheral layers of root sections.

The studies in which fluphenazine was used as a fluorescent probe for the localization of activated calmodulin also revealed a striking difference in localization between somatic and zygotic embryos and a resemblance between the localization during somatic embryogenesis and during zygotic embryo germination. A distinct polarized localization was observed in somatic embryos and young seedlings, but activated calmodulin was evenly distributed during the growth of zygotic embryos. In the base of somatic embryos and the root tip of young seedlings the cellular distribution was comparable. The fluorescent signal came from organelles, which sometimes were linked by small strands, surrounding the nucleus. The signal with fluphenazine appeared predominantly to be of vacuolar origin, although some cells possessed a signal which strongly suggested a localization in plastids (Figs. 7f and 9f). Occasionally nuclei stained positively (Fig. 9g).

The differences between the results obtained by either fluphenazine application or immunocytochemical techniques might be a direct result of the method of visualization. For immunolabelling the tissue was fixed and then processed for sectioning and incubation with antibodies. It is clear from other studies (e.g. Melan & Sluder 1992) that during this procedure proteins can be redistributed or differentially be extracted. A lack of calmodulin in vacuoles after immunolabelling might be the result of loss from the vacuole or a precipitation on the tonoplast. In working with fluorescent probes it should always be kept in mind that, in many cases, these probes are preferentially transferred to the vacuole (Oparka & Hawes 1992). Although a preferential accumulation of fluphenazine has never been reported before, the distinct vacuolar and nuclear site of localization could be the result of dye accumulation. As fluphenazine binds to calmodulin on the same position as calmodulin-binding proteins it has to compete with them in binding. If fluphenazine releases calmodulin from calmodulin-binding proteins present in the tonoplast and spreads out in the vacuole, it will lead to an

overall signal from this organelle.

In spite of the above mentioned drawbacks, we think it feasible to state that the amount and distribution of calmodulin vary strongly between different cells of one organism. Therefore, the action of calmodulin can directly be controlled by its level and distribution (see also Allan & Hepler 1989, Trewavas 1991) in contrast with the opinion of others (see the review by Poovaiah 1985) who state that the amount of calmodulin is never a limiting factor for its action. A tissue specific difference of calmodulin amount was also described for pea seedlings by Allan and Trewavas (1986), for a number of plant species by Lin *et al.* (1986), and for mays seedlings by Stinemetz *et al.* (1987). They all found that calmodulin is present in the highest amount in root tips. According to Poovaiah *et al.* (1987) root tips contain up to 4 times more calmodulin as compared to the root base.

All reports on calmodulin localization after tissue destruction described a predominantly cytoplasmic localization of calmodulin. Here, and in other immunocytochemical studies, an obvious organelle-bound localization was revealed. Butcher & Evans (1986) found calmodulin localized in protein body like organelles surrounding the nucleus in pea roots. Dauwalder *et al.* (1986) described a vacuolar presence of calmodulin and a general association of calmodulin with plastids. An explanation for this difference in calmodulin localization could be the presence of a loosely bound or easily extractable calmodulin in these organelles which could be lost during tissue destruction and organelle isolation and would increase the cytoplasmic portion (see also Van Eldik & Watterson 1985, Andreev *et al.* 1990).

The presence of calmodulin in plastids implies a role for calmodulin in starch biosynthesis and degradation during plant growth and differentiation (Mitsui *et al.* 1984, Preusser *et al.* 1988, Dreier *et al.* 1992), possibly by reversible, Ca^{2+} dependent, phosphorylation of proteins as was described for amyloplasts of sycamore cells (Ranjeva & Boudet 1987). In *Nicotiana tabacum* and *Datura innoxia* cell cultures a protein kinase was isolated from plastids and the activity of this enzyme correlates with rapid cell proliferation and starch accumulation (Böcher *et al.* 1985). Embryogenesis and germination go together with changes in the amount of starch and plastid differentiation and development (Halperin & Jensen 1967, Tisserat *et al.* 1979, Wurtele *et al.* 1988). Plastids are, together with vacuoles, the most variable structures during morphogenesis (Buvat 1989). Therefore, a first step in somatic embryogenesis might be a change in starch metabolism modulated by calmodulin. Michaux-Ferriere *et al.* (1992) described a change in starch composition of plastids during somatic embryogenesis of *Hevea brasiliensis*. A change in the amount of calmodulin during germination is described by Cocucci & Negrini (1991) for *Phacelia tanacetifolia* seeds. These authors linked calmodulin increase with the metabolic reactivation during germination. Another possibility is considered by Dauwalder *et al.* (1986) who con-

nected the presence of calmodulin in plastids, in the columella of the root cap, with signalling of changes in root orientation (see also Poovaiah *et al.* 1987).

The presence of calmodulin in the vacuole might be connected with the role of the vacuole in the regulation of $[Ca^{2+}]_c$. The vacuole is considered to be the most important Ca^{2+} store in plant cells (Evans *et al.* 1991, Johannes *et al.* 1992) and changes in $[Ca^{2+}]_c$ are considered to be under the control of a Ca^{2+}/nH^+ antiporter in the tonoplast which is greatly stimulated by calmodulin (Andreev *et al.* 1990).

A preferential presence in the protoderm during somatic embryogenesis is not restricted to calmodulin. Kiyosue *et al.* (1992) describe the presence of an embryogenic protein of carrot which appears in the protoderm of torpedo-shaped embryos after treatment with ABA. Sterk *et al.* (1991) found an almost exclusively protodermal presence of mRNA coding for a lipid transfer protein during carrot embryogenesis. Also concanavalin A-stainable glycoproteins are restricted to the protoderm in somatic embryos of carrot (Lo Schiavo *et al.* 1990). These facts point to the importance of the development of the protoderm during embryogenesis, as was also stated by Bruck & Walker (1985), Mayer *et al.* (1991) and De Jong *et al.* (1992) and is in strong contradistinction to the statement of Halperin (1966) that somatic embryos do not develop a defined protoderm.

In immature seeds calmodulin was conspicuously present in the outer layer of the endosperm. GP80, a glycoprotein isolated from carrot fruits, was also found predominantly in this layer (Torii *et al.* 1991). In Graminales the outer layer of the endosperm forms the aleurone layer, which is responsible for the hydrolysis of carbohydrates stored in the inner 'starchy' endosperm at germination (for review, see Jacobsen 1984). Ca^{2+} is involved in the regulation of the synthesis and activity of α-amylase in the barley aleurone (e.g. Bush *et al.* 1989). With regard to this the observation of Tretyn & Kopcewicz (1988) in the aleurone layer of oat is also interesting. Using CTC fluorescence and X-ray microanalysis these authors found a high level of Ca^{2+} to be present specifically in the aleurone layer. The distribution of calmodulin in the endosperm might point to a role for calmodulin in starch breakdown during germination of carrot seeds.

Carrot somatic embryogenesis is considered to be a good model system for zygotic embryogenesis (e.g. Choi & Sung 1989). From our results, however, it can be concluded that, at least regarding the distribution of calmodulin, striking differences exist between somatic and zygotic embryos and that strong similarities exist between somatic embryogenesis and zygotic embryo germination.

CHAPTER 4

DIGITONIN-AIDED LOADING OF FLUO-3 INTO EMBRYOGENIC PLANT CELLS

A.C.J. TIMMERS[1], H.-D. REISS[2] & J.H.N. SCHEL[1]

[1]Department of Plant Cytology and Morphology, Agricultural University, Arboretumlaan 4, 6703 BD Wageningen, The Netherlands
[2]Zellenlehre, Universität Heidelberg, Im Neuenheimer Feld 230, D-6900 Heidelberg, Federal Republic of Germany

Reprinted, with permission, from *Cell Calcium* 12:515-521 (1991)

SUMMARY

This paper describes a method to load embryogenic plant cells with fluo-3 in its cell impermeant form with the aid of digitonin. Attempts to load cells with fluo-3 AM were all unsuccessful. Presumably the indicator is cleaved outside the cells and can not penetrate in its acidic form. At a low pH fluo-3 enters the plant cells but normal Ca^{2+} homeostasis seems to be disturbed. Successful loading of fluo-3 was achieved by adding 0.1% digitonin during incubation with the Ca^{2+}-indicator. A bright fluorescence was observed in the epidermal layer of heart-shaped and torpedo-shaped somatic embryos of carrot with confocal scanning laser microscopy. Vacuoles were always without fluorescence which indicates that the dye, after loading, remains in the cytosol and does not leak out. The fluorescence intensity was sensitive to treatments with A23187 and EGTA. We conclude that fluo-3 can effectively be loaded, with the aid of digitonin, into plant embryogenic cells in liquid culture. Therefore we expect this technique to be very useful for the study of changes in cytosolic free Ca^{2+} levels during plant growth and development.

INTRODUCTION

For a detailed analysis of the distribution of free cytosolic Ca^{2+} with fluorescent indicators in living, intact plant cells in multicellular tissue, confocal scanning laser microscopy is the method of choice. Most CSLMs are equipped with an argon-ion laser with excitation wavelengths only in the visible region of the spectrum. From the recently developed long wavelength indicators (Minta *et al.*

1989), fluo-3 has the best fluorescence characteristics which makes it the most suitable dye for the study of Ca^{2+} with CSLM.

Most Ca^{2+} indicators can easily be loaded into animal cells in the form of acetoxymethyl (AM) esters (Tsien *et al.* 1985). After intracellular cleavage by esterases, Ca^{2+} binds to the free acid. Unfortunately, loading of plant cells with these AM esters still encounters some serious problems, such as extracellular ester hydrolysis (Cork 1985) or incomplete internal dye hydrolysis (Brownlee & Wood 1986). Methods of dye loading into plant cells are microinjection, electroporation or loading at low pH of the free acid of the indicator. Most plant cells possess a large vacuole which makes the cytoplasm, surrounding the vacuole, a small target for microelectrode insertion (Brownlee 1987). Electroporation is disruptive, and therefore, may well change both cytosolic Ca^{2+} levels and the cell's ability to regulate them (Gilroy *et al.* 1986). Loading at low pH has only been described for protoplasts (Bush & Jones 1987).

The present study describes the application of fluo-3 as an indicator of cytosolic Ca^{2+} in plant cells. The above mentioned problems were circumvented by using digitonin to permeabilize the plasma membranes, as was reported earlier for animal cells (Elias *et al.* 1978, Fiskum 1985). Because we are interested in the role of Ca^{2+} in plant embryogenesis, CSLM of carrot embryogenic cells was performed. These cells are easily maintained as a liquid culture and embryogenesis can be initiated and synchronized by transfer of proembryogenic masses from an auxin-containing to an auxin-free medium. Somatic embryos progress through the successive stages of globular, heart-shaped, and torpedo-shaped embryos comparable to their zygotic counterparts (Sung *et al.* 1984)

MATERIALS AND METHODS

Plant material and culture conditions

For all experiments a liquid cell culture of *Daucus carota* L. cv. Flakkese sg 766 Trophy, in B5 medium (Gamborg *et al.* 1968; Ca^{2+} concentration 1 mM), was used. Culture conditions and initiation of embryogenesis were essentially the same as described earlier (De Vries *et al.* 1988b). After initiation of embryogenesis, liquid cell cultures were maintained in Erlenmeyer flasks on a rotary shaker or in Petri dishes.

Dye loading protocols

Four different loading protocols for fluo-3 were tested.

1. Incubation of the culture with 20 μM fluo-3 AM (Molecular Probes Inc., Eugene, Oregon, USA; stock 1 mM in DMSO; Williams *et al.* 1990), added to the growth medium, for 1 to 7 hours or overnight.
2. as 1 with 0.02% Pluronic F-127 (according to the protocol of Molecular Probes; Poenie *et al.* 1986).
3. Incubation of the culture with 20 μM fluo-3 (Molecular Probes) at pH 4.5 as described by Bush and Jones

(1987) for indo-1. Dye loading was tested in the loading medium described by these authors or in B5 medium at pH 4.5. After loading cells were rinsed in B5 medium, pH 5.8.
4. Incubation of cells with 5, 10 or 20 μM fluo-3 in B5 medium supplemented with 0.025, 0.05 or 0.1 % digitonin for 1-2 hours. After a quick rinse in B5 medium (to remove the digitonin) the cells were incubated in B5 medium with fluo-3 for at least half an hour. Finally the cells were transferred into B5 medium without fluo-3.

For loading with chlorotetracycline (Sigma; CTC) embryos were incubated in B5 medium with 1.10^{-4} M CTC for 20 min and afterwards shortly rinsed in fresh B5 medium (Chapter 2). The specificity of the fluorescence signal for Ca^{2+} was checked by incubation in B5 medium supplemented with 1.10^{-6} M A23187 (Serva, stock $2.5.10^{-3}$ M in ethanol) or 1 mM EGTA (Sigma) and 1.10^{-5} M A23187.

Confocal microscopy

The confocal scanning laser microscope of Leica Lasertechnik GmbH (Heidelberg, FRG) was used in this study. The microscope was equipped with a multiline argon ion laser of which the 488 and 514 lines can be selected. For fluo-3 and CTC the 488 line was used. The emitted light passed two filters, BP 520-560 and LP 515, to reduce autofluorescence to near limit detection levels. Cells were observed with a 25-oil/0.75 (theoretical section thickness 2-3 μm), 40-oil/1.3 (theoretical section thickness 1-1.5 μm)or 100-oil/1.32 (theoretical section thickness 0.5-0.8 μm) objective in one or more optical sections which were stored in a RAM or directly on optical disk. From most embryos also the transmitted light signals were collected and stored. For additional information about the CSLM see Knebel *et al.* (1989).

RESULTS

All attempts to load the embryogenic cells with fluo-3 AM were without success. After 2 to 3 hours of incubation with fluo-3 AM only a slight increase in fluorescence could be observed (Fig. 1) which did not change even after an overnight incubation. The addition of Pluronic F-127 did not improve the results. Hand made 1 mm sections of torpedo-shaped embryos were used to check whether dye loading was prevented by an outer cuticle as was described for maize coleoptiles (Williams *et al.* 1990). A marked increase of fluorescence of plastids, mainly in the protoderm of the embryo, was observed after this action but no changes in fluorescence intensity could be provoked by adding either A23187 or EGTA. Although fluo-3 AM is hardly fluorescent, after a prolonged incubation background fluorescence increased strikingly.

After loading at pH 4.5 a strong fluorescence was observed in the cytoplasm of a collection of cells at the periphery of some embryos. These cells were in direct contact with the coverglass. Small embryos, which had no contact with the cover-

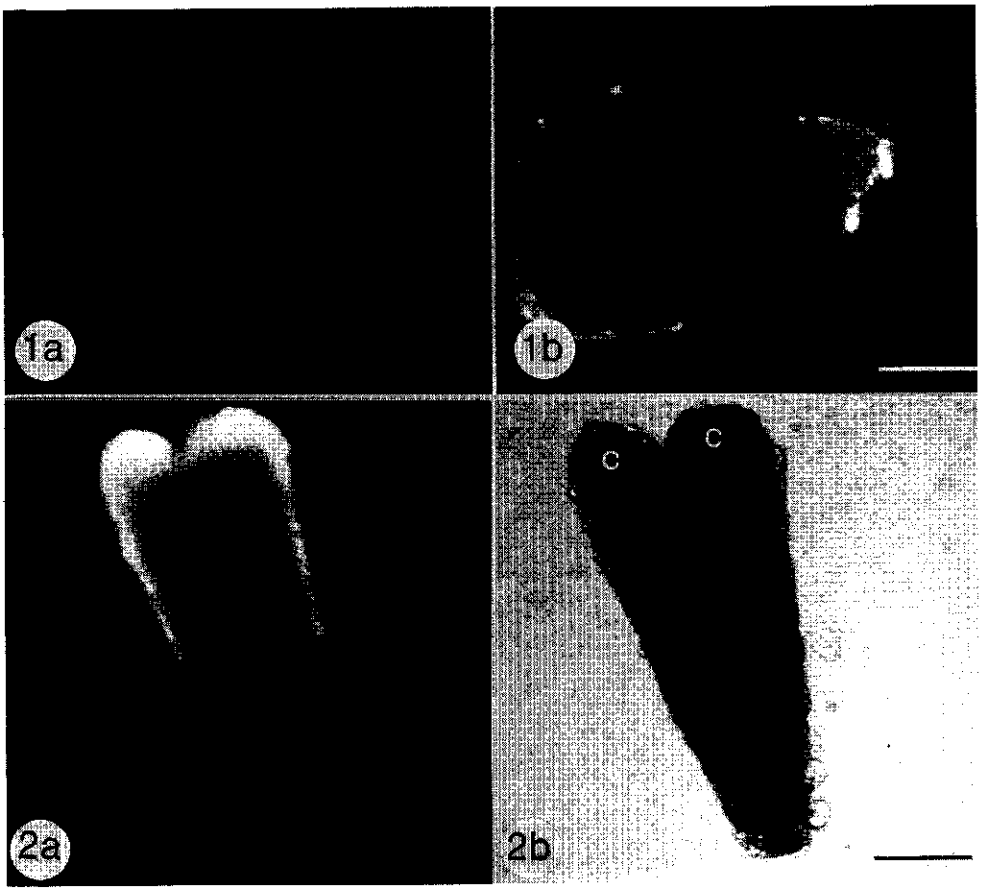

Figure 1. Heart-shaped somatic embryo before dye loading (**a**) and three hours after incubation in 20 μM fluo-3 AM (**b**). Only a slight increase in fluorescence could be observed. Scale bar 50 μm.

Figure 2. Torpedo-shaped somatic embryo loaded with fluo-3 in the presence of 0.1% digitonin. **a.** Confocal fluorescence image. **b.** Bright field image. Note the gradient in fluorescence intensity from cotyledons to base. Scale bar 100 μm.

glass, showed no signal. From this we concluded that, although dye loading is possible at pH 4.5, apparently the normal Ca^{2+} homeostasis is disturbed. The observed fluorescence signal might be the consequence of the pressure caused by the coverglass.

Incubation of embryos in growth medium supplemented with 20 μM fluo-3 and 0.1% digitonin resulted in a bright and defined, easily detect-

able fluorescent signal. The signal was most intense in the protoderm of the torpedo-shaped embryos (Fig. 2). Most embryos in this stage possessed a declining gradient in fluorescence intensity from cotyledons to base. Hardly any signal could be detected from the interior cells of the embryos when the voltage and offset values of the CSLM were optimal for collecting the signal of the protoderm. At maximum voltage the interior cells could faintly be seen. Higher magnifications of the surface cells of torpedo-shaped embryos revealed the cytosolic distribution of the fluorescence (Fig. 3). Cell walls and vacuoles were negative. In most cells nuclei were strongly fluorescent. Very prominent was the fluorescence of the nucleolus. The intensity of the fluorescence of the cytoplasm in one cell was not uniform and stronger fluorescent regions could be observed. In younger stages all embryogenic cells showed an intense signal

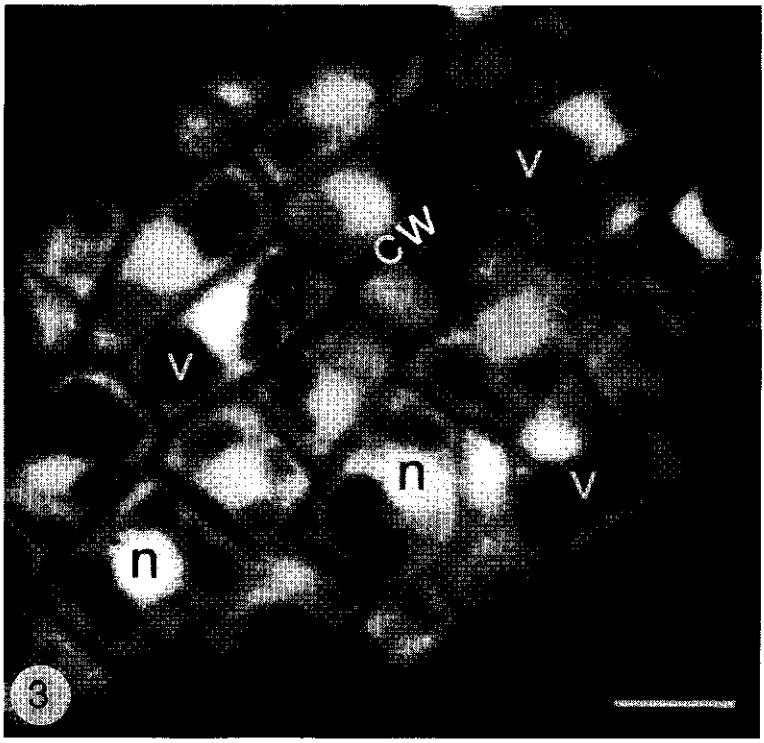

Figure 3. Optical section through the protoderm of a cotyledon from a torpedo-shaped somatic embryo loaded with fluo-3. Fluorescence is absent in cell walls and vacuoles while nuclei are strongly positive. Scale bar 10 μm.

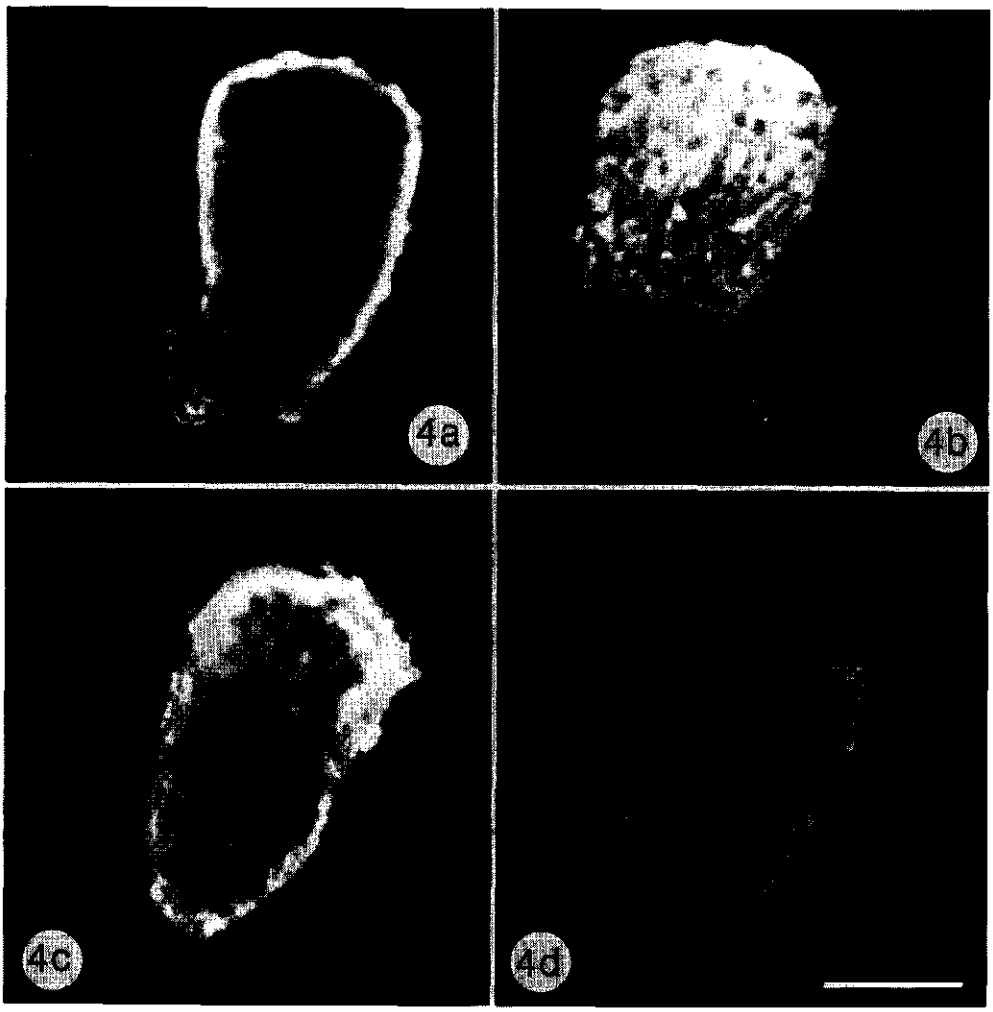

Figure 4. Confocal images of the centre of early torpedo-shaped somatic embryos loaded with fluo-3. **a.** Before incubation in 1.10^{-5} M A23187. **b.** The same embryo as in a after incubation in 1.10^{-5} M A23187 for one hour. The difference between fluorescence intensity in protoderm cells and interior cells has disappeared. **c.** Before incubation in A23187 and 1 mM EGTA. **d.** The same embryo as in c after incubation in A23187 and 1 mM EGTA for one hour. Although the overall intensity of fluorescence is diminished, the distinct distribution of the signal remains. Scale bar 150 μm.

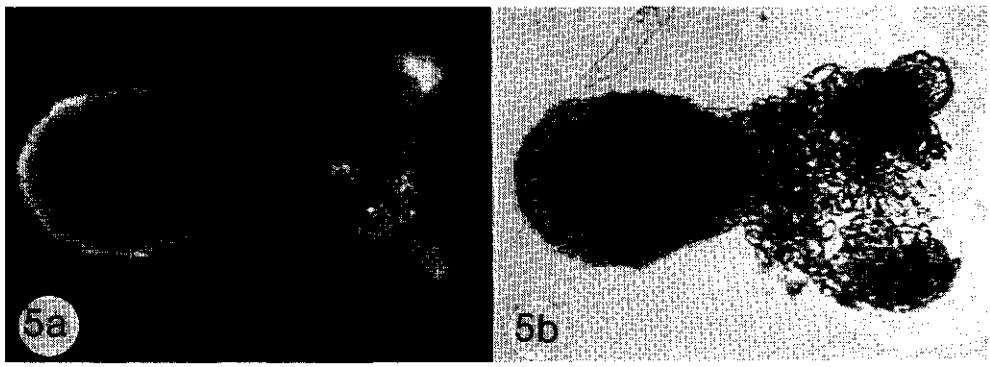

Figure 5. Fluorescence signal in a late globular staged embryo incubated with CTC, showing a similar labelling pattern as with fluo-3. **a.** Confocal fluorescence image. **b.** Bright field image. Scale bar 100 μm.

which was about 2 to 3 times higher than the signal from proembryogenic masses, the progenitor cells of the somatic embryos (results not shown). In later stages the strong difference between the fluorescence intensity of protoderm and interior cells was quite obvious.

High concentrations of digitonin (more than 0.1%) have been reported to disrupt the intracellular membranes (Fiskum 1985). Therefore, both for fluo-3 and digitonin the lowest concentrations which resulted in a good signal were determined. These were 20 μM fluo-3 and 0.1% digitonin respectively. Lower concentrations of both chemicals resulted in a lower signal. Minimum incubation time for a distinct signal was approximately 20 minutes. Postincubation in medium with fluo-3 but without digitonin had a positive effect on fluorescence intensity. When, during incubation with digitonin, Petri dishes were placed on a rotary shaker no fluorescent signal appeared. Shaking during the postincubation had no effect on the intensity of the signal. The best loading protocol for fluo-3 into somatic embryos proved to be an incubation in B5 medium supplemented with 20 μM fluo-3 and 0.1% digitonin for 1 hour, without shaking. Longer incubation times, till 2 hours, did not modify the distribution of fluo-3 fluorescence. Afterwards the embryos were carefully rinsed in B5 medium and postincubated in B5 medium with 20 μM fluo-3 for half an hour. After three rinses in B5 medium the embryos were observed with the CSLM.

After prolonged culture, redistribution of the dye was never observed. Even 24 hours after dye loading no vacuolar fluorescence, which would be the result of leakage or transport of the indicator into the vacuoles, could be detected. The embryos showed no visible damage, which might have resulted from the treat-

ment with digitonin. Early staged embryos, loaded with fluo-3 in the presence of digitonin, normally developed into torpedo-shaped embryos.

The signal was sensitive to treatments with A23187 and EGTA (Fig. 4). Incubating fluo-3 loaded embryos in medium with 1.10^{-5} M A23187 resulted in strongly fluorescent embryos without a clear difference in fluorescence intensity between protoderm and interior cells. One hour in medium with A23187 and 1 mM EGTA was sufficient to decrease the fluorescence intensity significantly, but the distinct distribution of the signal persisted.

Embryos, incubated in medium with CTC, showed the same overall distribution of fluorescence as with fluo-3 (Fig. 5). High magnification images were unfortunately not possible with CTC because of its fast bleaching.

DISCUSSION

The study of the intracellular distribution of free Ca^{2+} in plant cells is, in most cases, restricted to protoplasts (e.g. Bush & Jones 1987), single cells (Clarkson *et al.* 1988) or linearly arranged cells (Hepler & Callaham 1987). Williams *et al.* (1990) were the first to report the use of fluo-3 AM for the localization of Ca^{2+} in a multicellular, intact plant tissue, in combination with CSLM. They discussed and showed the advantages of the use of CSLM, in comparison with conventional wide-field microscopy, for the study of Ca^{2+} with fluorescent indicators. From their study it appeared that for effective dye loading in maize coleoptile tissue, the outer waxy cuticle must be removed. This resulted in a difference in loading capacity of cells caused by differences in the effectuality of cuticle removal. For our system, carrot somatic embryos, attempts to load fluo-3 AM were all unsuccessful. Sectioning of the embryos, to make the cells more accessible to the indicator, resulted in an increase of autofluorescence but did not promote the entry of the dye into the cells. The addition of Pluronic F-127, reported to improve dye uptake (Poenie *et al.* 1986), had no influence on dye loading. From the pronounced increase of fluorescence of the medium we conclude that fluo-3 AM is cleaved outside the cells, probably by esterases within the cell wall (Cork 1985), and can not enter the cells in its free acidic form. An attempt to load embryogenic cells with fluo-3 at low pH was only partially successful. The cells took up the dye, but only stressed or damaged cells showed a visible fluorescent signal.

This study has shown that embryogenic cells of carrot can effectively be loaded with fluo-3, if a low concentration of digitonin is added to the incubation medium. Digitonin is a steroid glycoside which forms insoluble complexes with cholesterol and other ß-hydroxysterols in the plasma membrane (Akiyama *et al.* 1980). This results in a major disordering of the lipid bilayer which can be visualized by electron microscopy as 4-5 nm pits in the external face of the plasma membrane (Seeman *et al.* 1973). In animal cells it has been used to selectively disrupt the plasma

membrane, which has a high cholesterol/phospholipid ratio, without disrupting intracellular membranes which have relatively little cholesterol (Colbeau *et al.* 1971). The minimum level of digitonin needed to permeabilize the animal plasma membranes for ions and molecules falls within the range of 0.005-0.10% (w/v). These levels have apparently little or no effect on the functional integrity of the endoplasmic reticulum membranes and do not alter Ca^{2+} uptake or distribution (Fiskum 1985). We have shown that similar procedures can be used to optimize fluo-3 loading into plant cells. When loaded the indicator remains in the cytosol and does not move into the vacuole as was observed after loading fluo-3 AM in the maize coleoptiles (Williams *et al.* 1990). The treatment of the cells with digitonin does not prevent their normal development into somatic embryos which indicates that the cells are still vital and in a good condition. The advantage of using the free acidic form of the dye instead of its ester is that the concentration of the indicator is not dependent on the esterase activity of the loaded cells. Differences in fluorescence intensity caused by possible differences in dye concentration are in this case very unlikely. From the confocal microscope images it is obvious that the protoderm of advanced embryogenic stages possesses a higher concentration of free cytosolic Ca^{2+} than the other cells of the embryos. Shortly after initiation of embryogenesis, embryogenic structures with a, relatively, high concentration of Ca^{2+} become visible. This points to a specific role of Ca^{2+} in carrot somatic embryogenesis as has been shown also by other evidence (Jansen *et al.* 1990).

The results obtained with CTC confirm the results obtained with fluo-3. Problems with penetration of the indicator into plant cells are not reported for CTC. As both indicators give comparable results, this adds to the validity of the presented loading protocol of fluo-3 into plant cells with the aid of digitonin.

The presented technique of dye loading makes it possible to study changes in cytosolic Ca^{2+} in response to stimuli which affect embryogenesis. Preliminary results (not shown) indicate a change in Ca^{2+} distribution resulting from the addition of 2,4-D. Therefore, we expect this technique to be very useful for the study of free cytosolic Ca^{2+} distribution in response to several environmental stimuli in living, unfixed and intact plants.

CHAPTER 5

LOCALIZATION OF CALCIUM DURING SOMATIC EMBRYOGENESIS OF *DAUCUS CAROTA* L.

A.C.J. TIMMERS & J.H.N. SCHEL

Department of Plant Cytology and Morphology, Agricultural University, Arboretumlaan 4, 6703 BD Wageningen, The Netherlands

Partially published in : Karssen, C.M., van Loon, L.C., Vreugdenhil, D. (eds) *Progress in Plant Growth Regulation*. Kluwer Academic Publishers, Dordrecht, pp. 347-353 (1991)

SUMMARY

The distribution of free cytosolic Ca^{2+} was studied by using fluo-3 as a fluorescent Ca^{2+} indicator, in combination with confocal scanning laser microscopy, during somatic embryogenesis of carrot. CTC fluorescence and antimonate precipitation were used as additional methods to confirm the results obtained with fluo-3. Carrot somatic embryogenesis was found to coincide with a rise in the level of free cytosolic Ca^{2+}. The level of Ca^{2+} was low in proembryogenic masses and high in later stages of embryogenesis. The highest signal was found in the protoderm of embryos from the late globular to the torpedo-shaped stage. A gradient in fluorescence intensity was observed very often along the longitudinal axis of the embryos. The most conspicuous intracellular signal was observed in the nucleus. Other organelles did not take up the dye and were always without fluorescence. Unfortunately, attempts to calibrate the $[Ca^{2+}]_c$ failed because of difficulties encountered by the determination of F_{min} and F_{max}. The changes in $[Ca^{2+}]_c$ observed are linked with physiological processes which are known to be important during somatic embryogenesis.

INTRODUCTION

Ca^{2+} ions are important in the regulation of growth and development of plants (Hepler 1988) and plant embryogenesis forms a good model system for understanding fundamental strategies of morphogenesis (Choi & Sung 1989). In a carrot suspension culture, somatic embryos can be obtained in large amounts from small clusters of cells, designated proembryogenic masses (Halperin 1966), after transfer from auxin-containing to auxin-free medi-

um. A rise in extracellular Ca^{2+} promotes carrot somatic embryogenesis (Jansen *et al.* 1990) and the transition from non-directed to organized growth during carrot somatic embryogenesis coincides with a rise in the level of Ca^{2+}, as was observed by CTC fluorescence (Chapter 2). CTC, however, is not specific for Ca^{2+} and its fluorescence does not allow the study of the distribution of cytosolic Ca^{2+} at the cellular level in a multicellular organism like a plant embryo. To study the distribution of Ca^{2+} at this higher resolution level we used confocal scanning laser microscopy in combination with fluo-3, a fluorescent Ca^{2+} indicator.

The examination of the distribution of Ca^{2+} with fluorescent indicators is not without difficulties and control experiments are necessary (e.g. Read *et al.* 1992). Therefore CTC fluorescence and antimonate precipitation were used as additional methods to confirm the results obtained with fluo-3.

The results show a sustained increase of $[Ca^{2+}]_c$ after the onset of embryogenesis and a distinct distribution of Ca^{2+} in somatic embryos in different developmental stages. The possible interactions of Ca^{2+} and 2,4-D and the potential actions of Ca^{2+} during carrot somatic embryogenesis are discussed.

MATERIALS AND METHODS

Plant material and culture conditions

For all experiments we used a liquid culture of *Daucus carota* L. cv. Flakkese sg 766 Trophy, maintained in B5 medium (Gamborg *et al.* 1968) supplemented with 1 μM 2,4-D. Embryogenesis was initiated by transferring an enriched fraction (size between 50 and 125 μm) to 2,4-D free B5 medium. After initiation of embryogenesis, liquid cultures were maintained in Erlenmeyer flasks on a rotatory shaker as described earlier (De Vries *et al.* 1988b) or in Petri dishes.

Dye loading protocols

Cells were loaded with fluo-3 (10 or 20 μM in B5 medium) with the aid of digitonin (0.1%) as described in Chapter 4. Chlorotetracycline (1.10^{-4} M, Chapter 2) and N-phenyl-1-naphtylamine (1.10^{-6} M; Saunders & Hepler 1981) were loaded by incubation for 20 min in the culture medium.

Confocal scanning laser microscopy

Since this study was accomplished in two laboratories two different confocal scanning laser microscopes were used. Most observations were made with the CSLM of Leica Lasertechnik GmbH (Heidelberg, FRG) equipped with a multiline argon ion laser from which the 488 line was selected (for more information, see Knebel *et al.* 1989) and Chapter 4). Quantifications were made with the Bio-Rad MRC 600 CSLM equipped with a multiline argon-krypton laser. The Bio-Rad MRC 600 was attached to a Nikon Diaphot inverted microscope equipped with a Fluor 20x/0.75, PlanApo 40x/0.95 and PlanApo 60x/1.40 oil objectives. Most observations were made with

the 20x objective and the pinhole open for 1/3. Images were taken after 10 to 20 times Kalman filtering and stored for further processing. Quantification attempts were undertaken with the use of only 1.10^{-5} M A23187 to determine F_{max} or with a combination of A23187 and 1mM EGTA to determine F_{min} (Thomas & Delaville 1991). Fluorescence intensities were measured by using the complex command stat which enables the measurement of the maximum, minimum and average fluorescence intensity of rectangles of any size. The fluorescence intensities were expressed in arbitrary values on a scale ranging from 0 to 255.

Electron microscopy

Calcium was visualized as calcium antimonate precipitates according to the two-step fixation protocol of Poenie and Epel (1987). Ultrathin sections were observed with a Jeol 1200 EX II electron microscope. The specificity of the method for detection of calcium was checked by incubation of sections in 1 mM EGTA (Serva) prior to observation.

RESULTS

Fluorescence microscopy

During the development of somatic embryos of carrot from proembryogenic masses a marked increase in fluo-3 fluorescence was observed. Most proembryogenic masses had a low overall level of fluorescence, indicating a low concentration of Ca^{2+} in this stage of embryogenesis (Figs. 1a, 1b). However, several different patterns of fluorescence were found, varying from one strongly fluorescent cell in a proembryogenic mass to proembryogenic masses with several cells with a moderately higher overall fluorescence (Figs. 1c, 1d). No obvious differences between fluorescence intensity of nuclei or other organelles and the cytoplasm were observed.

From 1 day after initiation of embryogenesis, strongly fluorescent structures, which resembled morphologically the first stages of embryogenesis, were observed in proembryogenic masses (Figs. 2a to 2d). The signal from the cells of these structures was 2 to 3 times higher than the signal from proembryogenic masses. Usually, several embryos, ranging from 3 to 10 or more, depending on the size of the proembryogenic mass, developed from one proembryogenic mass. During this stage, all cells of the embryo were strongly fluorescent (Figs. 2e, 2f). In globular-shaped embryos, present on proembryogenic masses 3 to 4 days after initiation of embryogenesis, fluorescence was more profound in the outer layers of the embryo than in the centre (Figs. 2g, 2h). Also in the heart-shaped and torpedo-shaped embryos the highly fluorescent signal was restricted to the outermost cell layers (Figs. 2i and 2k).

In every stage of embryogenesis gradients in fluorescence intensity were observed which were most significant in torpedo-shaped embryos. When present, the change in fluorescence intensity was always along the longitudinal axis of the

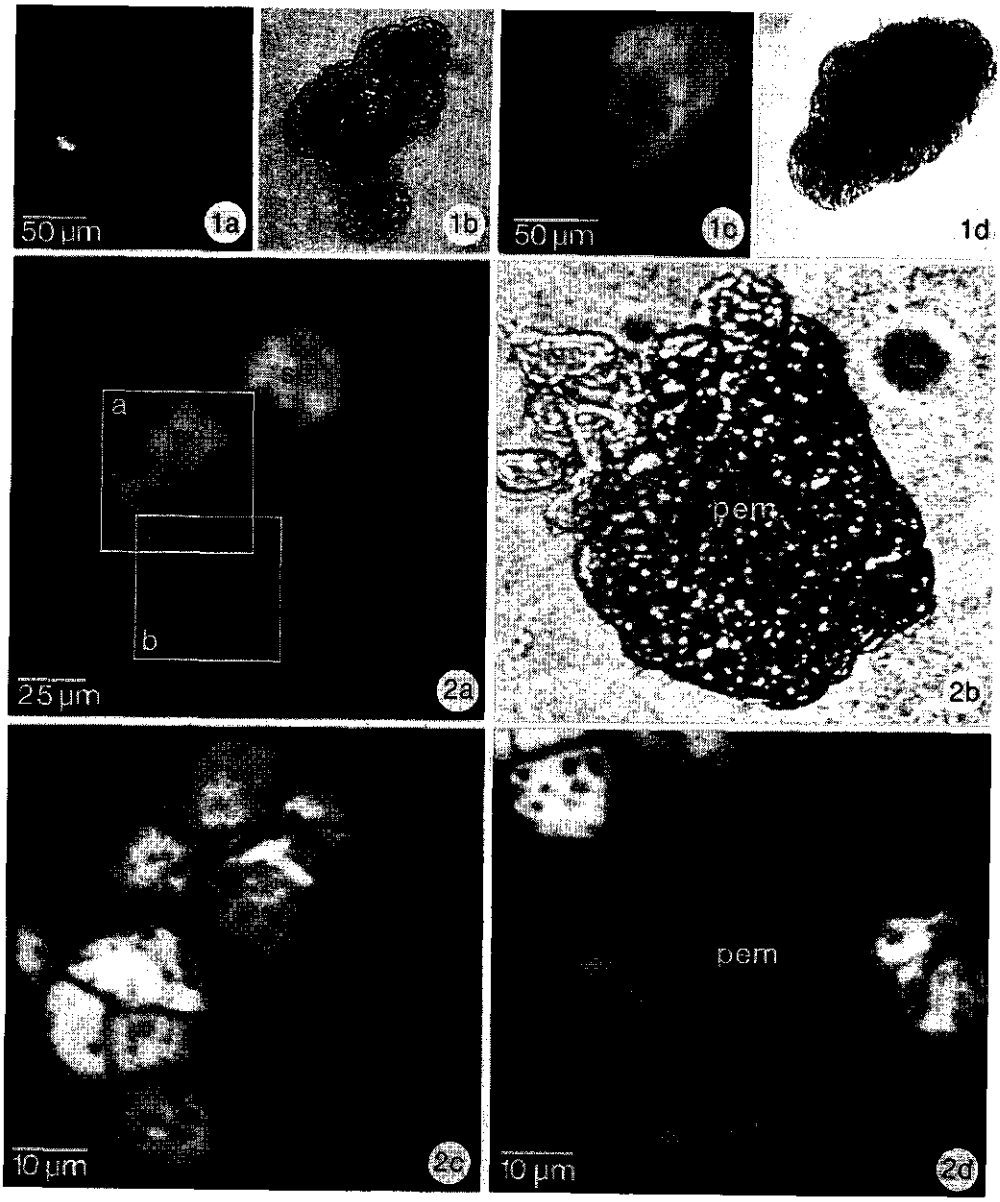

Figure 1. Confocal images of fluo-3 fluorescence in a carrot suspension culture before the initiation of embryogenesis. **a.** A proembryogenic mass with a low level of fluorescence indicating to a low $[Ca^{2+}]_c$. **b.** The bright field image of a. **c.** A proembryogenic mass showing a considerable variety in the level of fluorescence between the different individual cells. **d.** The bright field image of c.

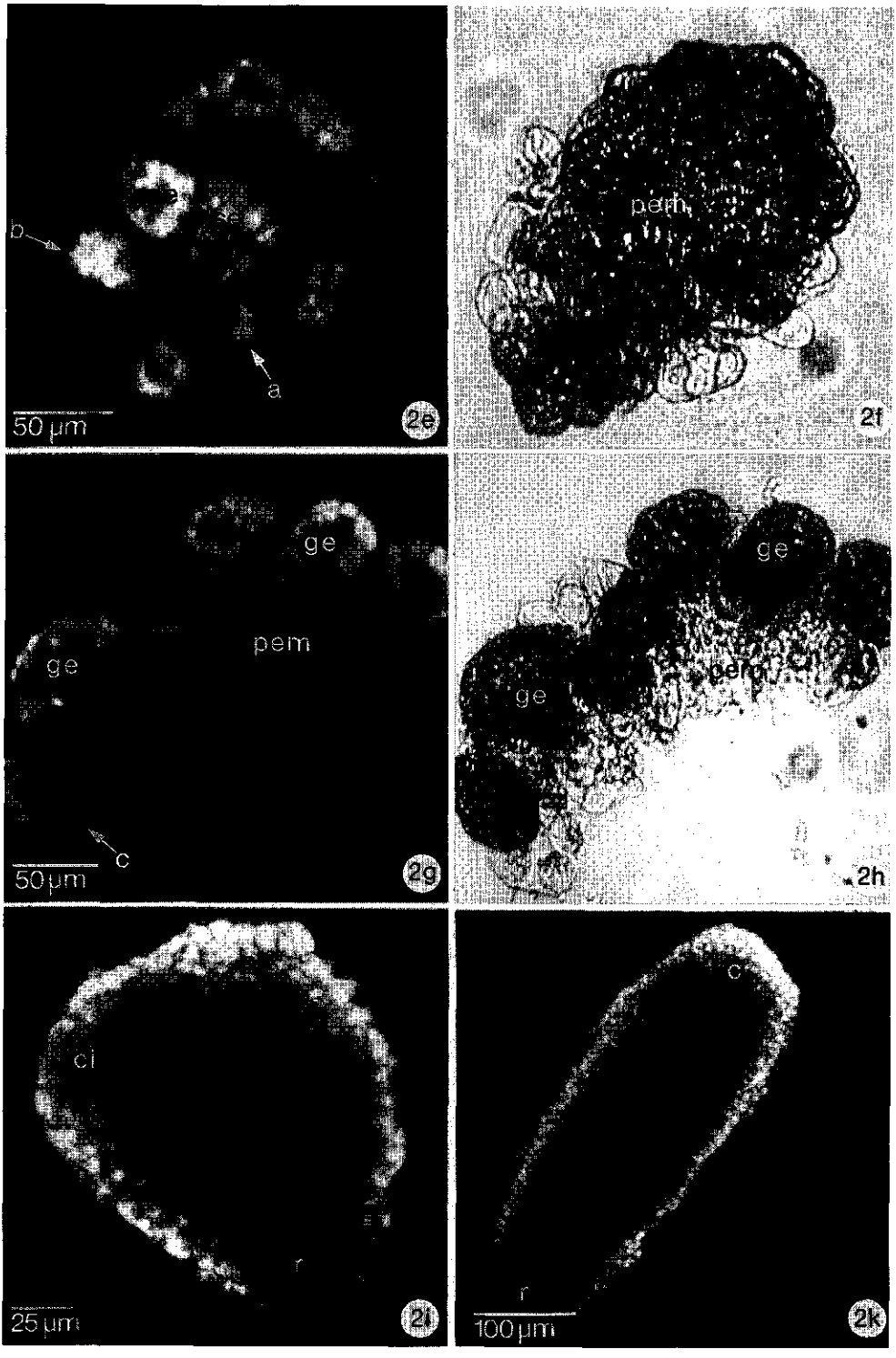
b
a
50 µm
2e
pem
2f
ge
pem
ge
c
50 µm
2g
ge
ge
2h
ci
r
25 µm
2i
c
r
100 µm
2k

Figure 2. Confocal images of fluo-3 fluorescence in a carrot suspension culture after the initiation of embryogenesis. **a.** Low magnification image of a proembryogenic mass 1 d.a.i. with three brightly fluorescent early stages of somatic embryogenesis. The areas outlined in the boxes are magnified in c (box a) and in d (box b). **b.** The bright field image of a. **c.** Higher magnification of two young somatic embryos from the area outlined in box a in Figure a. **d.** The part of the same proembryogenic mass just beneath the part in Figure c as outlined in box b in Figure a. Note the great difference in fluorescence intensity between the embryo and the non-embryogenic cells. **e.** A proembryogenic mass 2 d.a.i.. Many brightly fluorescent early staged embryos arise. **f.** The bright field image of e. **g.** Globular embryos, connected with each other by the remnants of the proembryogenic mass. The distribution of the fluorescence has changed from present overall in early staged embryos to mainly present peripheral in globular embryos which is indicated with the arrows a to c in Figures e and g. **h.** The bright field image of g. **i.** Early heart-shaped embryo with a strong fluorescence in the peripheral cell layers. **k.** Torpedo-shaped embryo, again with the strongest signal in the outer cell layers. Note the decrease in fluorescence intensity from cotyledons to root side of the embryo.

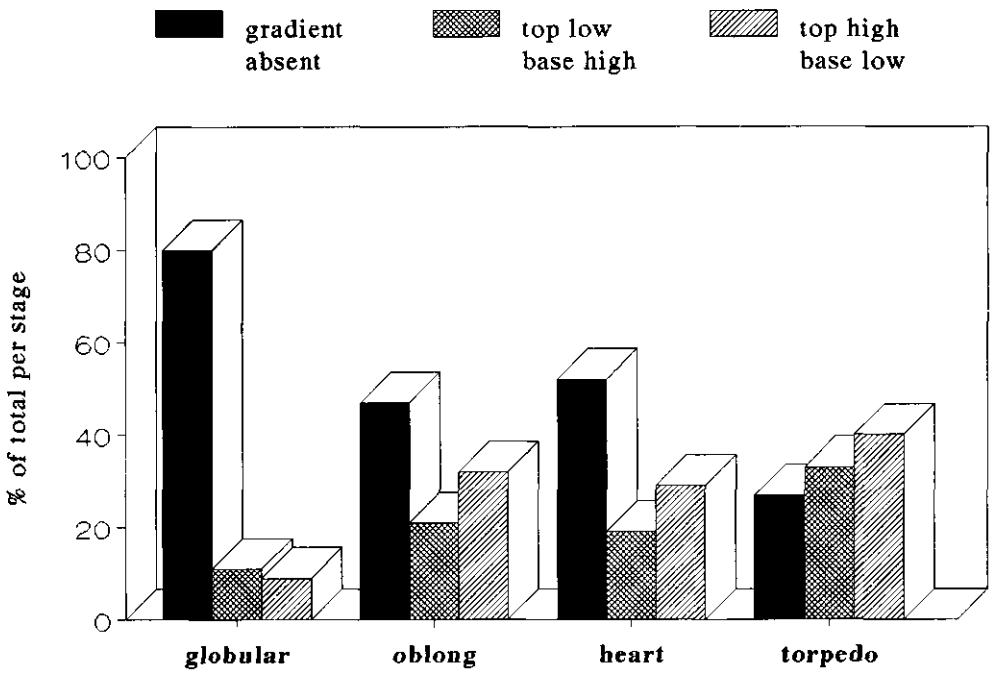

Figure 3. The occurrence of gradients in fluo-3 fluorescence in globular, oblong, heart-shaped and torpedo-shaped somatic embryos of carrot. Per stage, randomly, 50 embryos from a culture of 50 ml were examined on the presence or absence of a gradient and on its longitudinal direction.

Figure 4. Optical section through the protoderm of a cotyledon from a torpedo-shaped somatic embryo after loading with fluo-3. Note the absence of fluorescence from cell walls and vacuoles and the strong signal from nuclei.

embryo and could increase from embryo top to embryo base or vice versa (Fig. 3).

Higher magnifications of optical sections through the protoderm of a torpedo-shaped embryo revealed the cellular origin of the fluorescence (Fig. 4). All cells were highly fluores-

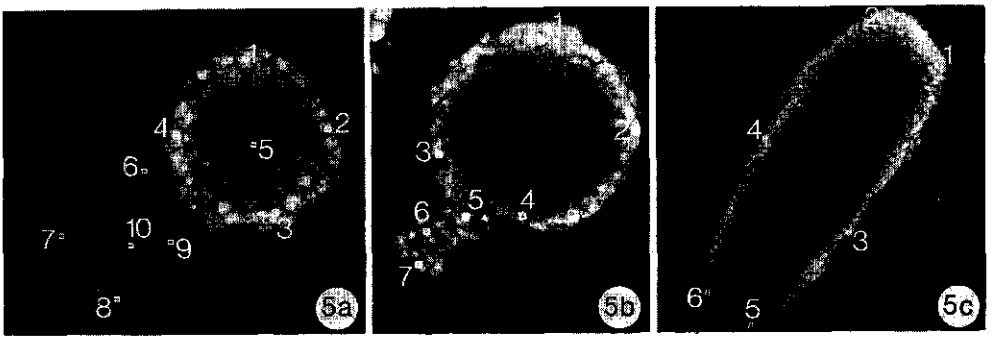

Figure 5. The intensity of fluo-3 fluorescence in different developmental stages of somatic embryogenesis of carrot. The intensity is expressed in arbitrary values in a scale ranging from 0 to 255 (see table) **a.** A globular embryo (numbers 1 to 5) and its proembryogenic mass (numbers 6 to 10) showing a considerable difference in fluorescence intensity (table, column 5a). **b.** An early (numbers 5 to 7) and a late globular embryo (numbers 1 to 4) with only a small difference in fluorescence intensity between the two (table, column 5b). **c.** Torpedo-shaped somatic embryo showing a gradient in fluorescence intensity from cotyledons (numbers 1 and 2) to root side (numbers 5 and 6, table, column 5c).

	5a	5b	5c
1	151	189	207
2	132	198	224
3	160	123	170
4	165	155	170
5	81	151	103
6	77	115	93
7	83	145	
8	110		
9	69		
10	95		

Figure 6. Fluorescence images of hand made sections through torpedo-shaped somatic embryos of carrot. The intensity of fluorescence is expressed in arbitrary values in a scale ranging from 0 to 255 (see table) **a.** Confocal image of fluo-3 fluorescence. Note the differences in fluorescence intensity between the protoderm (numbers 1, 3, 6 and 8; table, column 6a) and the cell layer directly adjacent to it (numbers 2, 4, 5 and 7; table, column 6a) **b.** Higher magnification of a part of a. (table, column 6b). **c.** Epi-fluorescence image of CTC fluorescence. Note the resemblance with the image of Fig. a. **d.** Epi-fluorescence image of NPN fluorescence. The intensity increases from the periphery to the middle of the section visualizing the distribution of membranes. Compare with Figs. a and c.

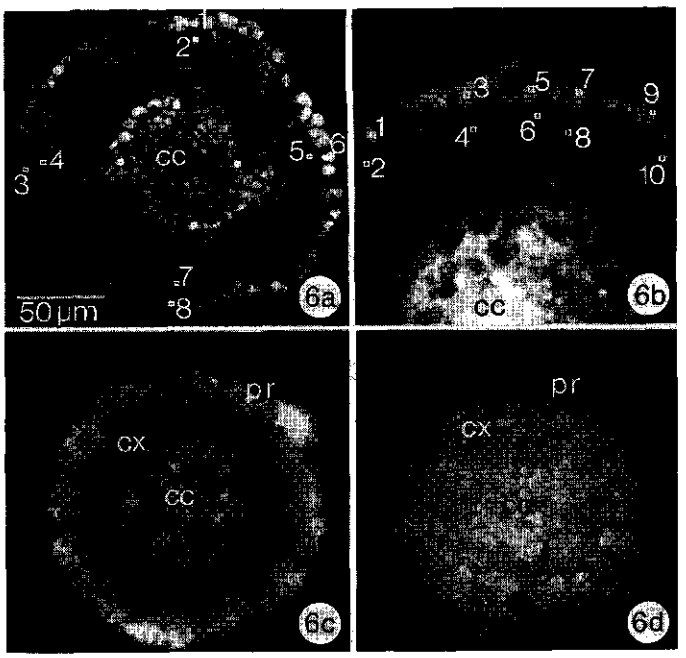

	6a	6b
1	148	143
2	139	96
3	98	142
4	105	110
5	109	145
6	201	115
7	85	145
8	113	108
9		120
10		116

cent, with the highest signal present in the nuclei. Especially nucleoli showed a striking fluorescence. In the cytoplasm, regions with varying intensities of fluorescence were observed. Cell walls, vacuoles and large organelles, presumably amyloplasts or proplastids, were always negative.

Attempts were undertaken to determine F_{min} and F_{max} for the calculation of $[Ca^{2+}]_c$ by incubation in A23187 and EGTA. It was, however, found that, although an increase was always observed with A23187 and a decrease with EGTA, no constant value for a number of embryos of F_{min} or F_{max} could be fixed. Sometimes the differences in fluorescence intensity before and after incubation in A23187 or EGTA were very small. Another limitation was the alteration of fluorescence intensity in various focus planes, caused by overlying structures, which is inevitable due to the different transparency of the tissues at different locations (see also Fricker & White 1992). From this we had to conclude that calculations were not possible under these conditions and we decided to give only the fluorescence intensities in arbitrary values with a scale ranging from 0 to 255.

Quantification of the fluorescence intensity demonstrated the differences in intensity between proembryogenic masses and embryos (Fig. 5a) and between different regions within a torpedo-shaped embryo (Figs. 3, 5c). In arbitrary values the average intensity of the proembryogenic mass in Fig. 5a was about the half of the intensity in the cells of the protoderm of the embryo (respectively 87 ± 16 and 152 ± 15). As can be seen in Fig. 5b, globular-shaped embryos do not differ much in fluorescence intensity during their development from early globular (average of 130 ± 15) to late globular (average of 166 ± 34 in the protoderm). In torpedo-shaped embryos (Fig. 5c) the intensity of the cotyledons was sometimes found to be twice as high as the intensity of the base.

Hand made sections of living torpedo-shaped embryos were loaded with fluo-3 to check whether the distribution observed was factual or was caused by difficulties in dye uptake by the interior cells. In these preparations the protoderm cells again possessed the highest signal in comparison with the signal from the interior cells. Interior cells, even when exposed directly to the medium, always possessed a low level of fluorescence intensity (results not shown).

Hand made sections of living torpedo-shaped embryos loaded with fluo-3, CTC or NPN were used to observe the differences between protoderm cells and interior cells (Fig. 6). With both Ca^{2+} indicators a strong signal was observed in sections through the embryos in the protoderm and the stele. With NPN only the stele showed a strong fluorescence, indicating a higher membrane content of this region which could account for the higher signal from the Ca^{2+} indicators. The fluorescence intensity in the cells of the protoderm was about 1.3 times the value found in the cortex cells.

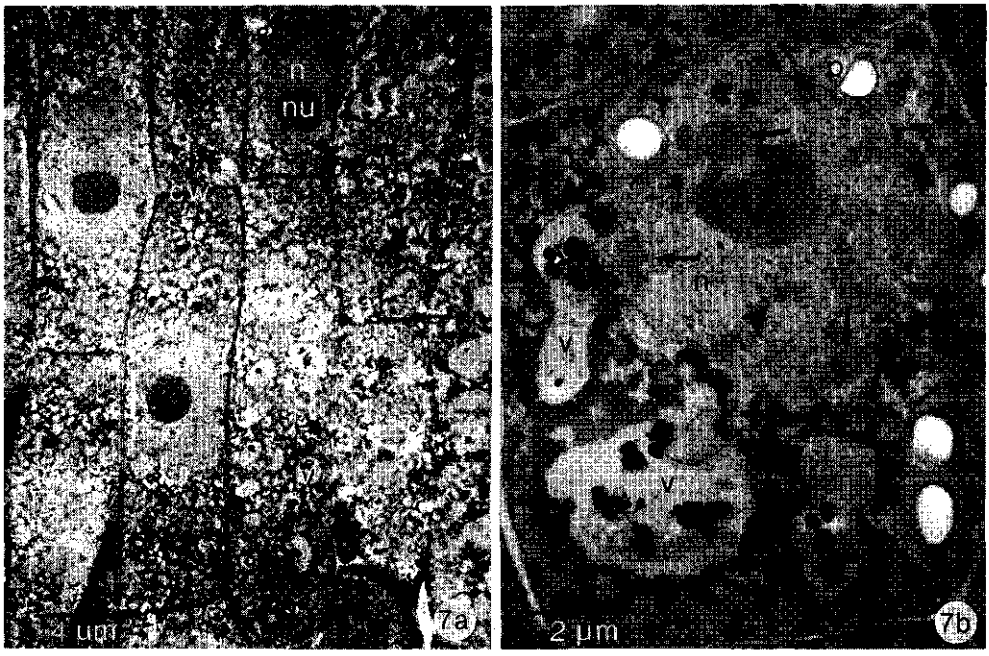

Figure 7. The distribution of antimonate precipitates in a section of a torpedo-shaped somatic embryo of carrot. **a.** Overview. Precipitates are mainly present in cell walls, vacuoles and nuclei. **b.** High magnification image of one cell. Note the high amount of precipitates present in the nucleolus and the presence in batches in the nucleus (arrows).

Electron microscopy

The distribution of calcium antimonate precipitates was only studied in torpedo-shaped embryos. Precipitates were mainly found in the cell wall, the nucleus and the vacuole (Fig. 7a). Erratically, precipitates were also found in amyloplasts. No differences were observed between protoderm cells and interior cells. Higher magnifications of nuclei revealed a fine precipitate, scattered over the nucleus with a high quantity in the nucleolus (Fig. 7b).

DISCUSSION

Carrot somatic embryogenesis coincides with a rise in the level of free cytosolic Ca^{2+}. The $[Ca^{2+}]_c$ in proembryogenic masses was found to be lower than the concentration in embryos and showed a greater variety, both within one proembryogenic mass and between proembryogenic masses, than in embryos. During early embryogenesis the highest $[Ca^{2+}]_c$ was observed in all embryo cells, while from the globular stage

on the highest $[Ca^{2+}]_c$ was found in the protoderm of the embryos. In embryogenic stages from late globular to torpedo-shaped, a gradient in $[Ca^{2+}]_c$ along the longitudinal axis of the embryo was often observed. The high signal in the protoderm was confirmed by CTC fluorescence of hand made sections through torpedo-shaped embryos. CTC has often been used as a probe for membrane-associated Ca^{2+}, but according to Dixon *et al.* (1984) the fluorescence intensity of CTC is directly correlated with the $[Ca^{2+}]_c$.

The most conspicuous intracellular signal was found in the nucleus. Dye accumulation in intracellular organelles has often been found to be a major problem in working with fluorescent Ca^{2+} indicators (e.g. Read *et al.* 1992) and Fricker & White (1992) found indo-1 to accumulate in the nucleus of *Commelina communis* guard cells after microinjection. The nucleus of sympathetic neurons isolated from the bullfrog by Hernandez-Cruz *et al.* (1990) accumulated fluo-3 but a Ca^{2+} gradient was also present. In our study the presence of Ca^{2+} in the nucleolus was confirmed by antimonate precipitation. Pyroantimonate forms precipitates not only with Ca^{2+}, but also with other divalent cations such as Mg^{2+} (Caswell 1979). The recently developed method of Poenie & Epel (1987), which was used here, includes the use of fluoride ions for the *in situ* precipitation of intracellular calcium during fixation. This leads to a very specific precipitation of antimonate with Ca^{2+}, which was not obtained with earlier antimonate precipitation protocols (Slocum & Roux 1982). Although we cannot exclude accumulation of fluo-3 in the nucleus of carrot embryos, antimonate precipitation confirms that the high fluorescence of this organelle certainly also indicates a high $[Ca^{2+}]$.

Attempts to calibrate $[Ca^{2+}]_c$ from the fluorescence intensity of fluo-3 were not possible because of the difficulties encountered by determining F_{min} and F_{max} with A23187 and EGTA. Also others have reported difficulties with *in situ* calibration using ionophores and EGTA (Hepler 1989, Guiragossian Kiss *et al* 1991, Read *et al.* 1992 and Bush 1992). To obtain sustained changes in $[Ca^{2+}]$ detergents are often used, but in our situation this would certainly lead to dye loss from the cells. Other problems with A23187 are its pH dependent activity and its aspecificity (Kell & Donath 1990). Hence new techniques have to be developed in order to quantify $[Ca^{2+}]_c$ reliably in carrot embryo cells.

The observed rise in $[Ca^{2+}]_c$ might be linked with the role of auxin in carrot somatic embryogenesis. Auxin is the most important factor for regulation of induction and development of embryogenesis and it has different effects in different phases of embryogenesis (Komamine *et al.* 1990). Auxin is essential for the induction of embryogenesis but inhibits the development of subsequent stages. In general, auxin treatment leads to an increase in $[Ca^{2+}]_c$ (e.g. Brummel & Hall 1987, Ettlinger & Lehle 1988) which is usually transient (Felle 1988). In a few cases also a decrease in $[Ca^{2+}]_c$ was observed after auxin treatment (Das *et al.* 1987, Tretyn *et al.* 1991).

The continuous presence of 2,4-D in the culture medium may cause a continuous change in $[Ca^{2+}]_c$ of cells which are sensitive to the action of 2,4-D, perhaps depending on the stage of the cell cycle they are in at that moment. The differences in $[Ca^{2+}]_c$ observed within one proembryogenic mass and between proembryogenic masses may be explained in this way. A direct consequence could be a distortion of auxin transport and prevention of the development of a polarized distribution of endogenous auxin, which is necessary to complete embryogenesis (Fujimura & Komamine 1979a). The importance of auxin transport during embryogenesis was already stressed by Schiavone & Cooke (1987) for carrot and by Chée & Cantliffe (1989) for *Ipomoea batatas*. Removal of 2,4-D from the culture medium then allows an auxin transport permissible with embryogenesis. The sustained increase in $[Ca^{2+}]_c$ in embryo cells might be caused by the action of endogenous cytokinin. The cytokinin zeatin stimulates embryogenesis (Fujimura & Komamine 1980, Li & Neumann 1985) and the action of cytokinins (reviewed by Kaminek 1992), is often connected with changes in $[Ca^{2+}]_c$. For example, in *Funaria hygrometrica*, cytokinin treatment leads to a sustained increase in $[Ca^{2+}]_c$ rather than a rapid spike (Saunders 1992).

A direct consequence of the sustained higher level of cytosolic Ca^{2+} might be a physical isolation of the embryogenic cells from the proembryogenic mass. An increase in $[Ca^{2+}]_c$ inhibits cell-to-cell transport in plants through closing of plasmodesmata (Tucker 1990). This physical isolation of initiating cells, prior to the onset of embryogenesis, seems to be an important initial event in somatic embryogenesis (Williams & Maheswaran 1986). In carrot, a physical isolation of cytoplasm as a result of plasmolysis has been reported to enhance embryogenesis (Wetherell 1984). The elevated $[Ca^{2+}]_c$ could also stimulate the synthesis and deposition of callose (see Kauss 1987) and so strengthen the isolation of the embryogenic cells. Callose deposition is reported to be an early marker of somatic embryogenesis from roots of a *Cichorium* hybrid (Dubois *et al.* 1990) and from leaves of *Camellia japonica* (Pedroso & Pais 1992). In this respect the observation of the absence of plasmodesmata in the zygote of barley by Norstog (1972) is worth mentioning.

In addition, the observed rise in $[Ca^{2+}]_c$ may also cause a partial disassembly of microtubules, allowing a rebuilding of the cytoskeleton in a highly ordered way (Steer 1988, Cyr 1991). The transition from non-directed growth (in proembryogenic masses) to embryo development goes together with a change in the distribution of microtubules from a rather random orientation to an ordered orientation, with adjacent cells having identical microtubular profiles (Wochok 1973). This change in the orientation of microtubules, as a consequence of an increase in $[Ca^{2+}]_c$, might be necessary for the coordinated behaviour of a group of cells, which is a prerequisite for a proper development of an embryo. A similar change in the orientation of microtubuli has been observed during

organogenesis in *Petunia hybrida* (Traas *et al.* 1990). Opposite observations, however, are also described. Dijak and Simmonds (1988) found no particular pattern of organization of cortical microtubules associated with early stages of embryogenesis from mesophyll protoplasts of *Medicago sativa*. However, the direct effect of a rise in $[Ca^{2+}]_c$ on the orientation of cortical microtubules in embryogenic cells of carrot has not been investigated and until then, the assumption of a link between the two remains speculative.

The relatively high $[Ca^{2+}]_c$ in the protoderm of somatic embryos confirms the importance of the protoderm in somatic embryogenesis, as was already stressed in Chapter 3. It may be linked with the synthesis and secretion of a number of substances to the medium by the protodermic cells. Extracellular proteins with various enzymatic activities have been isolated from the culture medium of carrot (De Vries 1992). One of them appeared to be a peroxidase isoenzyme (Cordewener *et al.* 1991). The synthesis and secretion of peroxidases has been proved to be under the control of $[Ca^{2+}]_c$ (Sticher *et al.* 1981). In this respect, the recent finding of Dietz *et al.* (1992) of a high concentration of calcium in the epidermis of barley in comparison with the level of the mesophyll is interesting. These authors proposed a separation of Ca^{2+} and PO_4^{3-} by compartmentation in different cell layers to avoid the formation of insoluble salts, which would prevent the normal PO_4^{3-} homeostasis of the cell. In other systems of somatic embryogenesis, the epidermis is not as evident as in carrot. Somatic embryos of alfalfa have a very rough, poorly-differentiated epidermis which is lost after pro-embryo formation (Xu & Bewley 1992).

Although the role of Ca^{2+} in plant gene expression is still hardly investigated (e.g. Guilfoyle 1989), the observed high level of Ca^{2+} in nuclei of embryogenic cells might point to a role of Ca^{2+} in the regulation of the expression of genes related to embryogenesis (Racusen & Schiavone 1988, Aleith & Richter 1990). In animal cells, enhancer elements which mediate Ca^{2+} dependent induction of gene expression are described (Lenormand *et al.* 1992). On the other hand, this may also indicate merely an overall higher level of gene expression in embryogenic cells as compared to the level in proembryogenic masses (Nomura & Komamine 1986a). In respect of this, the involvement of Ca^{2+} in nuclear protein phosphorylation is worth noting (Ranjeva & Boudet 1987). The high $[Ca^{2+}]$ in the nucleolus of eukaryotes (Campbell 1983) probably has a function in maintaining the structure of the nucleolus which is directly correlated with the production of ribosomes (Selzer *et al.* 1991).

In conclusion, we can state that carrot somatic embryogenesis coincides with a change in the level and distribution of Ca^{2+} and that this change can be linked with a number of physiological processes which are concerned in the growth and development of somatic embryos.

CHAPTER 6

PARALLELS BETWEEN THE DISTRIBUTION OF NEUTRAL RED, ACRIDINE ORANGE AND FLUPHENAZINE FLUORESCENCE DURING EMBRYOGENESIS OF *DAUCUS CAROTA* L.

A.C.J. TIMMERS, U.K. TIRLAPUR & J.H.N. SCHEL

Department of Plant Cytology and Morphology, Agricultural University, Arboretumlaan 4, 6703 BD Wageningen, The Netherlands

SUMMARY

The accumulation of neutral red and acridine orange, to indicate differences in vacuolar pH, were studied during embryogenesis of carrot. Neutral red accumulated barely in proembryogenic masses, but was present conspicuously in globular-shaped somatic embryos. From the late globular to the torpedo-shaped stage, it was mainly found in the root side of the embryo. Here, neutral red was predominantly present in large dark-red to purple stained vesicles. In the cotyledons neutral red was found in small orange vesicles. In zygotic embryos of carrot, the dye was uniformly distributed with no specific localization in organelles. During germination, however, neutral red accumulated preferentially in regions in the root side and the hypocotyl of the germling. Acridine orange was dispersed erratically in proembryogenic masses with a great variety in intensity. It was quite obviously present in early stages of somatic embryogenesis and restricted to the root side in late globular to torpedo-shaped embryos. Confocal images revealed the vacuolar presence of the fluorescence and the predominant presence in the protoderm. During germination of zygotic embryos, the signal changed from uniform to localized with sharp borders between fluorescent and non-fluorescent regions. Two to three days after the beginning of germination, acridine orange accumulated preferentially in the root tip of the germling. The distribution of the fluorescence from fluphenazine, a probe for activated calmodulin, more or less resembled the signal from acridine orange, although some differences were observed. All the three probes reacted in a similar manner to treatments with EGTA, A23187 or propionic acid. The role of calmodulin in the regulation of vacuolar pH and vacuo-

lar $[Ca^{2+}]$, as well as a possible role of calmodulin in the regulation of vacuolar digestion or movement, is discussed. Differences between somatic and zygotic embryogenesis and similarities between somatic embryogenesis and zygotic embryo germination are mentioned.

INTRODUCTION

Calcium ions and pH both influence somatic embryogenesis of carrot. Ca^{2+} must be present in the growth medium for embryogenesis, or even cell division and cell growth, to proceed. Increasing the $[Ca^{2+}]_e$ above 1 mM specifically stimulates embryogenesis, but has no influence on cell proliferation (Jansen *et al.* 1990). The pH of the medium changes during every culture cycle (Smith & Krikorian 1990a) and in hormone-free medium low pH_e mimics the inhibiting action of 2,4-D on embryogenesis (Smith & Krikorian 1990b). Carrot somatic embryogenesis coincides with a rise in $[Ca^{2+}]_c$ (Chapters 4 and 5) and electrical currents through torpedo-shaped somatic embryos are almost totally carried by protons (Brawley *et al.* 1984).

The $[Ca^{2+}]$ in the cytosol is linked with the pH of the cytosol. Small changes in pH_c are followed by larger changes in $[Ca^{2+}]_c$, probably by transfer of Ca^{2+} from the vacuole to the cytosol (Felle 1988). The tonoplast lacks a Ca^{2+} ATPase (Bush & Sze 1986) and transport of Ca^{2+} depends on the activity of a Ca^{2+}/nH^+ antiport system (Guern *et al.* 1989, Blackford *et al.* 1990) and the state of Ca^{2+} channels in the tonoplast (Johannes *et al.* 1992). From this it can be assumed that $[Ca^{2+}]_c$, $[Ca^{2+}]_v$, pH_c and pH_v are interrelated and that changes in pH_v are important in the regulation of the former three. Large changes in pH_v within one cell population have been described and the pH_v can vary between 6.5 and even 1 (Kurkdjian & Guern 1989). No histological reports are, however, available on the distribution of pH_v within one organism. As both pH and $[Ca^{2+}]$ are important factors in carrot embryogenesis, we decided to look at the distribution of pH_v during somatic and zygotic embryogenesis and during germination of carrot. Two pH probes which specifically accumulate in acidic compartments, neutral red (Nishimura 1982) and acridine orange (Gluck *et al.* 1982), were used. The distribution of these probes was compared with the distribution of fluphenazine, a fluorescent probe for activated calmodulin (Chapter 2).

MATERIALS AND METHODS

Plant material and culture conditions

Plant material and culture conditions were as described in Chapter 3.

Probe loading protocols

Proembryogenic masses, somatic embryos, zygotic embryos and young seedlings were incubated in either 70 μM neutral red (Merck), 3 μM acridine orange (Pharbil) or 20 μM fluphenazine.2HCl (Serva) for 20 min-

utes. After a short rinse with the incubation medium, the distribution of the dyes was observed.

Effect of A23187, EGTA and propionic acid on dye distribution

Torpedo-shaped somatic embryos were incubated for one hour in either 10 μM A23187 (Molecular Probes), 1 mM EGTA (Serva) or 50 mM propionic acid (Merck) in B5 medium. After one hour, either neutral red, acridine orange or fluphenazine was added as described above. The addition of EGTA, A23187 or fluphenazine did not change the pH of the medium. Propionic acid lowered the pH to 3.2.

Microscopy

Fluphenazine fluorescence was viewed with a Nikon Labophot microscope equipped with a 100 W mercury lamp and filter combination BP365/10, DM400, LP420. Acridine orange fluorescence was viewed with a Nikon Microphot-FXA equipped with a Xenon XPS-100 lamp and filter combination 470-490, DM500, LP510. Photographs were recorded on Kodak Ektachrome P800/1600. Neutral red was viewed with a Nikon Optiphot microscope. Photographs were recorded on Kodak Ektachrome 64T/EPY 135-36.

Confocal images were made with a Bio-Rad MRC 600 scanning laser microscope, equipped with an argon-krypton laser (Ion Laser Technology, Salt Lake City, USA), from which the 488 line was selected, and an argon ion UV-laser (Coherent Inc., Palo Alto, USA) from which the 364 line was used. Filter combinations were, respectively, 488/10, DM510LP, LP515 and DM380, LP460.

RESULTS

Distribution of neutral red during somatic embryogenesis

During somatic embryogenesis the staining with neutral red changed markedly from a slight, uniform staining to a substantial, polarized staining. Proembryogenic masses were only weakly stained without any granular or conspicuously vacuolar staining (Fig. 1). Shortly after the initiation of embryogenesis intensely stained globular structures were observed on proembryogenic masses (Fig. 2a) which contained uniformly distributed, dark-red organelles (Fig. 2b). The size of these organelles decreased from embryo base to embryo top. Oblong, heart-shaped and torpedo-shaped stages were all characterized by the presence of a clearly stained base with dark-red organelles. In the oblong stage the upper part of the embryo was practically without any stain (Fig. 2c), but as soon as the cotyledons appeared a faint orange stain was observed in them (Figs. 2d and 2f, colour plate). Stained organelles were restricted to base and cotyledons and were relatively large and dark-red to purple (Fig. 2e, colour plate) or relatively small and orange (Fig. 2f, colour plate) respectively. In older staged germinated embryos various patterns of neutral red staining were observed. The large, dark-red to purple organelles could cover an area as big as

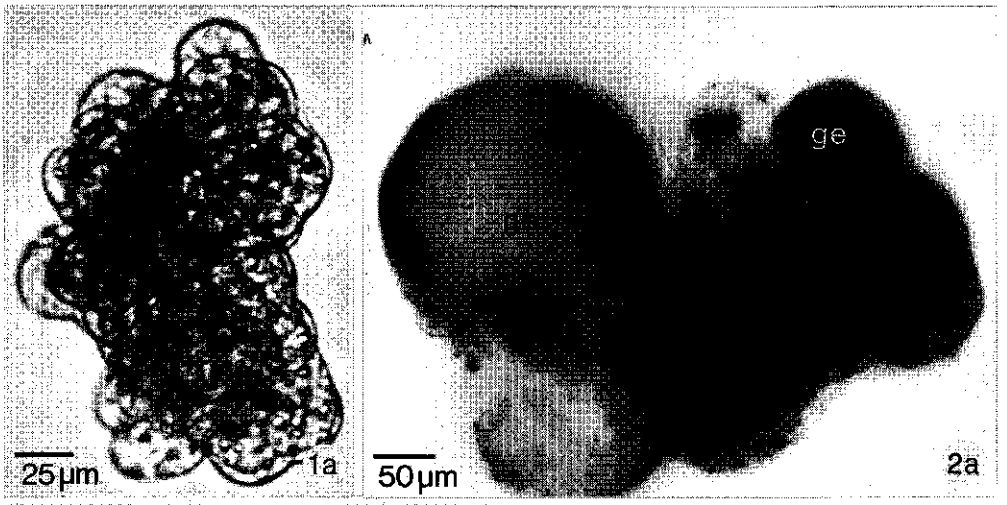
25 µm
1a
ge
50 µm
2a

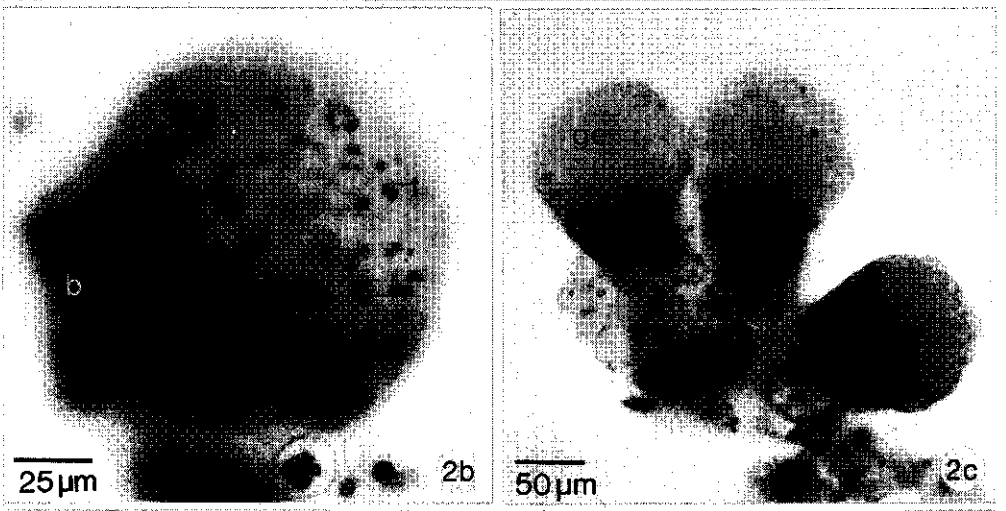
b
25 µm
2b
ge
50 µm
2c

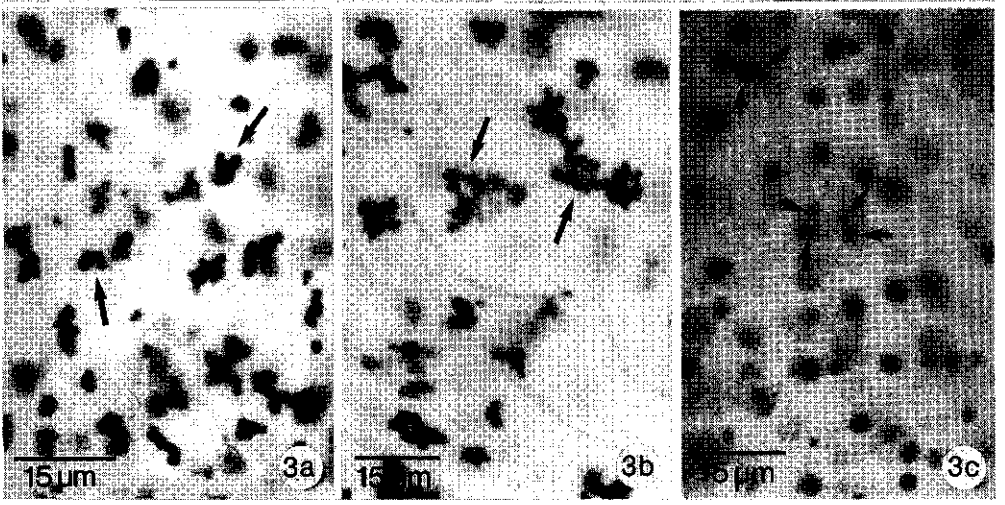
15 µm
3a
15 µm
3b
3c

the hypocotyl and root and contained an intervening lesser stained part just before the root tip (Fig. 2d, colour plate).

Higher magnification images revealed the cellular location of the neutral red stain in the various regions of germinated somatic embryos. In the region just below the hypocotyl, the cells usually contained one to a few dark-red to purple stained organelles (Fig. 3a, arrows). The cytoplasm and vacuoles possessed a faint red colour. More to the base of the embryo, clusters of purple stained small organelles (Fig. 3b, arrows) were found in the root hair region, where the cytoplasm and central vacuole were colourless. Below this region, the root tip, larger, round, purple stained organelles (Fig. 3c, arrows) were present again, embedded in a lilac stained cell content. An area with two neighbouring, different types of cellular localization forms the transition towards the hypocotyl, which is typified by cells with red stained vacuoles and cytoplasm (Fig. 3d, colour plate). A small number of large organelles with an intense annular staining was present in this region. The cotyledons contained small, orange-coloured, spherical organelles (Fig. 2f, colour plate).

Figure 1. Distribution of neutral red in a proembryogenic mass of carrot before the initiation of embryogenesis. Note the uniform distribution and the absence of neutral red accumulating organelles.

Figure 2. Distribution of neutral red in a suspension culture of carrot after the initiation of embryogenesis. **a.** A proembryogenic mass with 4 globular embryos 4 d.a.i. Neutral red accumulates in embryogenic structures and is present in a high amount in small vesicles scattered over the embryos. **b.** Globular embryo showing the presence of neutral red accumulating vesicles that increase in size from embryo top to embryo base. **c.** Three globular embryos 4 d.a.i. of embryogenesis showing a preferential accumulation of neutral red in the base (root side) of the embryos. **d.** Colour plate. Torpedo-shaped somatic embryo 14 d.a.i. showing the difference in colour of neutral red stain in cotyledons and root side. The strong neutral red accumulating vesicles cover the total lower part of the embryo. **e.** Colour plate. High magnification of the base of a torpedo-shaped embryo 4 d.a.i. showing the presence of neutral red both in the central vacuole of the cells and in smaller vesicles. **f.** Colour plate. High magnification of the cotyledons of the embryo in Fig. d. Neutral red accumulating vesicles are small and lighter in colour.

Figure 3. High magnification images of the accumulation of neutral red in different regions of a germinated somatic embryo of carrot. **a.** The region just beneath the hypocotyl. Neutral red accumulating vesicles are grouped and intensely stained (arrows). **b.** The root hair zone. Neutral red accumulating vesicles are clustered (arrows). **c.** The root tip. Neutral red accumulating vesicles are large and round (arrows). **d.** Colour plate. The hypocotyl. Besides in large round vesicles (arrows), neutral red also accumulates strongly in the central vacuole.


2d

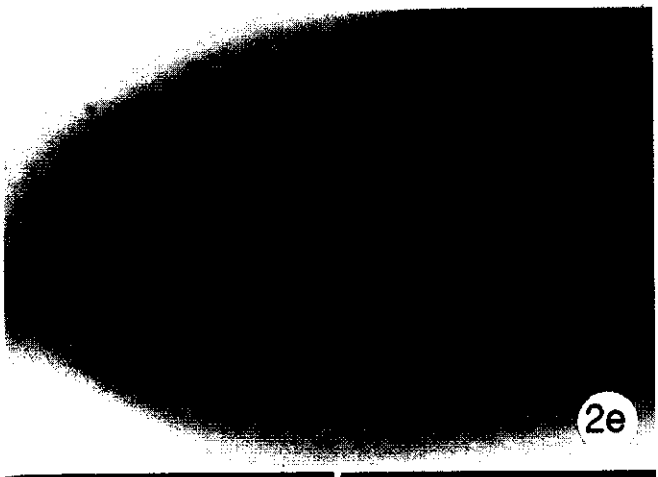
2e

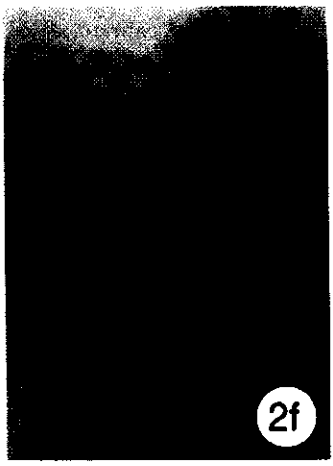
2f

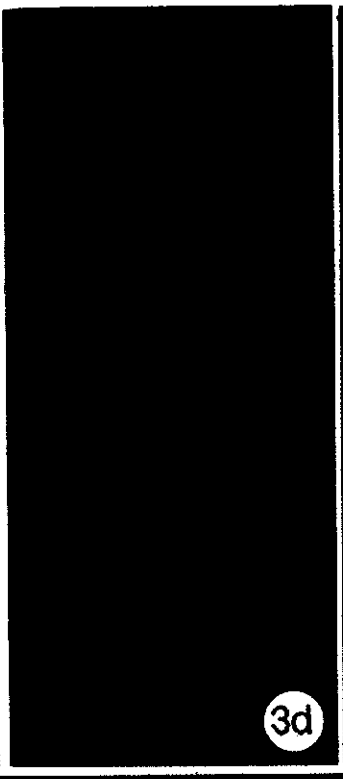
3d

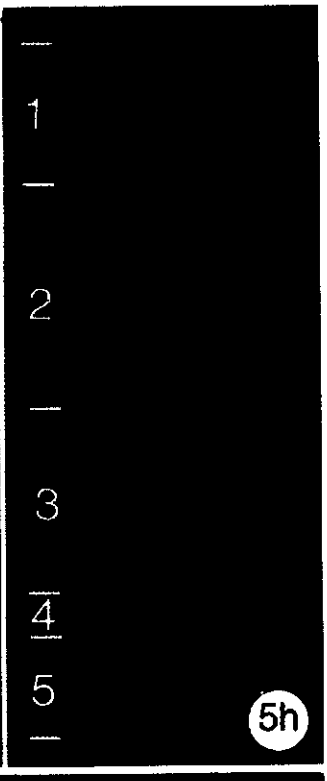
1
2
3
4
5
5h

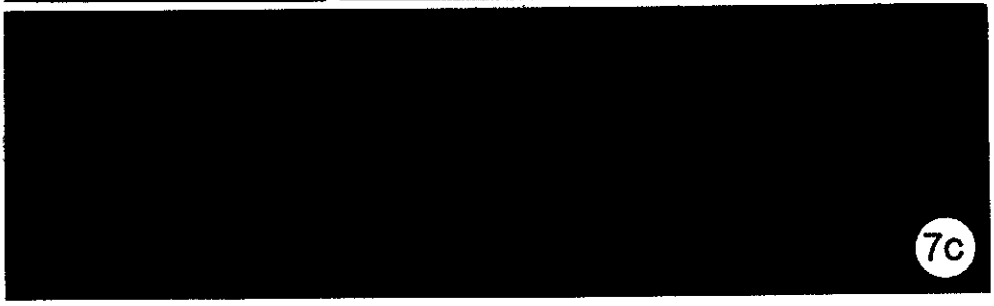
7c

Distribution of neutral red in germinated zygotic embryos

Zygotic embryos, incubated for one day in water to induce germination, stained intensely with neutral red. A precise observation of the distribution of the stain was not possible, however, because of their opacity. As far as it could be seen, the stain was uniformly distributed over the embryo, leading to overall stained cells without distinctly stained organelles. Nevertheless, these organelles were found in the regions which bordered on both sides of the root hair region of embryos incubated for more than one day. In some cells, these organelles were seen as spheres linked with each other by thin strains. The root hair region itself was almost colourless, without any organelle-bound neutral red stain (results not shown).

Distribution of acridine orange during somatic embryogenesis

During somatic embryogenesis the distribution of the fluorescence, caused by accumulation of acridine orange, changed from erratically dispersed over an embryo to clearly confined to a definite part of the embryos. A great diversity in the distribution of the fluorescence was observed in proembryogenic masses, ranging from almost non-fluorescent to strongly fluorescent (Figs. 4a, 4b). Cells with varying intensities of fluorescence were randomly distributed over the proembryogenic mass. The colour of the signal was either soft green or yellow. Shortly after initiation of embryogenesis, the yellow fluorescent regions were more localized (Figs. 5a, arrow, 5b) and early globular staged embryos possessed this kind of fluorescence, distributed uniformly (Figs. 6a and 6b). Oblong, heart-shaped and torpedo-shaped embryos were typified by a bright, yellow fluorescence of the base of the embryo (Figs. 5c to 5f and 6c and 6d). Besides a change from an evenly distributed presence of fluorescence to a polarized distribution, the signal also changed from overall present to more protoderm restricted (Figs. 6a to 6d). The size of the fluorescent region varied between different embryos, but primarily up to half of the embryo was fluorescent and a more or less sharp border separated it from a non-fluorescent cotyledonary region (Fig. 5e, arrow). Five regions, each with a characteristic configuration and colour of fluorescence, were observed in germinated somatic embryos (Fig. 5h, colour plate). The root tip showed a bright yellow fluorescence which originated from the vacuoles connected with each other by thin strands (Fig. 6e). A short, almost non-fluorescent, part separated the root tip from the root hair region. Numerous small organelles with an orange to red colour typified this region. These organelles were scattered over the entire region, both in the cells and in the root hairs. In the next part, the hypocotyl, the cells were almost totally filled with large, yellow to green-yellow vacuoles (Fig. 5g). Some small organelles characteristic for the root hair region, were also observed here. The picture of the cotyledons strongly resembled the one of the root hair region.

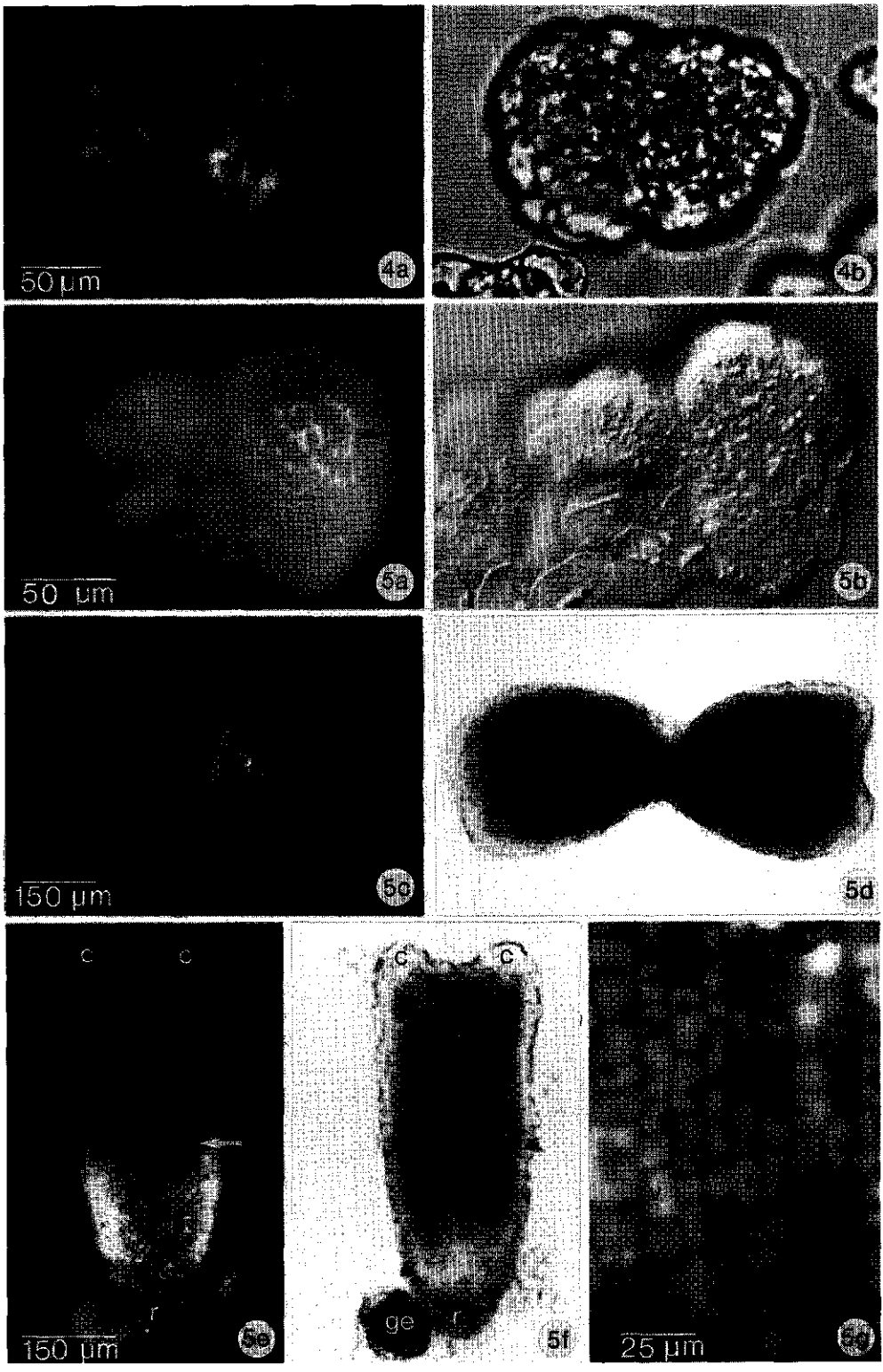
50 µm
4a
4b
50 µm
5a
5b
150 µm
5c
5d
c
c
r
150 µm
5e
c
c
ge
r
5f
25 µm
5g

Distribution of acridine orange in germinated zygotic embryos

At the start of germination the distribution of the fluorescence, caused by acridine orange, was almost uniform. Only the root tip possessed a lower intensity of fluorescence (Figs. 7a and 7b). The region with the low fluorescence varied in size and was sharply delineated from the bright, yellow-green fluorescent part of the embryo (Fig. 7b, arrow). Besides a difference in fluorescence intensity the two parts also differed in the colour of the fluorescence which was green in the root tip and bright, yellow in the other parts (Fig. 7c, colour plate). In both parts of the embryo the cellular distribution was comparable with the configuration found in the root tip of somatic embryos (Fig. 6e). No specifically fluorescent organelles could be distinguished in the cotyledons (Fig. 7a). Surprisingly, germlings, germinated one to two days before observation, showed a highly fluorescent root tip, green or yellow in colour, comparable with the situation in somatic embryos (Fig. 7d).

Distribution of fluphenazine fluorescence during somatic and zygotic embryogenesis.

The distribution of the fluphenazine fluorescence during carrot embryogenesis is already described in Chapters 2 and 3. In somatic embryos the signal changed from evenly distributed to clearly polarized and appeared to have a vacuolar origin. High magnification UV confocal images (Fig. 8) confirmed the vacuolar presence of fluphenazine fluorescence. The size of the fluorescent cell parts increased in the direction from embryo base to embryo top (Figs. 8a to 8c).

Figure 4. The distribution of acridine orange in a proembryogenic mass before the initiation of embryogenesis. **a.** Epi-fluorescence image showing a low and almost uniformly distributed fluorescence. **b.** The bright field image of a.

Figure 5. The distribution of acridine orange in a suspension culture of carrot after the initiation of embryogenesis. **a.** A proembryogenic mass 2 d.a.i. with a highly fluorescent group of cells (arrow) between less fluorescent ones. **b.** The bright field image of a. **c.** Two heart-shaped somatic embryos with a clearly polarized distribution of acridine orange fluorescence. **d.** The bright field image of c. **e.** A torpedo-shaped somatic embryo with an almost totally fluorescent lower part and a sharp border (arrow) with the non-fluorescent region. **f.** The bright field image of e. **g.** High magnification of the hypocotyl showing the accumulation of acridine orange in the central vacuole of the protoderm. **h.** Colour plate. A germinated somatic embryo showing five regions differing in colour and nature of acridine orange fluorescence. 1. cotyledons, 2. hypocotyl, 3. root hair zone, 4. root tip, 5. root tip with calyptra.

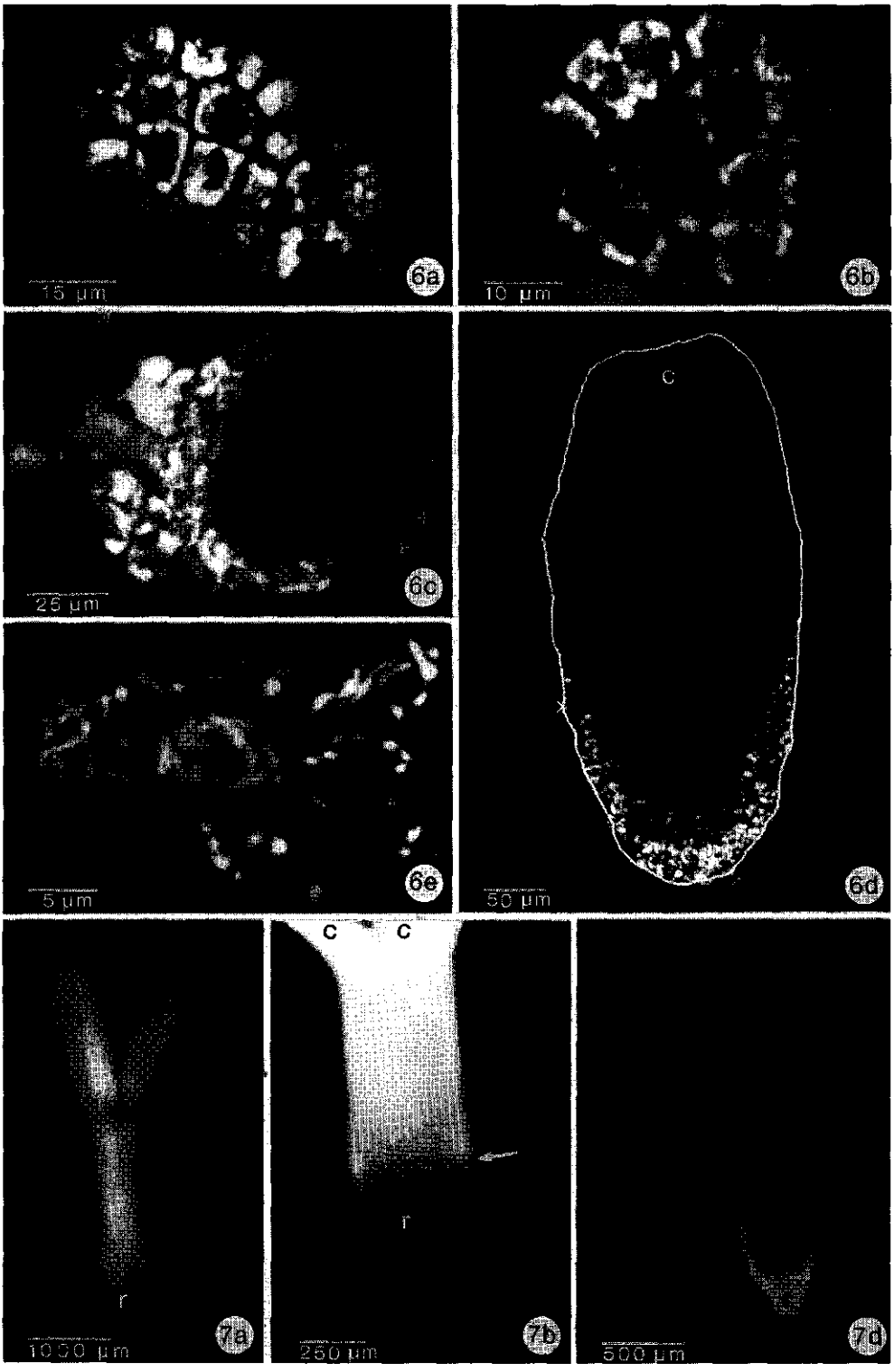
15 µm
6a
10 µm
6b
25 µm
6c
c
50 µm
6d
5 µm
6e
c
c
r
1050 µm
7a
r
250 µm
7b
500 µm
7c

Effects of A23187, EGTA or propionic acid on the distribution of neutral red, acridine orange or fluphenazine fluorescence

The distribution of the three probes used, observed after incubation of somatic embryos for one hour in A23187, EGTA or propionic acid, changed markedly but almost similarly. The addition of A23187 to the growth medium had no perceptible effect on the distribution of the signal from neutral red (not shown), acridine orange (Fig. 9a) or fluphenazine (Fig. 9b). The addition of EGTA, alone or in combination with A23187, led to a decrease of the signal with the three probes used. With neutral red, both the amount of stained organelles and the size of them decreased (not shown). The signal of acridine orange almost totally disappeared in most embryos (Fig. 9c), but a small number of them showed a faint, green fluorescence, restricted to the base of the embryo. Erratically distributed, intensely fluorescent regions, comparable with intensely stained regions after neutral red staining, were present (Fig. 9c). These regions, most likely, represent cells which are damaged by the treatment with EGTA. The results obtained with fluphenazine (Fig. 9d) were as those described for acridine orange. The addition of propionic acid led to a uniform distribution of the three probes used (Figs. 9e and 9f). The signal also changed from specifically organelle-bound to a less distinct distribution.

Figure 6. Confocal images of the distribution of acridine orange in different developmental stage of carrot somatic embryogenesis. **a.** Optical section through a globular embryo showing the accumulation of acridine orange in the vacuolar system. **b.** A globular embryo with a higher amount of fluorescence in the protoderm. **c.** Polarized localization of acridine orange fluorescence in a globular embryo. Fluorescence is almost totally restricted to the base. **d.** A torpedo-shaped embryo with a gradient in fluorescence intensity from cotyledon side to root side of the embryo. The white line marks the contour of the embryo. **e.** Optical section through the protoderm at the root side of a torpedo-shaped embryo at high magnification showing the accumulation of acridine orange in the vacuolar system, which consists of vesicles connected with tubules.

Figure 7. The distribution of acridine orange in germinated zygotic embryos of carrot. **a.** A seedling shortly after the induction of germination. Note the low level of fluorescence of the root tip. **b.** A seedling, one day after the stage as shown under a, with a strong fluorescent upper part and a sharp border (arrow) with the lower part, considerable in size, which is almost non-fluorescent. **c.** Colour plate. Higher magnification of the border region between the fluorescent upper part and the less fluorescent lower part of the embryo from b. Note the change in colour from green to yellow in the direction from root tip to cotyledons. **d.** A seedling, five days after the stage as shown under a, with the fluorescence restricted to the extreme root tip of the plantlet.

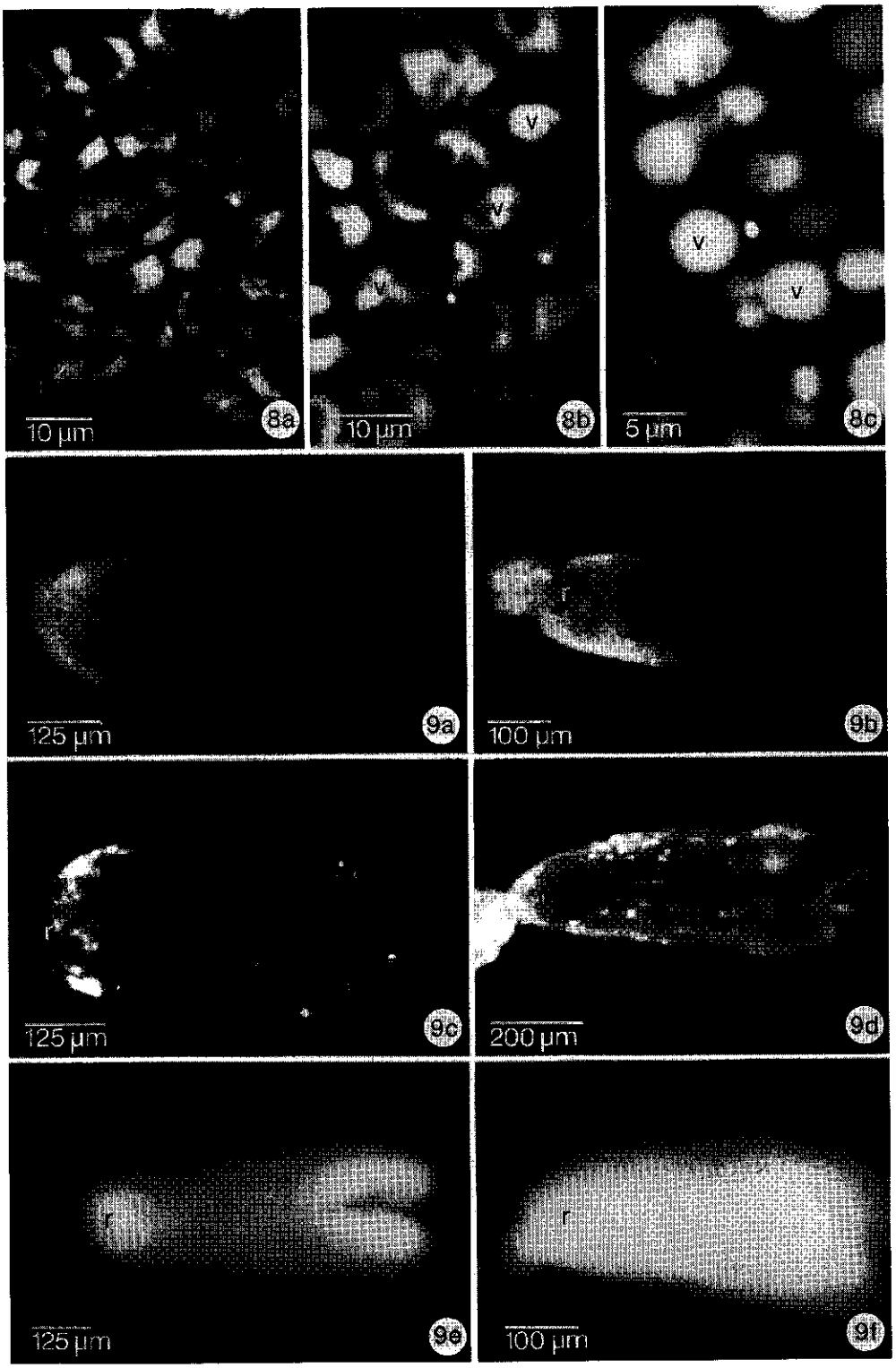
v
v
v
v
v
10 µm
8a
10 µm
8b
5 µm
8c
125 µm
9a
100 µm
9b
r
125 µm
9c
200 µm
9d
r
125 µm
9e
r
100 µm
9f

Figure 8. UV-confocal images of fluphenazine fluorescence of the outer cell layer in different regions of a torpedo-shaped somatic embryo of carrot. **a.** The extreme root tip with small fluorescent organelles. **b.** The fluorescence pattern some 50 μm above the region shown in a. The fluorescence pattern indicates to a presence of the signal in vacuoles. **c.** The middle of the embryo, about 100 μm above the region shown in a. Again the signal is present in the vacuoles which have reached a considerable size.

Figure 9. The effect of treatments with A23187, EGTA and propionic acid on the distribution of acridine orange and fluphenazine fluorescence in torpedo-shaped somatic embryos of carrot. **a.** A23187 and acridine orange. No change in the pattern due to the treatment with A23187 is obvious. **b.** A23187 and fluphenazine. As with acridine orange no change can be observed. **c.** EGTA and acridine orange. The signal almost totally disappears. The strongly fluorescent spots are damaged cells. **d.** EGTA and fluphenazine. The signal is reduced considerably in intensity. Also here, damaged cells are strongly fluorescent. **e.** Propionic acid and acridine orange. A strong, overall present, signal is observed. **f.** Propionic acid and fluphenazine. As with acridine orange, also here the polarized distribution has disappeared.

DISCUSSION

The distribution of neutral red, acridine orange and fluphenazine during carrot embryogenesis and germination showed striking resemblances between the three probes used. They showed the highest signal in the basal part of the somatic embryo from the oblong to the torpedo-shaped stage, all three were evenly distributed in zygotic embryos and all three reacted in a similar manner to treatments with A23187, EGTA and propionic acid. Differences, however, were also observed. During early stages of germination of zygotic embryos acridine orange fluorescence was very weak in the root tip and a sharp border was present between this region and the strongly fluorescent hypocotyl. Fluphenazine fluorescence was found to be present evenly distributed during this stage of germination (see Fig. 9a, Chapter 3) and increased in intensity in the subsequent stage with an almost exclusive presence in the root tip of the embryo (Fig. 9b, Chapter 3).

At the cellular level the differences between the three probes were more profound. Neutral red accumulated preferentially into small, isolated, spherical vacuoles, while acridine orange and fluphenazine were found in an elaborate network of tubules and vesicles (Figs. 6 and 8). A similar cellular picture was obtained by Cole *et al.* (1990) with carrot cells and protoplasts, shortly after incubation in FITC, and they consider this cell compartment to be the provacuolar apparatus (Buvat & Robert 1979). In the hypocotyl of germinated zygotic embryos both neutral red and acridine orange were present in the large vacuole of the cells of this region

(Figs. 3d and 5g). Fluphenazine fluorescence, however, was never observed in the vacuoles of the hypocotyl.

Neutral red and acridine orange are weak bases and will therefore accumulate, in a pH dependent way, in acidic compartments of cells by an ion-trap mechanism (Oparka 1991). The dye passes the tonoplast as the lipophilic free base, becomes protonated in the vacuolar lumen and is trapped as its cation. The signal intensity depends on the amount of accumulated dye. Both dyes, however, also change the pH of the vacuole. Acridine orange was found to increase the permeability of membranes for protons in tonoplast vesicles of oat and red beet roots and thereby reduced the differences in pH between these vesicles (Pope & Leigh 1988). Felle (1988) described a change in vacuolar pH of *Riccia fluitans* from 5.1 to 5.35 after the addition of 50 μM neutral red. These probes can, therefore, only be used reliably to visualize differences in weak base uptake by vacuoles in different plant cells. They are not effective for the exact measurement of vacuolar pH and only give an impression of the distribution of changes in vacuolar pH along a plant species. Additional limitations concerned with the use of acridine orange as a pH probe are discussed by Palmgren (1991).

Neutral red has been found to stain lysosomes (Allison & Young 1964), acid phosphatase positive granules in HeLa cells (Robbins *et al.* 1964), vacuoles of *Ricinus communis* (Nishimura 1982) and autophagic vacuoles in *Dictyostelium discoideum* (Yamamoto & Takeuchi 1983). Acridine orange has been found to stain lysosomes *in vivo* metachromatically (Koenig 1963, Allison & Young 1964), acid phosphatase multivesicular bodies in HeLa cells (Robbins *et al.* 1964) and the prelysosomal acidic compartment of *Dictyostelium discoideum,* thereby varying in colour from bright yellow to deep orange (Padh *et al.* 1989).

As mentioned above, the elaborate network of tubules which stains with acridine orange and fluphenazine in the root side of the embryo resembles the network described by Cole *et al.* (1990) for carrot cells and protoplasts. These tubules show considerable saltatory movements and are connected with small mobile and highly fluorescent vacuoles, which fuse to form larger vacuoles. A colocalization of acridine orange and calmodulin has been reported for lysosomes in several types of animal cells by Nielsen *et al.* (1987). In *Dictyostelium discoideum*, however, acidic compartments visualized with acridine orange, were clearly distinct from vacuoles which where rich in calmodulin (Zhu & Clarke 1992). Calmodulin immunofluorescence was concentrated in the periphery of contractile vacuoles and proved to be associated with an unconventional myosin. From this, it can be concluded that either calmodulin might be involved in the digestion of cellular material in autophagic vacuoles or is related with the saltatory movements of vacuolar tubules.

The differences, found between the various stages of embryogenesis, strongly suggest that along the longitudinal axis of somatic embryos

distinct differences in the pH_v exist. Large differences in pH_v have been described for many plants and can range from 6.5 to even 1.0 (Kurkdjian & Guern 1989). The staining pattern of neutral red also suggests acidic vesicles, possibly autophagic vacuoles, to be present besides the central vacuole. The pH_v and the pH_c are linked, but respond differently to changes in pH_e. Large changes in pH_e are not followed by large changes in pH_c, but change the pH_v dramatically (Raven 1990). The gradient observed in pH_v, might therefore be linked with a gradient in the pH of the apoplast as was also described for pea roots by Dorhout & Kollöffel (1992). These authors concluded that root cells of pea varied in their proton extrusion activity depending on cell type and location. This corresponds well with the results of Brawley *et al.* (1984) who described an electrical current through carrot somatic embryos which was almost totally carried by protons.

The gradient in pH_v was not found during zygotic embryogenesis. This may reflect the differences between the development of the vacuolar apparatus during somatic and zygotic embryogenesis. The process of vacuolization occurs much earlier in the development of somatic embryos than in zygotic embryos (Schiavone & Cooke 1985). During zygotic embryogenesis an overall reduction in the size of the vacuole occurs (see e.g. Norstog 1972, Van Lammeren 1986). An increase in vacuolar size and the existence of a gradient in pH_v coincide with germination of zygotic embryos. Therefore, we conclude that the development of the vacuole during somatic embryogenesis differs from the development of the vacuole during zygotic embryogenesis and shows resemblances with the development of the vacuole during germination of zygotic embryos.

Fluphenazine.2HCl has been used in a few lower plant systems (Cotton & Vanden Driessche 1987, Haußer *et al.* 1984) and during carrot somatic embryogenesis as a probe for activated calmodulin (Chapter 2). It binds reversibly and rather specifically to the Ca^{2+}/calmodulin complex (Levin & Weiss 1977) and can be photooxidized to fluorescent derivatives, thereby stabilizing the binding to calmodulin (Prozialeck *et al.* 1981). Both the binding of Ca^{2+} as the binding of fluphenazine to calmodulin are pH dependent. The binding of Ca^{2+} to calmodulin decreases with decreasing pH (e.g. Cox *et al.* 1988, Iida & Potter 1986) while the binding of phenothiazines to calmodulin decreases distinctly above pH 8 (Weiss *et al.* 1985). It is, therefore, quite surprising to find the highest amount of activated calmodulin, as indicated by fluphenazine fluorescence, in the most acidic compartment of the cell, i.e. the vacuole. However, fluphenazine should be non-fluorescent when it is not bound to calmodulin which suggest a presence of calmodulin in the fluorescent vacuole. A possible explanation might be that fluphenazine accumulates, in a pH dependent manner, in acidic compartments. There it might bind to the Ca^{2+}/calmodulin complex or aspecifically to calmodulin because of the high concentration of fluphenazine which leads to aspecific binding of the probe to calmodulin (Allan &

Hepler 1989).

The presence of fluphenazine might also have changed the location of calmodulin in the vacuole. If calmodulin is present in the tonoplast, bound to calmodulin-binding proteins, fluphenazine competes in binding with these proteins and releases calmodulin from them, resulting in free floating calmodulin in the vacuole.

The results with EGTA and propionic acid are also difficult to explain. Since a low signal from fluphenazine following a treatment with EGTA is accompanied by a low signal from acridine orange and neutral red, it appeared that a treatment with EGTA not only lowered $[Ca^{2+}]_e$ but also increased pH_v which has been reported to be followed by a decrease in $[Ca^{2+}]_v$ (Felle 1988). The free $[Ca^{2+}]_v$ is in the mM range. With a K_d of 10^{-6} this decrease in $[Ca^{2+}]_v$ cannot be enough to influence the binding of calmodulin to Ca^{2+} under normal physiological conditions. Therefore, we conclude that, from the results obtained, it is impossible to deduce whether the fluphenazine fluorescence reflects the distribution of activated calmodulin or results from accumulation of fluphenazine in acidic compartments (see also discussion Chapter 3). Another point against the presence of calmodulin in the vacuole is that, considering the low pH and the presence of possibly inhibiting phenolic compounds, it is unlikely to find the localization of biosynthetic reactions in the vacuole (see also Strack *et al.* 1987).

Summarizing, we conclude that a full explanation of the distribution patterns of neutral red, acridine orange and fluphenazine is not possible with just the results presented here, and needs further research. However, the distribution pattern of these three dyes shows marked differences between somatic and zygotic embryogenesis and resemblances between somatic embryogenesis and zygotic embryo germination.

CHAPTER 7

A COMPARATIVE STRUCTURAL STUDY OF SOMATIC AND ZYGOTIC EMBRYOGENESIS OF *DAUCUS CAROTA* L.

A.C.J. TIMMERS

Department of Plant Cytology and Morphology, Agricultural University, Arboretumlaan 4, 6703 BD Wageningen, The Netherlands

SUMMARY

A comparative structural study of carrot somatic and zygotic embryogenesis and germination was undertaken to obtain further evidence to interpret differences observed in the distribution of anti-calmodulin, fluphenazine fluorescence, Ca^{2+}, neutral red and acridine orange. The most obvious cellular differences observed between somatic and zygotic embryos were the proportion of vacuolation, the plastid composition and the lipid body content. Somatic embryos and germinated zygotic embryos were rich in vacuoles, while torpedo-shaped zygotic embryos contained only a few small vacuoles per cell. Somatic embryos and germinated zygotic embryos contained large amyloplasts, completely filled with starch grains, while zygotic embryos were almost starchless. Zygotic embryos, however, were rich in lipid bodies, which were not very abundant in somatic embryos and germinated zygotic embryos. The structural differences noticed are discussed in relation to the distribution of anti-calmodulin, fluphenazine fluorescence, Ca^{2+}, neutral red and acridine orange. It is concluded that distinct structural differences exist between somatic and zygotic embryos of carrot which can be linked with differences in the distribution of anti-calmodulin, fluphenazine, acridine orange and neutral red.

INTRODUCTION

Carrot somatic embryogenesis is often used as a model system for zygotic embryogenesis (e.g. Choi & Sung 1989). In the previous chapters, however, conspicuous differences in the distribution of anti-calmodulin, fluphenazine, acridine orange and neutral red were described for somatic and zygotic embryos. Strong similarities were found in the distribution of these dyes during somatic embryogenesis and during germina-

tion of zygotic embryos. In somatic embryos, calmodulin was found to be especially abundant in plastids located in the protoderm, but in zygotic embryos this distribution pattern was never observed. Therefore, this study was undertaken to ascertain structural and ultrastructural differences between somatic and zygotic embryos of carrot which could possibly be linked with the differences described above.

Carrot somatic embryogenesis has been studied extensively at the light microscopical and electron microscopical level (Halperin & Jensen 1968, Wochok 1973, Street & Withers 1974, Wilson *et al.* 1974), but zygotic embryogenesis was only studied at the light microscopical level (Borthwick 1931). Just one report is available where a comparison is made of the ultrastructure between somatic and zygotic embryos of carrot, but this report focuses mainly on the composition and number of lipid bodies (Dutta *et al.* 1991). Xu & Bewley (1992) investigated the morphological changes occuring during the development of embryos of alfalfa by scanning electron microscopy. They found major differences between somatic and zygotic embryos in the development of the suspensor, the epidermis and the cotyledons.

In this Chapter a comparison of the structure between somatic and zygotic embryos of carrot is made at the light and electron microscopical level, and the differences are discussed in respect of the distribution of anti-calmodulin, fluphenazine, Ca^{2+}, acridine orange and neutral red. The protoderm of somatic embryos has been found to be high in $[Ca^{2+}]_c$ in comparison with the concentration in the other cells of an embryo. Since the ER is considered to be important in the regulation of $[Ca^{2+}]_c$ (Somlyo 1984) $KMnO_4$ was used both as secondary fixative and contrast enhancer to observe differences in the amount or distribution pattern of ER during somatic and zygotic embryogenesis.

Figure 1. Sections through proembryogenic masses of carrot before the initiation of embryogenesis. **a.** A proembryogenic mass consisting of cells varying considerably in cytoplasmic content. **b.** A proembryogenic mass consisting of highly vacuolated cells.

Figure 2. Sections through different developmental stages of somatic embryogenesis of carrot. **a.** A proembryogenic mass 2 d.a.i. consisting of a part with highly vacuolated cells and a part consisting of cytoplasm rich cells. **b.** A higher magnification of the the area outlined in the box in a, showing the difference in vacuolation between proembryogenic and embryogenic cells. **c.** A globular somatic embryo showing the distribution of vacuoles and plastids in this stage. Note the difference between top and base in plastid composition. **d.** A torpedo-shaped embryo showing the distribution of vacuoles and plastids in this stage. Vacuoles are predominantly present in the cortex and plastids vary in their starch content from cotyledons to base. Compare with Fig. 5b and Fig. 8b. **e.** Root side of a torpedo-shaped embryo showing the presence of large amyloplasts (arrows) in this region of the embryo. Compare with Fig. 5d and Fig. 8a.

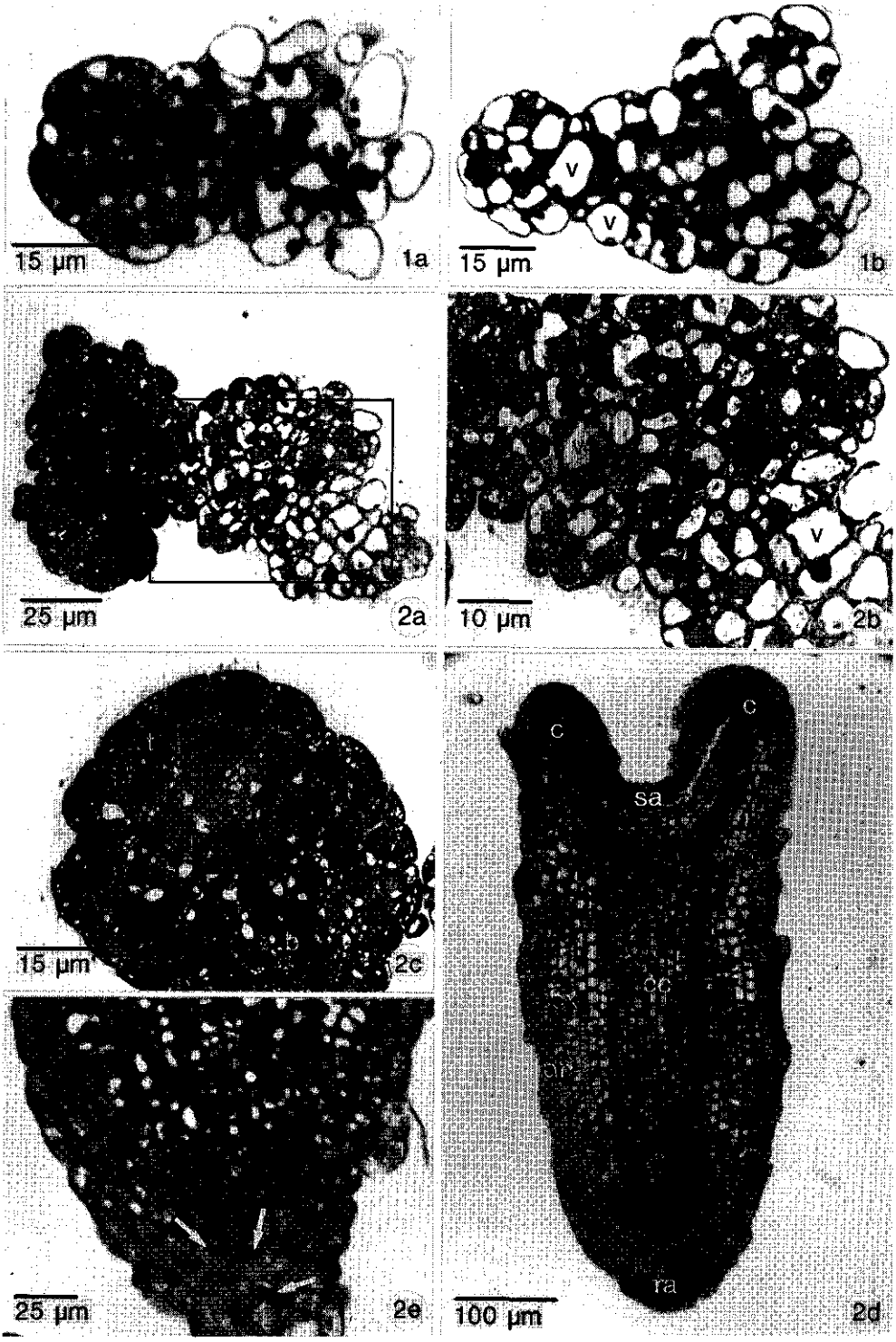
15 µm
1a
v
v
15 µm
1b
25 µm
2a
v
10 µm
2b
15 µm
2c
c
c
sa
cc
ra
25 µm
2e
100 µm
2d

MATERIALS AND METHODS

Plant material and tissue culture conditions

Plant material and tissue culture conditions were as described in Chapter 3.

Specimen preparation for microscopy

Fixation and embedding were the same for all specimens used. Proembryogenic masses, somatic, zygotic and germinated zygotic embryos were fixed in 2.5% glutaraldehyde (Merck) in 0.1 M PIPES buffer, pH 7 (Merck), for 2-3 hours. After two rinses with buffer they were transferred to deionized water on ice. The material was then incubated for 20 min in 6% $KMnO_4$ (Merck) on ice and rinsed with water. Dehydration was performed with ethanol, and Spurr's resin (Serva) was used for embedment. Sections were made with a LKB 8800 Ultratome III. Semithin sections were observed unstained or stained with toluidine blue (1% solution in deionized water). Ultrathin sections were observed with a JEOL 1200 EX II electron microscope at 80 kV.

RESULTS

Somatic embryogenesis

During somatic embryogenesis, from proembryogenic mass to torpedo-shaped embryo, noticeable changes were observed in the proportion of vacuolation and plastid content of the cells. Proembryogenic masses usually had two types of cells (Figs. 1a, 1b). Most cells had a large vacuole and a small amount of cytoplasm in which large plastids, almost totally filled with starch, were present. A few cells in a proembryogenic mass were highly cytoplasmic with small vacuoles, mitochondria, lipid bodies, proplastids, amyloplasts and a large nucleus with a nucleolus which varied in size considerably (Fig. 3).

After initiation of embryogenesis the number of highly cytoplasmic cells increased (Fig. 2a) and embryos arose from these cells. In this stage, proembryogenic masses consisted of cells which varied considerably in vacuole and plastid composition (Fig. 2b). Globular embryos were characterized by cells with small vacuoles and small plastids (Fig. 2c). The starch content of the plastids in-

---

Figure 3. Peripheral proembryogenic cell before the initiation of embryogenesis. Note the large amyloplasts present frequently in cells of this stage of embryogenesis.

Figure 4. Electron microscopical observations of peripheral cells of somatic embryos of carrot. **a.** A protoderm cell from a globular embryo. Ultrastructurally, no obvious differences with the proembryogenic cell, shown in Fig. 3, are observable. **b.** A torpedo-shaped embryo. Besides in the amount of vacuolation no conspicuous ultrastructural differences between the several cell layers are present. Compare with Fig. 6a and Fig. 9a.

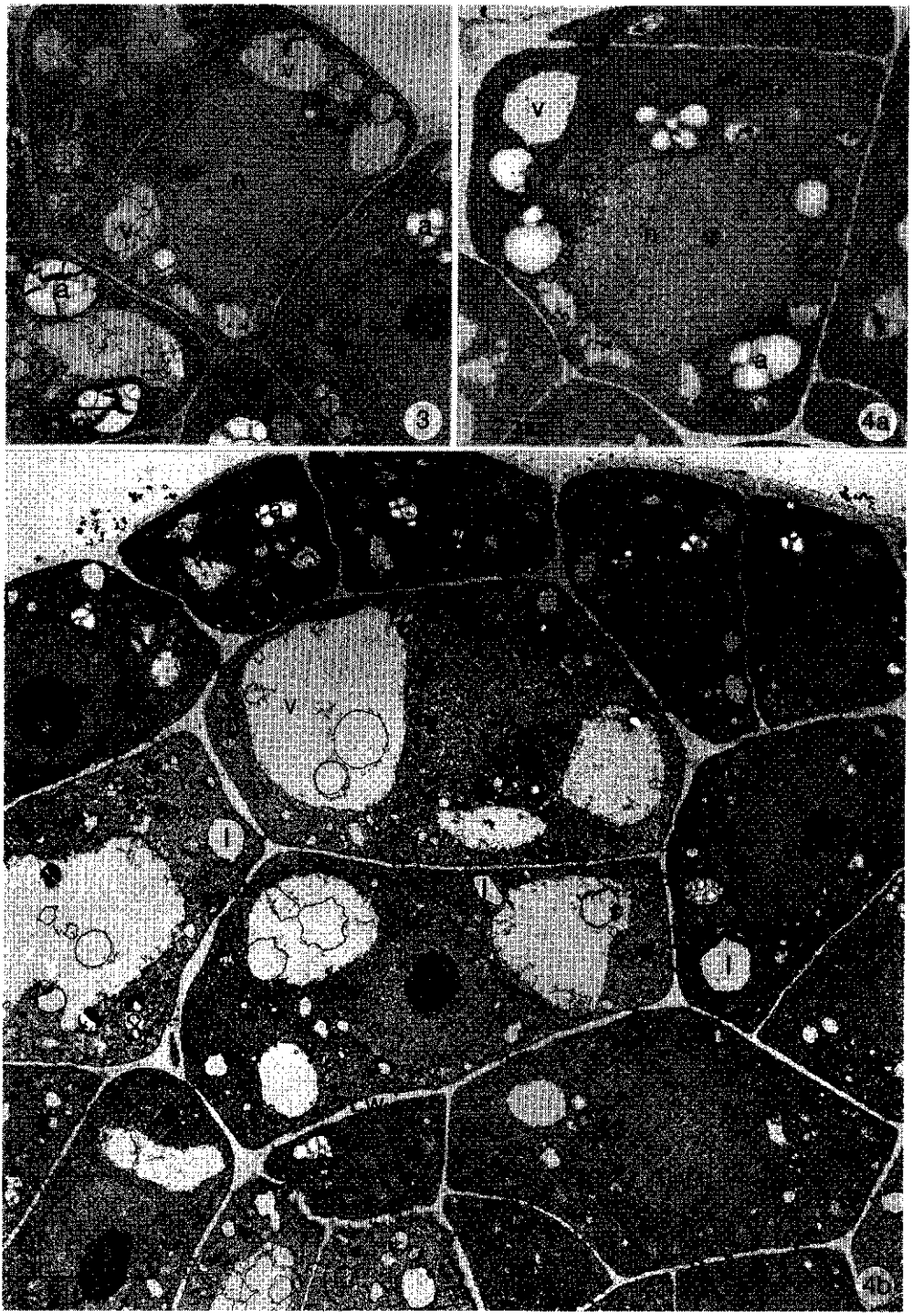
v
v
a
3
v
a
4a
v
v
v
l
l
l
4b

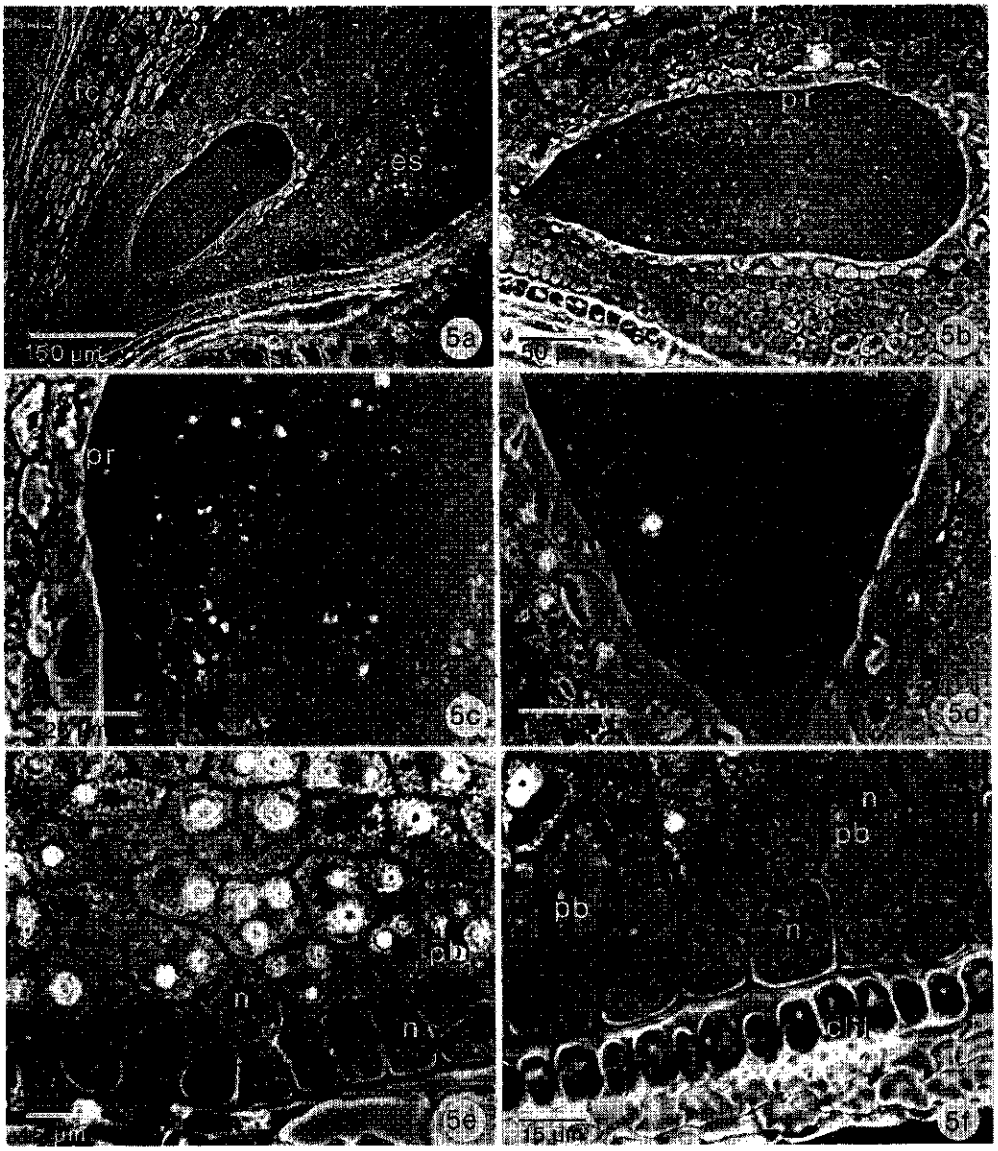

Figure 5. Light microscopical images of sections through immature seeds of carrot. **a.** A part of a longitudinal median section showing the embryo and the surrounding tissues. **b.** Torpedo-shaped embryo showing the uniformity of the different cell layers. Compare with Fig. 2d and Fig. 8b. **c.** High magnification image of the middle of a longitudinal section of a torpedo-shaped embryo. No obvious structural differences between the different cell layers are present. **d.** Section through the root side of the developing embryo with highly cytoplasmic cells. Compare with Fig. 2e and Fig. 8a. **e.** The peripheral cell layers of the endosperm at the concave side of the immature seed showing the difference in structure between the most outer cell layer and the more inner layers. **f.** The peripheral cell layers of the immature seed at the convex side, with the seed coat, consisting of cells which contain a few large chloroplasts.

creased from embryo top to embryo base. Ultrastructurally these cells resembled the highly cytoplasmic cells of proembryogenic masses (compare Fig. 3 with 4a).

Vacuolation was quite obvious in especially the central cells of heart-shaped and torpedo-shaped embryos (Fig. 2d). Large amyloplasts were present in the future root side of these embryos (Fig. 2e, arrows). Besides the level of vacuolation and plastid composition, no striking differences were observed between cells of different cell layers (Fig. 4b). No differences were observed in the amount and distribution of ER between proembryogenic mass cells and embryo cells or between cells from different cell layers of torpedo-shaped embryos.

Zygotic embryogenesis

Of zygotic embryogenesis only heart-shaped and torpedo-shaped embryos were studied. In contrast with somatic embryos, zygotic embryos consisted of cells which were virtually uniform in size, vacuolation and plastid composition (Figs. 5a to 5d). Very prominent was the large nucleus with a large nucleolus (Figs. 5c, 5d). Protoderm cells were slightly smaller than the other cells (Fig. 5c). The large amyloplasts found in torpedo-shaped somatic embryos were totally absent in torpedo-shaped zygotic embryos (Fig. 5d, compare with Fig. 2e).

At the ultrastructural level the large amount of lipid bodies, present in all cells of an embryo, was obvious (Fig. 6a). Proplastids, mitochondria and ER were found in a small amount. Vacuoles were small or totally absent (Fig. 6b). As in somatic embryos, no striking differences were observed between cells of different cell layers (Fig. 6a).

Heart-shaped and torpedo-shaped embryos of carrot were completely surrounded by endosperm (Figs. 5a, 5b). The endosperm which was present as an oval, oblong region at the micropylar end of the seed and which directly surrounded the embryo (Fig. 5a) consisted of cells from which the cell walls were partially digested and the cytoplasm contained a large vacuole and plastids with starch grains (Fig. 7a). Three types of cells were distinguished in the remaining larger part the endosperm from their appearance with phase contrast microscopy and toluidine blue staining intensity. The outer layer of the endosperm was characterized by a darker appearance with phase contrast microscopy (Fig. 5e) and more intense staining with toluidine blue (not shown). Electron microscopical observations of this cell layer showed that a low number of lipid bodies was present in these cells, but that the ER was present conspicuously in a high amount and arranged in parallel layers (Fig. 7b). An other type of cells characterized by a lighter appearance with phase contrast microscopy (Fig. 5a) and weaker staining with toluidine blue (not shown) was present at the extreme micropylar region of the endosperm. Ultrastructurally, no marked differences were observed between these two cell types and the third type of endosperm cells which filled most of the immature seed. The latter type had thick cell walls and was almost com-

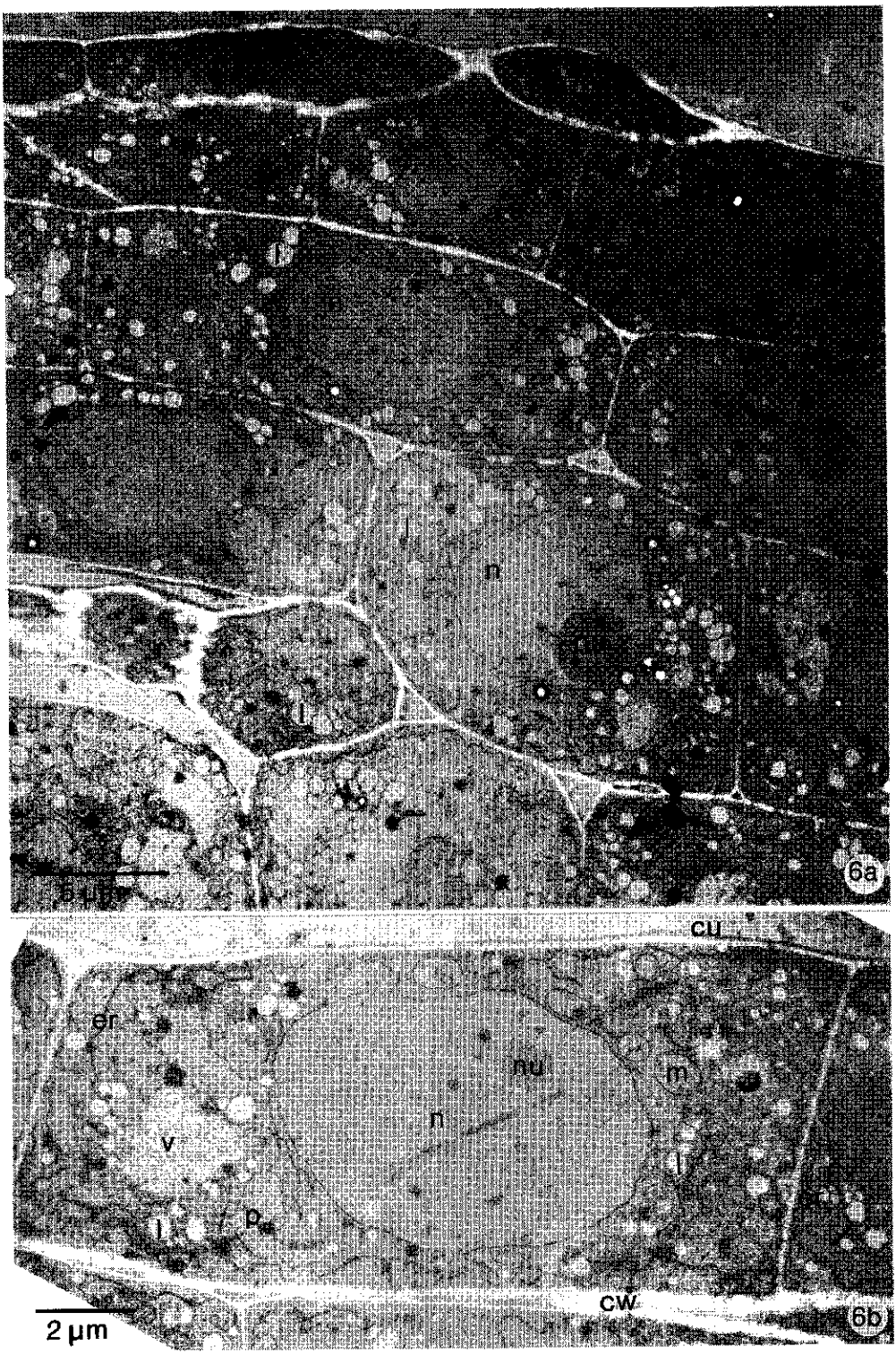
n
l
5 µm
6a
cu
er
nu
m
n
v
l
p_x
cw
2 µm
6b

Figure 6. Electron microscopical observations of the peripheral cells of zygotic embryos of carrot. **a.** A longitudinal section through the hypocotyl showing the uniformity at the ultrastructural level of the four peripheral cell layers. Compare with Fig. 4b and 9a. **b.** A protoderm cell. Note the presence of lipid droplets and the absence of amyloplasts.

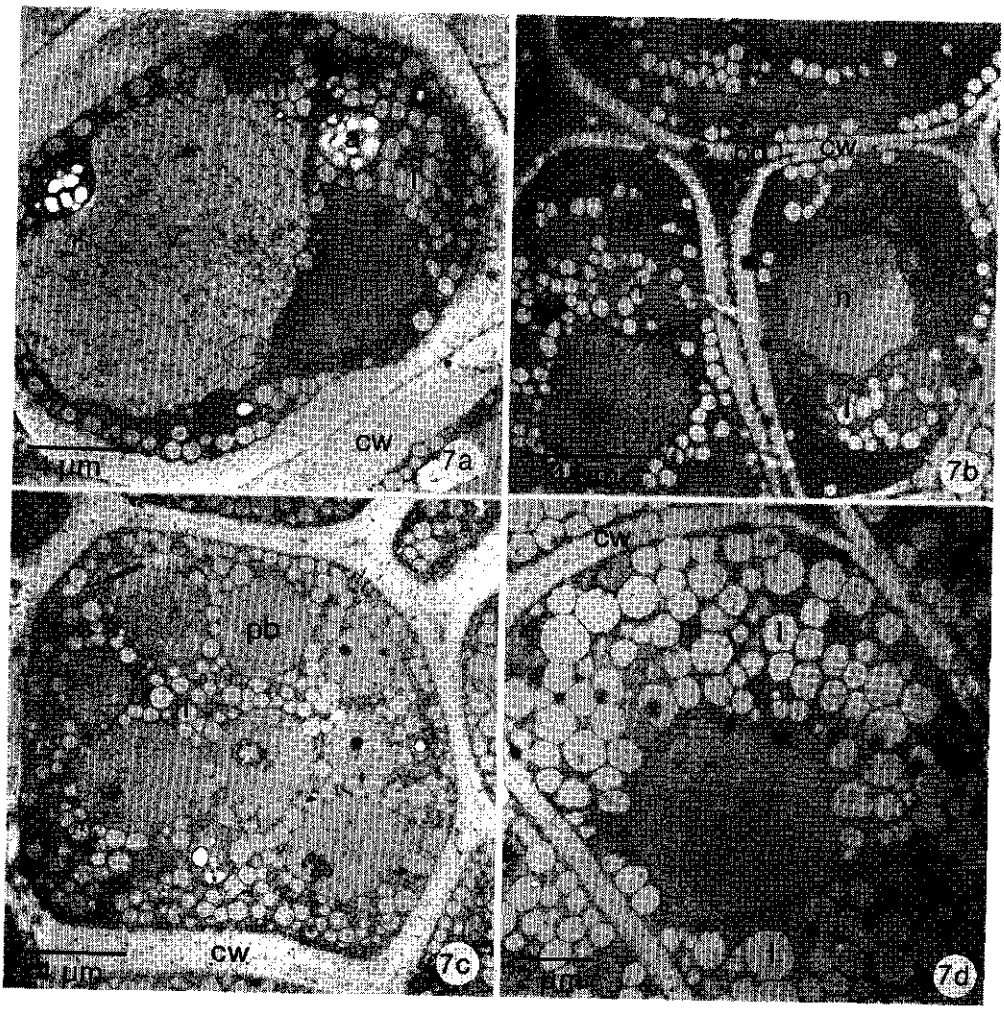

Figure 7. Electron microscopical observations of the endosperm of immature seeds of carrot. **a.** A cell of the endosperm directly surrounding the embryo. The cell walls are very thick and the cells contain amyloplasts and lipid droplets together with a large vacuole. **b.** The outermost cell layer at the concave side of the endosperm showing the high ER content of these cells. **c.** A cell in the middle of the endosperm, containing large protein bodies, some with electron dense inclusions, and a great number of lipid droplets. **d.** A cell in the middle of the endosperm, with only lipid droplets.

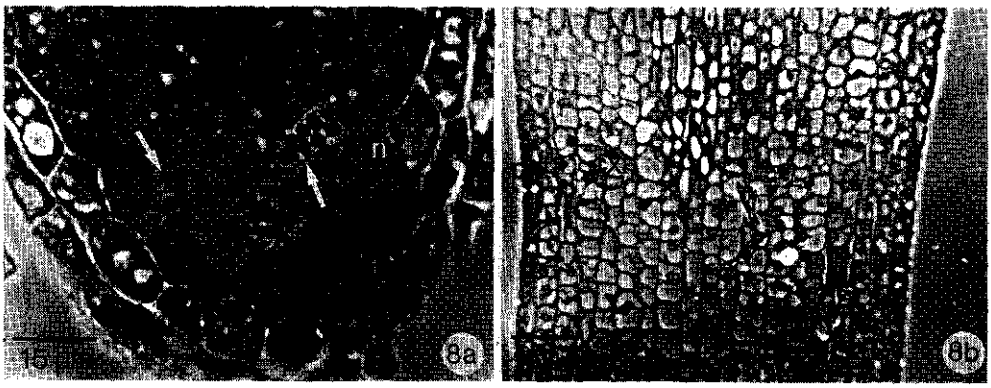

Figure 8. Light microscopical images of longitudinal sections through germinated zygotic embryos of carrot. **a.** Section through the root side of a germling, showing the presence of large amyloplasts (arrows). Compare with Fig. 2e and Fig. 5d. **b.** The hypocotyl showing the difference in vacuolation between the different cell layers in this region of the germling. Compare with Fig. 2d and Fig. 5b.

pletely filled with lipid bodies (Fig. 7d). A number of them contained large protein bodies enclosing globoids of various sizes and angular shapes (Fig. 7c). Jacobsen *et al.* (1976) titled these organelles as the aleurone grains in endosperm of *Apium graveolens*.

The endosperm was surrounded by integuments. At the convex side of the mericarp the first integumental layer was a chloroplast containing cell layer (Fig. 5a and 5f) which was absent at the other side of the mericarp (Fig. 5a). The cells had a few large chloroplasts and a large central vacuole.

Germination

Germination of zygotic embryos of carrot was characterized by marked changes in the plastid composition and changes in the proportion of vacuolation. Cells varied in their plastid composition according to their location. Large amyloplasts were observed only in the root region of the seedling and they were very conspicuous in the calyptra cells (Figs. 8a and 9b). The size and starch content of the amyloplasts increased from the centre to the periphery of the calyptra (Fig. 9a). Epidermal cells of seedlings in this region were characterized by a large nucleus with a very large nucleolus (Fig. 9c). The cytoplasm further included some proplastids, mitochondria, lipid bodies, ER and numerous ribosomes. Vacuoles were either absent or very small. Ultrastructurally, these cells resembled the cells of the root meristem (compare Fig. 9c with Fig. 9d).

Vacuolation was especially present in cells of the cortex of the hypocotyl region of the young seedling (Figs. 8b and 9e). Vacuoles increased in size from epidermis to stele and appeared to exist of vesicles connected

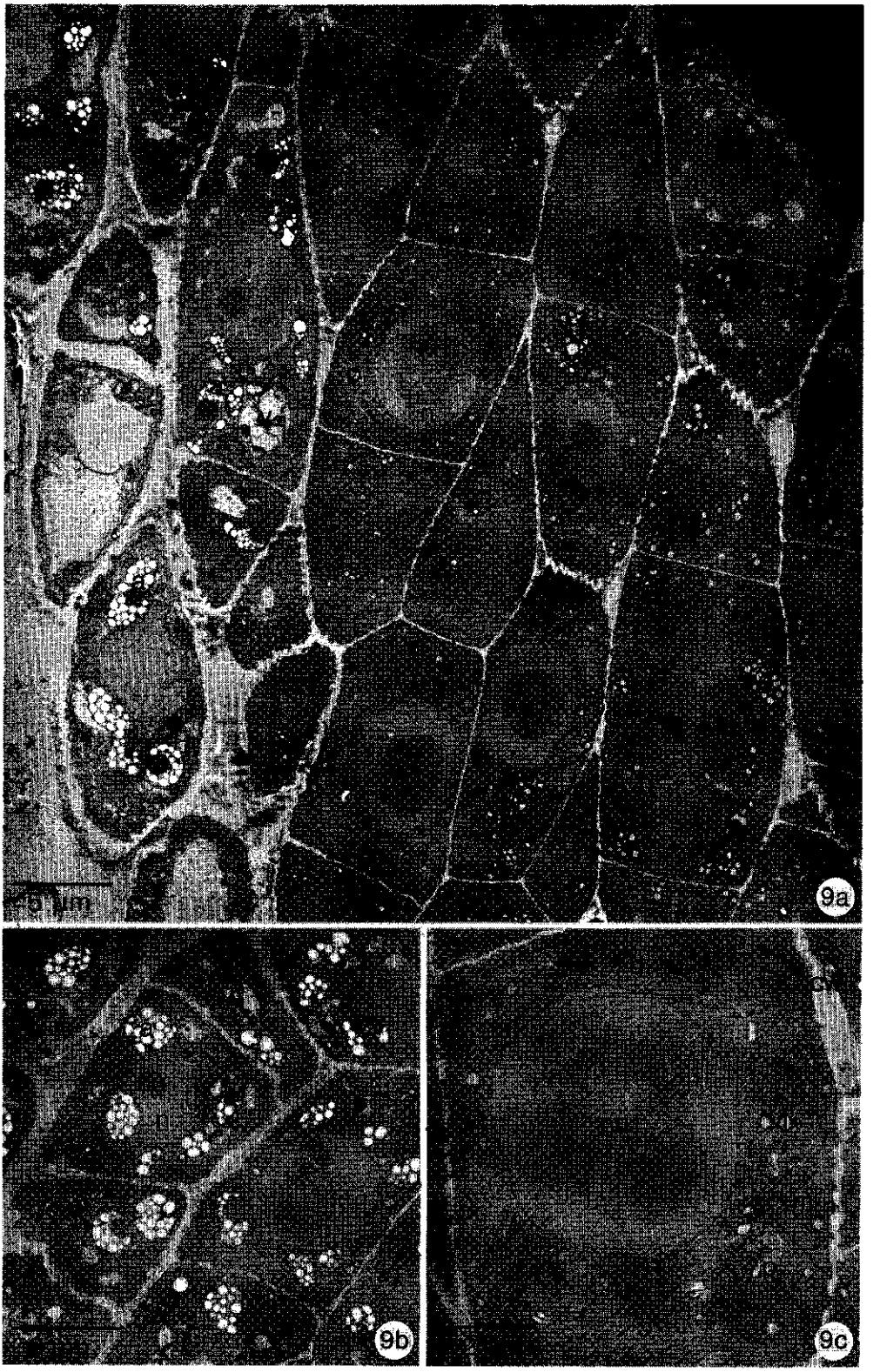
50 µm
9a
9b
9c

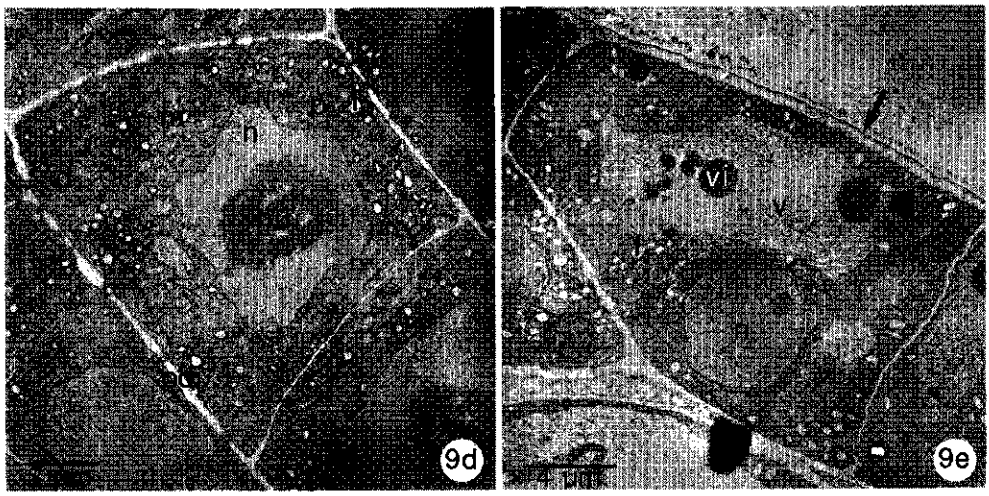

Figure 9. Electron microscopical observations on longitudinal sections through germinated zygotic embryos of carrot. **a.** Overview of a part of the root tip, showing the differences in plastid composition and vacuolation of the different cell layers. Compare with Fig. 4b and Fig. 6a. **b.** Calyptra and root tip cells, containing a number of large amyloplasts. Note the size of the nucleolus in comparison with the size in Fig. 9c. **c.** Epidermal cell at the root side of a germling. The cell contains a large nucleus with a prominent nucleolus, numerous proplastids, mitochondria, dictyosomes and some ER profiles. **d.** Root meristem cell. Compare with Fig. 9c and note the resemblance. **e.** Epidermal cell in the hypocotyl of a germling, containing a large vacuole with a few non-identifiable spherical inclusions. The arrow indicates the cuticle. Compare with Figs. 3, 4 and 6.

by tubules. A clear cuticle was observed on the outer walls of the epidermal cells in this region (Fig. 9e, arrow).

DISCUSSION

The most distinct cellular differences between somatic and zygotic embryogenesis of carrot observed in this study are the proportion of vacuolation, the plastid composition and the lipid body content of the embryo cells. The proportion of vacuolation was found to be high in proembryogenic masses, low in early stages of somatic embryogenesis and to increase again from the stage of the heart-shaped embryo (see also Halperin & Jensen 1967). On the contrary, the proportion of vacuolation was very low during zygotic embryogenesis, which corresponds to the general decrease in vacuolation during zygotic embryogenesis (Buvat 1989). An increase in the proportion of vacuolation was not found before germination of zygotic embryos. This dif-

ference in vacuole size and number between somatic and zygotic embryos of carrot was also described by Schiavone & Cooke (1985).

Plastids in proembryogenic masses were usually filled with large starch grains. In early stages of somatic embryogenesis the starch content was low but it increased in later stages, especially at the future root side of the embryo, as was also found by Halperin & Jensen (1967). In comparison, zygotic embryos contained no plastids filled with large starch grains but they contained only small plastids with short membrane profiles and sometimes small starch grains. However, in the root tip of germinated zygotic embryos amyloplasts were very conspicuous, particularly in the calyptra cells.

Somatic embryos of carrot differ in their lipid body number, but ordinarily only a few lipid bodies per cell were observed during this study. All cells of a zygotic embryo of carrot were found to contain abundant lipid bodies. During germination the lipid body number was low in comparison with the number in zygotic embryos and it resembled the number in somatic embryos. The lipid body number and area occupied by lipid bodies per cell in somatic embryos, however, are strongly dependent on the sucrose and sorbitol content of the medium (Dutta *et al.* 1991). According to these authors, differences in lipid body composition and number do not exist between somatic embryos and early stages of zygotic embryogenesis. Nevertheless, in the present study, cells in the later stages of development of zygotic embryos were found to be filled with compressed lipid bodies, along with some protein bodies.

In the previous Chapters the localization of calmodulin, Ca^{2+} and the distribution of neutral red and acridine orange during somatic and zygotic embryogenesis of carrot have been described. In somatic embryos, calmodulin was found to be associated with plastids, present in the protoderm, but in zygotic embryos, calmodulin was more restricted to the cytoplasm and distributed more uniformly. From the results of this study it can be concluded that calmodulin is predominantly present in starch containing plastids in the protoderm of somatic embryos, which are absent in the protoderm of zygotic embryos. They are present again in calyptra cells during germination and then also are calmodulin positive (Chapter 3). Although not completely clear from earlier results (see Chapter 6), also the distribution of fluphenazine might be linked with the starch content of plastids in the protoderm of somatic embryos. From apex to base both the starch content of plastids in the protoderm and the signal of fluphenazine increases. The possible implications of this with regard to a role of calmodulin in gravitropism or the regulation of starch biosynthesis were already discussed in detail in Chapter 3.

The high content of calmodulin found in the outer layer of the endosperm coincides with a high membrane content of this cell layer. Since the association of calmodulin with a variety of intracellular membranes, especially SER, is described for rat cerebellum cells (Lin *et al.* 1980), also in these endosperm cells cal-

modulin might be present, bound to membranes or sequestered in the lumen of the ER.

During somatic embryogenesis fluphenazine, acridine orange and neutral red staining was almost completely restricted to the base of the embryo, but evenly distributed in zygotic embryos (Chapter 6). These differences in distribution between zygotic and somatic embryos are linked with differences in vacuolation between these two. Vacuoles are absent or very small in zygotic embryos but abundant in somatic embryos and during germination of zygotic embryos. No further structural signs for the observed differences along the longitudinal axis of somatic embryos and germinated zygotic embryos in neutral red or acridine orange distribution were found.

The $[Ca^{2+}]_c$ was found to be high in the protoderm during somatic embryogenesis (Chapter 5). In this study we did not find any correlation between the proportion of ER, vacuolation or any other ultrastructural sign, and the differences observed in $[Ca^{2+}]_c$.

Somatic embryogenesis of carrot is regarded to be quite similar with zygotic embryogenesis of carrot (e.g. Choi & Sung 1989). In this study, however, it has been shown that during their development, distinct structural differences exist between somatic and zygotic embryos. Remarkable structural similarities exist between somatic embryos and germinated zygotic embryos. Some of the differences could be linked with differences in the distribution of anti-calmodulin, fluphenazine, acridine orange and neutral red, but not with differences in $[Ca^{2+}]_c$.

CHAPTER 8

GENERAL DISCUSSION

EMBRYOGENESIS OF CARROT

Somatic embryogenesis: proliferation and embryo initiation

A suspension culture of carrot has two manifestations: 1. The proliferating culture, grown in the presence of 2,4-D, composed of single cells of various shapes and sizes, and cell clusters, comprised of vacuolated cells or cells rich in cytoplasm, or a mixture of the two. 2. The embryogenic culture, grown in the absence of 2,4-D, in which, besides the components of the proliferating culture, embryos in different developmental stages are present. Fujimura & Komamine (1980) revealed four phases in the early process of embryogenesis, designated phase 0 to phase 3 (Fig. 1). In phase 0, competent single cells (state 0) form proembryogenic masses (state 1) in the presence of auxin. During this phase the induction of embryogenesis occurs and the proembryogenic masses gain the ability to develop to embryos when auxin is removed from the medium. The subsequent phase, phase 1, starts by transfer of state 1 proembryogenic masses to the auxin-free medium. During phase 1, proembryogenic masses proliferate slowly and apparently without differentiation. After this phase, rapid cell divisions occur in certain parts of the proembryogenic mass, leading to the formation of globular embryos. This phase is designated phase 2. In the final phase, phase 3, plantlets develop from globular embryos through heart-shaped and torpedo-shaped embryos.

During this study the greatest diversity of localizations with probes for cytosolic free Ca^{2+}, calmodulin and vacuolar pH was observed in proembryogenic masses (state 1), competent to form embryos. Hence it appears that, although the presence of 2,4-D in the medium prevents the outgrowth of embryos, it apparently does not prevent the cells of proembryogenic masses from obtaining structural properties characteristic for cells of embryos. In the presence of 2,4-D embryo initiation does take place but the subsequent coordinated growth to globular-shaped embryos is inhibited by 2,4-D which results in cell divisions randomly in orientation, consequently leading to unorganized growth. If, as it appears, the presence of 2,4-D in the medium leads to a continuous change in the physiological state of the cells, expressed as changes in the level of cytosolic free Ca^{2+} and calmodulin and changes in vacuolar pH, the inhibiting action of 2,4-D could result from the prevention, by 2,4-D, of the formation of a physiological state neces-

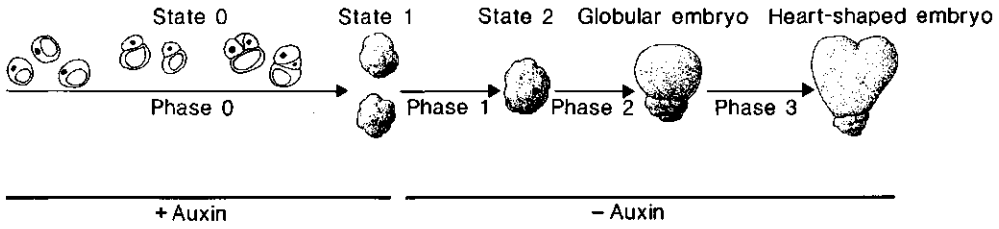

Figure 1. Carrot somatic embryogenesis. Schematic representation of the subsequent stages and phases of development during carrot somatic embryogenesis. (After Komamine *et al.* 1990).

sary for coordinated growth of a group of cells. It has been reported that 2,4-D causes oscillations in $[Ca^{2+}]_c$ and pH in coleoptiles of mays (Felle 1988). This leads to the conclusion that proembryogenic masses are apparently not composed of only undifferentiated suspension cells but also of cells committed to undergo embryogenesis but lacking the possibility of cooperation. The removal of 2,4-D from the growth medium then abolishes the continuous change in the physiological state of the cells, thereby allowing coordinated growth to occur. This is expressed as the growth of a predestined shape, the globular embryo, in which the level and distribution of cytosolic free Ca^{2+} and calmodulin are cooperatively regulated.

Somatic embryos are thought to arise from one superficial cell of a proembryogenic mass after the removal of 2,4-D from the growth medium. However, from the observations described in Chapters 3 and 5, a multicellular origin appears also to occur. Many proembryogenic masses contain, already in medium with 2,4-D, groups of cells with properties characteristic for cells of embryos, but they are not arranged in an embryogenic configuration. Although no serial observations of these groups of cells were made, it is proposed that such a group develops as a whole into an embryo after the removal of 2,4-D from the growth medium. In proembryogenic masses, where at the time of 2,4-D removal such groups were not present, a single cell origin of embryos occurs. In this case, the superficial cells possess the properties characteristic for cells of an embryo in the 2,4-D depleted medium and they directly continue their development into globular embryos. Two modes of somatic embryogenesis, unicellular and multicellular, are also described for *Hevea brasiliensis* (Michaux-Ferrière *et al.* 1992) and might explain the great diversity in localization patterns of free cytosolic Ca^{2+}, calmodulin and vacuolar pH during the initial phases of somatic embryogenesis described in this study.

From the number of processes mentioned in Table 1 in Chapter 1

and the results described in this study it is indisputable that an accurate regulation of $[Ca^{2+}]_c$ and the distribution of calmodulin is important for the proper development of somatic embryos of carrot. To begin with, Ca^{2+} has to be present in the surrounding medium as a prerequisite of any growth and increasing its concentration promotes embryogenesis (Jansen *et al.* 1990). This corresponds with earlier studies on the role of Ca^{2+} in cell growth and proliferation (Hepler 1988), mitosis and cytokinesis (Hepler 1989), organogenesis (Hush *et al.* 1991) and germination (Cocucci & Negrini 1991).

Differentiation of plant cells depends on the presence or absence of certain plant growth regulators such as auxins and cytokinins. These substances also influence the $[Ca^{2+}]_c$ and an interaction between Ca^{2+} and plant growth regulators during somatic embryogenesis seems very probable. As already pointed out in Chapter 5 the continuous presence of a high concentration of 2,4-D in the growth medium could possibly prevent potential embryogenic cells to develop into an organized structure by continuously changing the $[Ca^{2+}]_c$ which, in its turn, leads to a distortion of auxin transport and prevention of a polarized distribution of endogenous auxin necessary to complete embryogenesis (Fujimura & Komamine 1979a).

The synthesis of extracellular substances, such as components of the cell wall and extracellular enzymes, has been reported to be influenced by Ca^{2+} (Penel *et al.* 1986, Brummel & Maclachlan 1989). The high $[Ca^{2+}]$ found in the periphery of somatic embryos might point to a specific role of Ca^{2+} in the synthesis or secretion of extracellular compounds. An example could be the lipid transfer protein from which it is described that its mRNA is relatively abundant in the protoderm of somatic and zygotic embryos of carrot but is present in very small amounts in proembryogenic masses (Sterk *et al.* 1991).

From this study, and studies performed by others (e.g. Dreier *et al.* 1992), it seems very probable that calmodulin is involved in starch metabolism. Both in somatic embryos and in germinated zygotic embryos calmodulin is mainly associated with starch-containing plastids. A first step in somatic embryogenesis could therefore be a change in starch metabolism, or more in general a change in carbohydrate metabolism (Greger & Bertell 1992). This change could be modulated by calmodulin, possibly through reversible phosphorylation of protein kinases present in plastids. Further research on the correlation of carbohydrate metabolism with embryogenesis is therefore expedient and will certainly lead to a more fundamental insight in the regulation of somatic embryogenesis in general.

The high concentration of Ca^{2+} found in especially nuclei of embryos points to a specific role of Ca^{2+} in gene expression during somatic embryogenesis. Differences in gene expression during embryogenesis are mainly quantitative. The protein pattern and gene-expression programs of proembryogenic masses differ little with those of somatic embryos (Wilde *et al.* 1988). There-

fore it appears that a high concentration of Ca^{2+} in the nucleus of a plant cell facilitates the transcription of DNA into RNA, possibly by changing the structure of the chromatin.

Finally, morphogenesis is directly influenced by changes in $[Ca^{2+}]_c$ through the action of Ca^{2+} on the assembly and disassembly of microtubules (Cyr 1991). Marked changes in the orientation of microtubules during somatic embryogenesis of carrot are reported (Wochok 1973) and a role of Ca^{2+} in this process is evident.

Establishment of polarity

The expression of polarity during somatic embryogenesis was found to be completely different from the expression of polarity during zygotic embryogenesis. From the late globular stage on, polarity was perceptible along the longitudinal axis of the embryo in the distribution of fluo-3 and fluphenazine fluorescence, the distribution of neutral red and acridine orange, and in plastid composition (Fig. 2). Very often, these gradients of substances preceded the morphological polarity. From a number of observations, it is suggested that cotyledon development was preceded by or coincided with a high $[Ca^{2+}]$ and with the presence of small particles which obtained an orange colour after neutral red treatment of the embryos. At the root side of the embryos the cells change from having a high signal from fluphenazine, acridine orange and neutral red to a low signal as they become more distant from the root tip. Therefore, in this respect, these cells in the root side change their composition, in contrast to the cells of the cotyledon side of the embryo, resulting in a completely different way of development of the root and cotyledon side of a somatic embryo which is expressed as tissue polarity.

As described in Chapters 2, 3, 5 and 7 these uneven distributions can be linked with polarity in the location of processes, important in plant growth and differentiation, such as carbohydrate metabolism, action of plant growth regulators, gene expression, phosphorylation of proteins and the orientation of microtubuli. Other examples, such as direction of electrical currents and auxin transport, are described by Brawley *et al.* (1984) and Schiavone & Cooke (1985, 1987). The further development of the embryo depends on the proper establishment of this polarity during the transition from the globular to the heart-shaped embryo. The prevention of this establishment, by e.g. heat shock (Zimmerman *et al.* 1989) or addition of 2,4-D (Sung *et al.* 1984), leads to abnormal embryo

Figure 2. Polarity during carrot somatic embryogenesis. Survey of the distribution of fluo-3, anti-calmodulin, fluphenazine, neutral red, acridine orange and plastids during carrot somatic embryogenesis. **a.** Proembryogenic mass. **b.** Several globular-shaped somatic embryos on the surface of a proembryogenic mass. **c.** A proembryogenic mass with one heart-shaped somatic embryo. **d.** Torpedo-shaped somatic embryo.

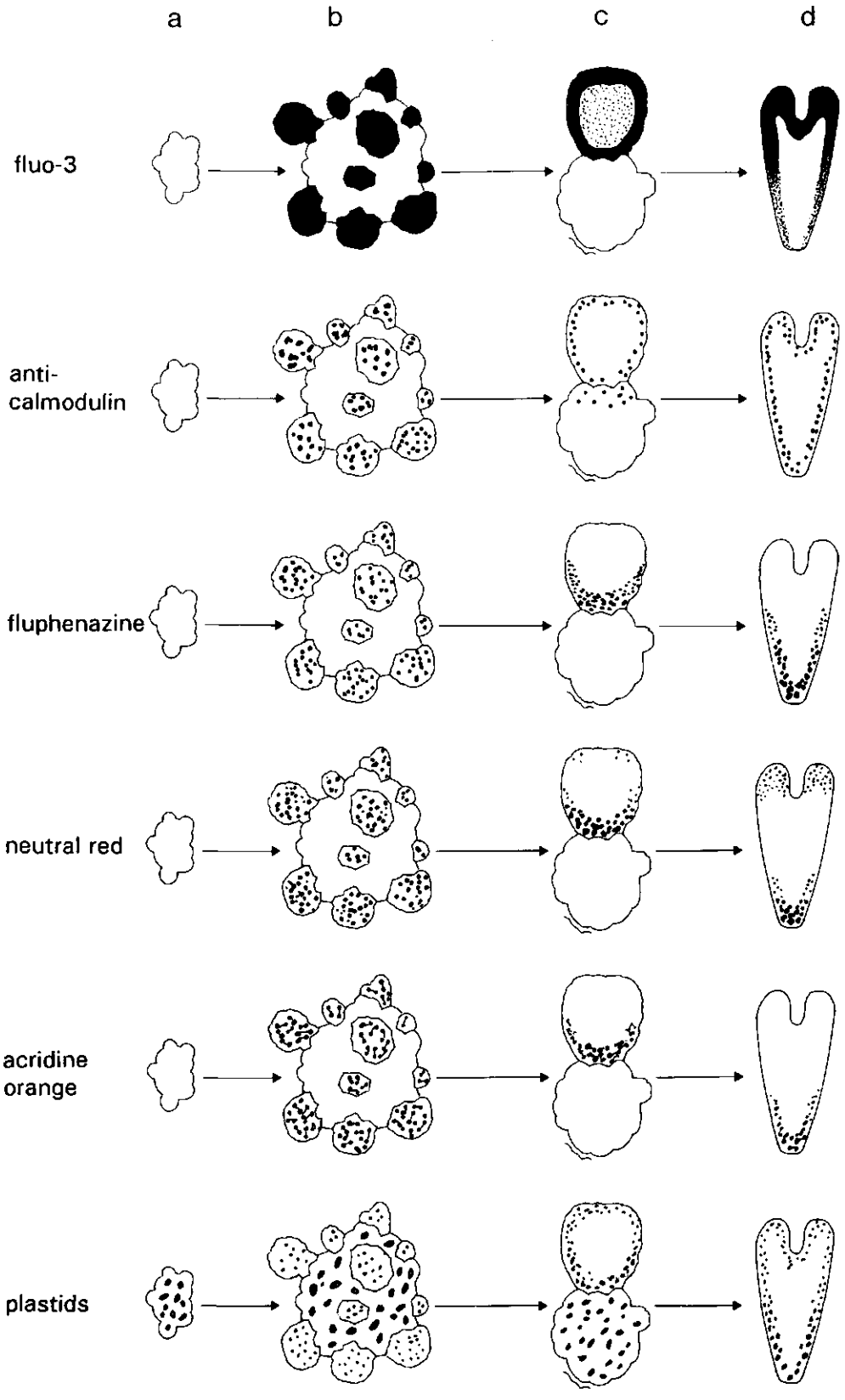
a
b
c
d
fluo-3
anti-
calmodulin
fluphenazine
neutral red
acridine
orange
plastids

growth and giant globular-shaped embryos. It is, therefore, surprising that, during zygotic embryogenesis, besides morphological polarity, any other light microscopical, or even electron microscopical, observable sign of tissue polarity is hard to perceive (Chapters 3, 6 and 7; see also Raghavan 1986 for other plant species). Zygotic embryos are surrounded by endosperm and connected with maternal tissues which are involved in the proper development of the embryo and the establishment of its polarity. During somatic embryogenesis these tissues are absent and the establishment of polarity has to reside in the embryo itself. A comparable expression of tissue polarity in zygotic embryos, as seen during somatic embryogenesis, was not found until germination. From this the conclusion can be made that physiologically somatic embryos resemble germinating zygotic embryos. The absence of dormancy in tissue culture of carrot can then be considered as a direct consequence of this. Somatic embryos develop directly into seedlings, without a period of dormancy, because they already started germination at the beginning of their development, i.e. after transfer of proembryogenic masses to auxin-free medium.

Somatic embryogenesis versus zygotic embryogenesis

Somatic embryogenesis of carrot is considered to be similar to zygotic embryogenesis (Choi & Sung 1989) and it has been a model system for understanding plant embryogenesis since its discovery by Reinert and Steward (Reinert 1958, Steward *et al.* 1958), although comparative studies on zygotic and somatic embryogenesis are very scarce (see e.g. Xu & Bewley 1992 for embryogenesis of alfalfa). From this study, however, it is indisputable that major differences exist between somatic and zygotic embryos of carrot. Taking the results together, instead of resembling zygotic embryogenesis, structurally, the process of somatic embryogenesis resembled to a higher extent the process of zygotic embryo germination.

The most prominent differences between the two types of embryogenesis were the proportion of vacuolation and plastid composition of the embryos. Vacuoles and plastids are the most variable structures with regards to morphology (Buvat 1989), but in addition to the differentiating evolution of the cell, they are influenced by many factors, such as the time of the day and, in tissue culture, medium composition. These differences can therefore be the direct consequence of the differences in osmolarity and nutrient composition of the medium surrounding the somatic or zygotic embryo. Somatic embryos generally grow and develop under hypotonic conditions (Fry 1990), while the fluid surrounding the zygotic embryos is considered to be more isotonic with the embryo (Gates & Greenwood 1991). The optimal sucrose concentrations during embryogenesis *in vitro* are reported to decrease with the development of the embryos. Early stages of embryogenesis of *Datura stramonium* require 8% sucrose for optimal growth, while 0.1-1% is optimal for

mature embryos. More negative osmotic values during early embryogenesis are supposed to slow down growth, thereby permitting normal differentiation and development. Increased levels of sucrose during the culture of mature stages of embryogenesis prevent precocious germination by inhibiting exponentional growth of the embryo (Gates & Greenwood 1991).

The sucrose concentration of the medium was found to influence the number of lipid bodies per cell in torpedo-shaped embryos of carrot also (Dutta *et al.* 1991). Increasing the sucrose concentration from 2% to 4% more than doubled the number of lipid bodies. Cells of torpedo-shaped zygotic embryos contained a high number of lipid bodies, more comparable to the number found in somatic embryos grown in high sucrose concentrations.

The structural differences observed between somatic and zygotic embryos can, accordingly, be regarded as resulting from differences in the composition of the medium surrounding the embryo. It remains unclear wether these differences are not only the consequence of exogenous factors, but are also inherent to the processes of somatic and zygotic embryogenesis and reflect a more fundamental difference between the two. It is obvious, however, that, if compared to *in vivo* plant development, during carrot somatic embryogenesis two processes intermingle, i.e. embryogenesis and germination. For practical plant breeding this could mean that comparative studies on zygotic embryogenesis, germination and somatic embryogenesis of certain plant species, might lead to more insight into the physiology of somatic embryogenesis.

In conclusion, somatic embryogenesis of carrot can be used as a model system for plant morphogenesis, but it should be remembered that somatic embryogenesis differs from zygotic embryogenesis and that comparative studies are needed to transfer results and conclusions obtained from studies of somatic embryogenesis to zygotic embryogenesis.

CONCLUDING TECHNICAL CONSIDERATIONS

Localization of calcium

Calcium can be localized in plant cells by a number of techniques of which three were used in this study. All of them, however, have their drawbacks and their advantages (Caswell 1979, Scarpa 1985, Read *et al.* 1992). Although it was possible to load the fluorescent Ca^{2+} indicator fluo-3 successfully into embryogenic plant cells (Chapter 4) it was found to be impossible to calibrate the $[Ca^{2+}]_c$ adequately (Chapter 5). *In situ* determination of F_{min}, being the fluorescence intensity in the absence of Ca^{2+}, and F_{max}, being the fluorescence intensity at saturating Ca^{2+}, is necessary for a reliable calibration of $[Ca^{2+}]_c$ (Thomas & Delaville 1991). Ca^{2+} ionophores, such as A23187 and ionomycin, and Ca^{2+} chelators, such as EGTA, are used for this purpose. The reaction of plant cells to these chemicals can, however, vary considerably in inten-

sity and speed. Besides permeabilizing the plasma membrane for Ca^{2+}, A23187 also has an effect on its integrity (Kell & Donath 1990). The action of A23187 is strongly pH dependent and not specific for Ca^{2+}. Permeabilizing the plasma membrane with digitonin or CHAPS to increase or decrease $[Ca^{2+}]_c$, as used by e.g. Guiragossian Kiss *et al.* (1991), forms no alternative because this would certainly also lead to dye loss from the cytosol. Quenching the fluorescence with Mn^{2+}, which is successful with quin-2, fura-2 and indo-1, will, unfortunately, not work with fluo-3 (Thomas & Delaville 1991). In addition, the level of fluorescence is dependent on the amount of the probe, which can vary as a result of unequal distribution, due to specific accumulation of the probe, within or between cells.

Consequently, it must be concluded that accurate calibration of $[Ca^{2+}]_c$ using fluo-3 in combination with CSLM is very difficult and always doubtful. The problems can be bypassed to some extent by using dual-excitation dyes such as indo-1. This probe, however, is excited with UV light and UV confocal microscopy is presently repleted with a number of technical problems (Fricker & White 1992). Therefore the conclusion of the foregoing is that the reliable determination of $[Ca^{2+}]_c$ in embryogenic plant cells, with fluorescent probes in combination with CSLM, is not yet possible and awaits further technical improvements.

Localization of calmodulin

Immunolocalization of calmodulin in plant tissues at the light microscopical level is possible after removal of the embedding medium, e.g. polyethylene glycol, or after cryosectioning of unembedded material. Apparently, the antigenic sites are then exposed sufficiently to allow antibody binding. Calmodulin has been detected in this way in a number of plant species (see Chapter 3). The localization at the electron microscopical level proved, however, to be more difficult. No convincing labelling was found in this study after embedment of somatic embryos of carrot in either London Resin White, London Resin Gold or Lowicryl K4M. Also Gubler *et al.* (1990) and Zhu & Clarke (1992) described a notable decrease in antibody binding to calmodulin after resin embedment. The immunolocalization of calmodulin appears to require tissue free of resin and is therefore only feasible at the electron microscopical level after ultrathin cryosectioning or by preembedment labelling techniques.

The results described in this study with fluphenazine require some additional comments. Fluphenazine has been used in some plant systems as a probe for the Ca^{2+}/calmodulin complex, designated as activated calmodulin (Chapters 2, 3 and 6). The signal of fluphenazine was, however, predominantly observed in the vacuole, an organelle of which it is unlikely to expect calmodulin to be present in high amounts (see discussion Chapter 6). Furthermore, differences were found between localization of calmodulin with immunolabelling and with fluphenazine fluorescence (Chapter 3). The signal from fluphenazine changed after

incubation of embryos with Ca^{2+} ionophores and Ca^{2+} chelators, but also after changing the pH of the cytosol with a weak acid like propionic acid. Localization studies of calmodulin with only fluphenazine as the indicator must, therefore, be looked upon with great suspicion, although fluphenazine binds specifically with activated calmodulin *in vitro* (Prozialeck *et al.* 1981), and has been used to isolate calmodulin from tissue extracts (Charbonneau & Cormier 1979).

REFERENCES

Akiyama T, Takagi S, Sankawa U, Inari S, Saito H (1980) Saponin-cholesterol interaction in the multibilayers of egg yolk lecithin as studied by deuterium nuclear magnetic resonance: Digitonin and its analogues. Biochemistry 19:1904-1911

Aleith F, Richter G (1990) Gene expression during induction of somatic embryogenesis in carrot cell suspensions. Planta 183:17-24

Allan E, Hepler PK (1989) Calmodulin and calcium-binding proteins. In: Marcus A (ed) The biochemistry of plants, vol. 15, Molecular biology, Academic Press, New York, pp. 455-484

Allan EEF, Trewavas AJ (1986) The concentration of calmodulin alters during early stages of cell development in the root apex of *Pisum sativum*. In: Trewavas AJ (ed) Molecular and cellular aspects of calcium in plant development. Plenum Press, New York, London, pp. 311-312

Allison AC, Young MR (1964) Uptake of dyes and drugs by living cells in culture. In: Life Sciences, vol. 3, Pergamon Press, pp. 1407-1414

Ammirato PV (1987) Organization events during somatic embryogenesis. In: Green CE, Somers DA, Hackett WP, Biesboer DD (eds) Plant tissue and cell culture. Alan R Liss, New York, pp 57-81

Ammirato PV (1989) Recent progress in somatic embryogenesis. IAPTC Newslett. 57:2-16

Andreev IM, Koren'kov V, Molotkovsky YG (1990) Calmodulin stimulation of Ca^{2+}/nH^{+} antiport across the vacuolar membrane of sugar beet taproot. J. Plant Physiol. 136:3-7

Anraku Y, Ohya Y, Iida H (1991) Cell cycle control by calcium and calmodulin in *Saccharomyces cerevisiae*. Biochim. Biophys. Acta 1093:169-177

Ashley CC, Campbell AK (1979) Detection and measurement of free Ca^{2+} in cells. Elsevier/North-Holland Biomedical Press, Amsterdam, New York, Oxford

Banuelos GS, Bangerth F, Marschner H (1987) Relationship between polar basipetal auxin transport and acropetal Ca^{2+} transport into tomato fruits. Physiol. Plant. 71:321-327

Bednarska E (1991) Calcium uptake from the stigma by germinating pollen in *Primula officinalis* L. and *Ruscus aculeatus* L. Sex. Plant Reprod. 4:36-38

Bhojwani SS, Razdan MK (1983) Plant tissue culture: Theory and practice. Elsevier, Amsterdam, Oxford, New York, Tokyo. pp 91-112

Biro RL, Daye S, Serlin BS, Terry ME, Datta N, Sopory SK, Roux SJ (1984) Characterization of oat calmodulin and radioimmunoassay of its cellular distribution. Plant Physiol. 75:382-386

Blackford S, Rea PA, Saunders D (1990) Voltage sensitivity of H^{+}/Ca^{2+} antiport in higher plant tonoplast suggests a role in vacuolar calcium accumulation. J. Biol. Chem. 265:9617-9620

Blinks JR, Mattingly PH, Jewell BR, Van Leeuwen M, Harrer GC, Allen DG (1978) Practical aspects of the use of aequorin as a calcium indicator: assay, preparation, microinjection and interpretation of signals. Methods Enzymol. LVII:292-328

Blinks JR, Wier WG, Hess P, Prendergast FG (1982) Measurement of Ca^{2+} concentrations in living cells. Progr. Biophys. Mol. Biol. 40:1-114

Böcher M, Erdmann H, Heim S, Wylegalha C (1985) Protein kinase activity of *in vitro* cultured plant cells in relation to growth and starch metabolism. J. Plant Physiol. 119:209-218

Borle AB, Freudenrich CC, Snowdowne KW (1986) A simple method for incorporating aequorin into mammalian cells. Am. J. Physiol. 251:C323-C326.

Borle AB, Snowdowne KW (1987) Methods for the measurement of intracellular ionized calcium in mammalian cells: comparison of four classes of Ca^{2+} indicators. In: Cheung WY (ed) Calcium and cell function, vol. VII, Academic Press, New York, pp. 159-200

Borthwick HA (1931) Development of the macrogametophyte and embryo of *Daucus carota*. Bot. Gaz. 92:23-44

Bourbouloux A, Roblin G, Fleurat-Lessard P (1992) Calcium involvement in the IAA-induced leaflet opening of *Cassia fasciculata*. J. Exp. Bot. 43:63-71

Braam J (1992) Touch-induced regulation of expression of the calmodulin-related TCH genes and thigmomorphogenesis in *Arabidopsis*. In: Karssen CM, Van Loon LC, Vreugdenhil D (eds) Progress in Plant Growth Regulation. Kluwer Academic Publishers, Dordrecht, Boston,

London, pp. 82-95.
Brady RC, Cabral FR, Schibler MJ, Dedman JR (1985) Cellular localization of calmodulin and calmodulin-acceptor proteins. In: Marmé D (ed) Calcium and Cell Physiology. Springer Verlag Berlin, pp. 140-147
Brand JJ, Becker DW (1984) Evidence for direct roles of calcium in photosynthesis. J. Bioenerg. Biomembr. 16:239-248
Brauer M, Sanders D, Stitt M (1990) Regulation of photosynthetic sucrose synthesis: a role for calcium?. Planta 182:236-243.
Brawley SH, Wetherell DF, Robinson KR (1984) Electrical polarity in embryos of wild carrot precedes cotyledon differentiation. Proc. Natl. Acad. Sci. USA 81:6064-6067
Brownlee C (1987) Microelectrode techniques and plant cells. In: Standen NB, Gray PTA, Whitaker MJ (eds) Microelectrode techniques. Cambridge, The Company of Biologists Limited
Brownlee C, Wood JW (1986) A gradient of cytoplasmic free calcium in growing rhizoids of *Fucus serratus*. Nature 320:624-626
Bruck DK, Walker DB (1985) Cell determination during embryogenesis in *Citrus jambhiri*. II. Epidermal differentiation is a one-time event. Am. J. Bot. 72:1602-1609
Brummel DA, Hall JL (1987) Rapid cellular responses to auxin and the regulation of growth. Plant Cell Environ. 10:523-543
Brummel DA, Maclachlan GA (1989) Calcium antagonist TMB-8 inhibits cell wall formation and growth in pea. J. Exp. Bot. 40:559-565
Bush DS (1992) The role of Ca^{2+} in the action of GA in the barley aleurone. In: Karssen CM, Van Loon LC, Vreugdenhil D (eds) Progress in Plant Growth Regulation. Kluwer Academic Publishers, Dordrecht, Boston, London, pp. 96-104
Bush DS, Jones RL (1987) Measurement of cytoplasmic calcium in aleurone protoplasts using Indo-1 and Fura-2. Cell Calcium 8:455-472
Bush DS, Jones RL (1988) Cytoplasmic calcium and α-amylase secretion from barley aleurone protoplasts. Eur. J. Cell Biol. 46:466-469
Bush DS, Sticher L, Huystee RV, Wagner D, Jones RL (1989) The calcium requirement for stability and enzymatic activity of two isoforms of barley aleurone α-amylase. J. Biol. Chem. 264:19392-19398
Bush RD, Sze H (1986) Calcium transport in tonoplast and endoplasmic reticulum vesicles isolated from cultured carrot cells. Plant Physiol. 80:549-555
Butcher R, Evans DE (1986) The control of calmodulin synthesis and localisation in pea root tissue. In: Trewavas AJ (ed) Molecular and cellular aspects of calcium in plant development. Plenum Press, New York, London, pp. 319-320
Buvat R (1989) Ontogeny, cell differentiation, and structure of vascular plants. Springer-Verlag, Berlin
Buvat & Robert (1979) Vacuole formation in the actively growing root meristem of barley (*Hordeum sativum*). Am. J. Bot. 66:1219-1237
Campbell AK (1983) Intracellular calcium. J. Wiley & Sons, New York, pp. 85-134
Caswell AH (1979) Methods of measuring intracellular calcium. Int. Rev. Cytol. 56:145-181
Charbonneau H, Cormier M (1979) Purification of plant calmodulin by fluphenazine-sepharose affinity chromatography. Biochem. Biophys. Res. Commun. 90:1039-1047
Chaubal R, Reger BJ (1992) Calcium in the synergid cells and other regions of pearl millet ovaries. Sex. Plant Reprod. 5:34-46
Chée RP, Cantliffe DJ (1989) Inhibition of somatic embryogenesis in response to 2,3,5-triiodobenzoic acid and 2,4-dichlorophenoxyacetic acid in *Ipomoea batatas* (L.) cultured *in vitro*. J. Plant Physiol. 135:398-403
Choi JH, Sung ZR (1989) Induction, commitment, and progression of plant embryogenesis. In: Kung S-D, Arntzen CJ (eds) Plant Biotechnology. Butterworth, Boston, London, pp. 141-160
Clarkson DT, Brownlee C, Ayling SM (1988) Cytoplasmic calcium measurements in intact higher plant cells: results from fluorescence ratio-imaging of fura-2. J. Cell Sci. 91:71-80
Cocking EC (1987) Plant cell biology in the 21st century: The needs of plant cell and tissue culture. In: Green CE, Somers DA, Hackett WP, Biesboer DD (eds) Plant Tissue and Cell Culture. Plant Biotechnology vol. 3, Alan R. Liss, New York, pp. 3-15
Cocucci M. Negrini N (1991) Calcium-calmodulin in germination of *Phacelia tanacetifolia* seeds:

effects of light, temperature, fusicoccin and calcium-calmodulin antagonists. Phys. Plant. 82:143-149

Colbeau A, Nachbaur J, Vignais PM (1971) Enzymatic characterization and lipid composition of rat liver subcellular membranes. Biochim. Biophys. Acta 249:462-492

Cole L, Coleman J, Evans D, Hawes C (1990) Internalisation of fluorescein isothiocyanate and fluorescein isothiocyanate dextran by suspension-cultured carrot cells. J. Cell Sci. 96:721-730

Cordewener J, Booij H, Van de Zand H, Van Engelen F, Van Kammen A, De Vries S (1991) Tunicamycin-inhibited carrot somatic embryogenesis can be restored by secreted cationic peroxidase isoenzymes. Planta 184:478-486

Cork RJ (1985) Problems with the application of quin-2 AM to measuring cytoplasmic free calcium in plant cells. Plant, Cell and Environm. 9:157-161

Cotton G, Vanden Driessche T (1987) Identification of calmodulin in *Acetabularia*: its distribution and physiological significance. J. Cell Sci. 87:337-347

Cox JA, Comte M, Mamar-Bachi A, Milos M, Schaer J-J (1988) Cation binding to calmodulin and relation to function. In: Gerday C, Gilles R, Bolis L (eds) Calcium and calcium binding proteins. Springer-Verlag, Berlin, Heidelberg, pp. 141-162

Cyr RJ (1991) Calcium/calmodulin affects microtubule stability in lysed protoplasts. J. Cell Sci. 100:311-317

Das R, Bagga S, Sopory SK (1987) Involvement of phosphoinositides, calmodulin and glyoxylase I in cell proliferation in callus cultures of *Amaranthus paniculatus*. Plant Sci. 53:45-51

Dauwalder M, Roux SJ, Hardison L (1986) Distribution of calmodulin in pea seedlings. Immunocytochemical localization in plumules and root apices. Planta 168:461-470

De Jong AJ, Cordewener J, Lo Schiavo F, Terzi M, Vandekerckhove J, Van Kammen A, De Vries SC (1992) A carrot somatic embryo mutant is rescued by chitinase. The Plant Cell 4:425-433

De Vries SC, Booij H, Meyerink P, Huisman G, Dayton Wilde H, Thomas TL, Van Kammen A (1988a) Acquisition of embryogenic potential in carrot cell-suspension cultures. Planta 176:196-204

De Vries SC, Booij H, Janssens R, Vogels R, Saris L, Lo Schiavo F, Terzi M, Van Kammen A (1988b) Carrot somatic embryogenesis depends on the phytohormone-controlled presence of correctly glycosylated extracellular proteins. Genes & Develop. 2:462-476

De Vries SC (1992) Secreted proteins as modulators of plant embryogenesis. In: Karssen CM, Van Loon LC, Vreugdenhil D (eds) Progress in Plant Growth Regulation. Kluwer Academic Publishers, Dordrecht, Boston, London, pp. 340-346

Dedman JR, Potter JD, Jackson RL, Johnson JD, Means AR (1977) Physicochemical properties of rat testis Ca^{2+}-dependent regulator protein of cyclic nucleotide phosphodiesterase: relationship of Ca^{2+}-binding, conformational changes and phosphodiesterase activity. J. Biol. Chem. 252:8415-8422

Dela Fuente RK (1984) Role of calcium in the polar secretion of indoleacetic acid. Plant Physiol. 76:342-346

Dietz K-J, Schramm M, Lang B, Lanzl-Schramm, Dürr C, Martinoia E (1992) Characterization of the epidermis from barley primary leaves. II. The role of the epidermis in ion compartmentation. Planta 187:431-437

Dijak M, Simmonds DH (1988) Microtubule organization during early direct embryogenesis from mesophyll protoplasts of *Medicago sativa* L. Plant Sci. 58-183-191

Dixon D, Brandt N, Hayes DH (1984) Chlorotetracycline fluorescence is a quantitative measure of the free internal Ca^{2+} concentration achieved by active transport. *In situ* calibration and application to bovine cardiac sarcolemmal vesicles. J. Biol. Chem. 259:13737-13741

Dorhout R, Kollöffel C (1992) Determining apoplastic pH differences in pea roots by use of the fluorescent dye fluorescein. J. Exp. Bot. 43:479-486

Dreier W, Preusser E, Gründel M (1992) The regulation of the activity of soluble starch synthase in spinach leaves by a calcium-calmodulin dependent protein kinase. Biochem. Physiol. Pflanzen 188:81-96

Dubois T, Guedira M, Dubois J, Vasseur J (1990) Direct somatic embryogenesis in leaves of *Cichorium*. A histological and SEM study of early stages. Protoplasma 162:120-127

Dutta PC, Appelqvist L-Å, Gunnarsson S, Von Hofsten, A (1991) Lipid bodies in tissue culture,

somatic and zygotic embryo of *Daucus carota* L.: a qualitative and quantitative study. Plant Sci. 78:259-267

Elias PM, Goerke J, Friend DS (1978) Freeze-fracture identification of sterol-digitonin complexes in cell and liposome membranes. J. Cell Biol. 78:577-596

Epel D (1990) The initiation of development at fertilization. Cell Differ. Dev. 29:1-12

Esau K (1977) Anatomy of seed plants. John Wiley & Sons, New York

Ettlinger C, Lehle L (1988) Auxin induces rapid changes in phosphatidylinositol metabolites. Nature 331:176-178

Evans DE, Briars S-A, Williams LE (1991) Active calcium transport by plant cell membranes. J. Exp. Bot. 42:285-303

Felle H (1988a) Auxin causes oscillations of cytosolic free calcium and pH in *Zea mays* coleoptiles. Planta 174:495-499

Felle H (1988b) Cytoplasmic free calcium in *Riccia fluitans* L. and *Zea mays* L.: Interactions of Ca^{2+} and pH? Planta 176:248-255

Felle H (1989) pH as a second messenger in plants. In: Boss WF, Morré DJ (eds) Second messengers in plant growth and development. Plant Biology vol. 6, Alan R Liss, New York, pp. 57-80

Felle HH, Rück A, Peters WS (1992) The role of cytosolic calcium, pH and auxin-induced electrical responses for elongation growth in maize. In: Karssen CM, Van Loon LC, Vreugdenhil D (eds) Progress in Plant Growth Regulation. Kluwer Academic Publishers, Dordrecht, Boston, London, pp. 663-667

Ferguson IB, Drøbak BK (1988) Calcium and the regulation of plant growth and senescence. Hort Sci. 23:262-266

Fienberg AA, Choi JH, Lubick WP, Sung ZR (1984) Developmental regulation of polyamine metabolism in growth and differentiation of carrot culture. Planta 162:532-539

Fiskum G (1985) Intracellular levels and distribution of Ca^{2+} in digitonin permeabilized cells. Cell Calcium 6:25-37

Frelin C, Vigne P, Ladoux A, Lazdunski M (1988) The regulation of the intracellular pH in cells from vertebrates. Eur. J. Biochem. 174:3-14

Fricker MD, White N (1992) Wavelength considerations in confocal microscopy of botanical specimens. J. Microsc. 166:29-42

Fry SC (1990) Roles of the primary cell wall in morphogenesis. In: Nijkamp HJJ, Van der Plas LHW, Van Aartrijk J (eds) Progress in plant cellular and molecular biology. Kluwer Academic Publishers, Dordrecht, pp. 504-513

Fujimura T, Komamine A (1975) Effects of various growth regulators on the embryogenesis in a carrot cell suspension culture. Plant Sci. Lett. 5:359-364

Fujimura T, Komamine A (1979a) Involvement of endogenous auxin in somatic embryogenesis in a carrot cell suspension culture. Z. Pflanzenphysiol. 95:13-19

Fujimura T, Komamine A (1979b) Synchronization of somatic embryogenesis in a carrot cell suspension culture. Plant Physiol. 64:162-164

Fujimura T, Komamine A (1980) Mode of action of 2,4-D and zeatin on somatic embryogenesis in a carrot cell suspension culture. Z. Pflanzenphysiol. 99:1-8

Gamborg OL, Miller RA, Ojiama K (1968) Plant cell cultures. Exp. Cell Res. 50:151-158

Gates JC, Greenwood MS (1991) The physical and chemical environment of the developing embryo of *Pinus resinosa*. Am. J. Bot. 78:1002-1009

Gilroy S, Fricker MD, Read ND, Trewavas AJ (1991) Role of calcium in signal transduction of *Commelina* guard cells. The Plant Cell 3:333-344

Gilroy S, Fricker MD, Read ND, Trewavas AJ (1992) The role of Ca^{2+} and ABA in the regulation of stomatal aperture. In: Karssen CM, Van Loon LC, Vreugdenhil D (eds) Progress in Plant Growth Regulation. Kluwer Academic Publishers, Dordrecht, Boston, London, pp. 105-115

Gilroy S, Hughes WA, Trewavas AJ (1986) The measurement of intracellular calcium levels in protoplasts from higher plants. FEBS Lett. 199:217-221

Gilroy S, Hughes WA, Trewavas AJ (1989) A comparison between quin-2 and aequorin as indicators of cytoplasmic calcium levels in higher plant cell protoplasts. Plant Physiol. 90:482-491

Giuliano G, Rosellini D, Terzi M (1983) A new method for the purification of the different stages of carrot embryoids. Plant Cell Rep. 2:216-218

Gluck S, Cannon C, Al-Awqati Q (1982) Exocytosis regulates urinary acidification in turtle bladder by rapid insertion of H^+ pumps into the luminal membrane. Proc. Natl. Acad. Sci. 79:4327-4331

Goddard RH, La Claire JW (1991) Calmodulin and wound healing in the coenocytic green alga *Ernodesmis verticillata* (Kützing) Børgesen. Immumofluorescence and effects of antagonists. Planta 183:281-293

Goldberg RB, Barker SJ, Perez-Grau L (1989) Regulation of gene expression during plant embryogenesis. Cell 56:149-160

Greger M, Bertell G (1992) Effects of Ca^{2+} and Cd^{2+} on the carbohydrate metabolism in sugar beet (*Beta vulgaris*). J. Exp. Bot. 43:167-173

Gubler F, Jablonsky PP, Duniec J, Hardham AR (1990) Localization of calmodulin in flagella of zoospores of *Phytophtora cinnamomi*. Protoplasma 155:233-238

Guern J, Mathieu Y, Kurkdjian A, Manigault P, Manigault J, Gillet B, Beloeil JC, Lalemand J-Y (1989) Regulation of vacuolar pH of plant cells. II. A ^{31}P NMR study of the modifications of vacuolar pH in isolated vacuoles induced by proton pumping and cation/H^+ exchanges. Plant Physiol. 89:27-36

Guilfoyle TJ (1989) Second messengers and gene expression. In: Boss WF, Morré DJ (eds) Second messengers in plant growth and development. Plant Biology vol. 6, Alan R Liss, New York, pp. 315-326

Guiragossian Kiss H, Evans ML, Johnson JD (1991) Cytoplasmic calcium levels in protoplasts from the cap and elongation zone of maize roots. Protoplasma 163:181-188

Halperin W (1966) Alternative morphogenetic events in cell suspensions. Am. J. Bot. 53:443-453

Halperin W, Jensen WA (1967) Ultrastructural changes during growth and embryogenesis in carrot cell cultures. J. Ultrastruct. Res. 18:428-443

Hari V (1980) Effect of cell density changes and conditioned media on carrot cell embryogenesis. Z. Pflanzenphysiol. 96:227-231

Haugland RP (1992) Handbook of fluorescent probes and research chemicals. Molecular Probes Inc. Eugene, USA.

Haußer I, Herth W, Reiss H-D (1984) Calmodulin in tipgrowing plant cells, visualised by fluorescing calmodulin binding phenothiazines. Planta 162:33-39

Havelange A (1989) Levels and ultrastructural localization of calcium in *Sinapis alba* during the floral transition. Plant Cell Physiol. 30:351-358

Hayashi M, Mitsui T, Akazawa T (1989) Regulatory role of Ca^{2+} on the level of α-amylase mRNA in rice seed. Plant Physiol. Biochem. 27:349-354

Henshaw GG, O'Hara JF, Webb KJ (1982) Morphogenetic studies in plant tissue cultures. In: Yeoman MM, Truman DES (eds) Differentiation *in vitro*. Cambridge University Press, New York, pp. 231-251

Hepler PK (1988) Calcium and development. In: Greuter W, Zimmer B (eds) Proc. XIV Int. Bot. Congr., Koeltz, Koningstein/Taunus, pp. 225-240

Hepler PK (1989) Calcium transients during mitosis: observations in flux. J. Cell Biol. 109:2567-2573

Hepler PK, Callaham DA (1987) Free calcium increases during anaphase in stamen hair cells of *Tradescantia*. J. Cell Biol. 105:2137-2143

Hepler PK, Wayne RO (1985) Calcium and plant development. Ann. Rev. Plant Physiol. 36:397-439

Hernandez-Cruz A, Sala F, Adams PR (1990) Subcellular calcium transients visualized by confocal microscopy in a voltage-clamped vertebrate neuron. Science 247:858-862

Hernandez-Nistal J, Rodriguez D, Nicolas G, Aldasoro JJ (1989) Abscisic acid and temperature modify the levels of calmodulin in embryonic axes of *Cicer arietinum*. Physiol. Plant. 75:255-2600

Herth W, Reiss H-D, Hartmann E (1990) Role of calcium ions in tip growth of pollen tubes and moss protonema cells. In: Tip growth in plant and fungal cells. Academic Press, New York, pp. 91-118

Hush JM, Overall RL, Newman IA (1991) A calcium influx precedes organogenesis in *Graptopetalum*. Plant Cell Environm. 14:657-665

Iida S, Potter JD (1986) Calcium binding to calmodulin. Cooperativity of of the calcium-binding sites. J. Biochem. 99:1765-1772

Jablonsky PP, Grolig F, Perkin JL, Williamson RE (1991) Properties of monoclonal antibodies to plant

calmodulin. Plant Sci. 76:175-184
Jacobsen JV (1984) Regulation of protein synthesis in aleurone cells by gibberellins and abscisic acid. In: Crozier A (ed) The biochemistry and physiology of gibberellins. Praeger, New York, pp. 159-187
Jacobsen JV, Pressman E, Pyliotis NA (1976) Gibberellin-induced separation of cells in isolated endosperm of celery seed. Planta 129:113-122
Jansen MAK, Booij H, Schel JHN, De Vries SC (1990) Calcium increases the yield of somatic embryos in carrot embryogenic suspension cultures. Plant Cell Rep. 9:221-223
Johannes E, Brosman JM, Sanders D (1992) Parallel pathways for intracellular Ca^{2+} release from the vacuole of higher plants. Plant J. 2:97-102
Jones RL, Deikman J, Melroy D (1986) Role of Ca^{2+} in the regulation of α-amylase synthesis and secretion in barley aleurone. In: Trewavas AJ (ed) Molecular and cellular aspects of calcium in plant development. Plenum Press, New York, London, pp. 49-56
Kaesser W, Koyro, H-W, Moor, H (1989) Cryofixation of plant tissues without pretreatment. J. Microsc. 154:279-288
Kaminek M (1992) Progression in cytokinin research. Trends Biotechn. 10:159-164
Kauss H (1987) Some aspects of calcium dependent regulation in plant metabolism. Ann. Rev. Plant Physiol. 38:47-72
Kell A, Donath E (1990) Effect of ionophore A23187 on plasma membrane integrity in isolated protoplasts of *Avena sativa*. Plant Sci. 69:135-138
Kiyosue T, Nakayama J, Satoh S, Isogai A, Suzuki A, Kamada H, Harada H (1992) Partial amino-acid sequence of ECP31, a carrot embryogenic cell protein, and enhancement of its accumulation by abscisic acid in somatic embryos. Planta 186:337-342
Knebel W, Quader H, Wijnaendts-Van Resandt R, Engelhardt H (1989) Application of confocal laser scanning microscopy in plant biology. Ber. Bunsenges Phys. Chem. 93:380-386
Knight MR, Campbell AK, Smith SM, Trewavas AJ (1991) Transgenic plant aequorin reports the effects of touch and cold-shock and elicitors on cytoplasmic calcium. Nature 352:524-526
Koenig H (1963) Vital staining of lysosomes by acridine orange. J. Cell Biol. 19:87A
Komamine A, Matsumoto M, Tsukahara M, Fujiwara A, Kawahara R, Ito M, Smith J, Nomura K, Fujimura T (1990) Mechanisms of somatic embryogenesis in cell cultures - physiology, biochemistry and molecular biology. In: Nijkamp HJJ, Van der Plas LHW, Van Aartrijk J (eds) Progress in plant cellular and molecular biology. Kluwer Academic Publishers, Dordrecht, pp. 307-313
Kretsinger RH (1979) The information role of calcium in the cytosol. Adv. Cyclic Nuc. Res. 11:1-26
Kropf DL (1992) Establishment and expression of cellular polarity in fucoid zygotes. Microbiol. Rev. 56:316-339
Kurkdjian A, Guern J (1989) Intracellular pH: measurement and importance in cell activity. Ann. Rev. Plant Physiol. Plant Mol. Biol. 40:271-303
Lambert AM, Vantard M, Van Eldik L, De Mey J (1983) Immunolocalization of calmodulin in higher plant endosperm cells during mitosis. J. Cell Biol. 97:40A
Lenormand P, Pribnow D, Rodland KD, Magun BE (1992) Identification of a novel enhancer element mediating calcium-dependent induction of gene expression in response to either epidermal growth factor of activation of protein kinase C. Mol. Cell. Biol. 12:2793-2803
Levin RM, Weiss B (1975) Mechanism by which psychotropic drugs inhibit cyclic AMP-phophodiesterase in brain. Mol. Pharmacol. 12:581-589
Levin RM, Weiss B (1977) Binding of trifluperazine to the calcium dependent activator of cyclic AMP-phosphodiesterase. Mol. Pharmacol. 13:690-697
Li TR, Neumann K-H (1985) Embryogenesis and endogenous hormone content of cell cultures of some carrot varieties (*Daucus carota* L.). Ber. Deutsch. Bot. Ges. 98:227-235
Lin CT, Dedman JR, Brinkley BR, Means AR (1980) Localization of calmodulin in rat cerebellum by immunoelectron microscopy. J. Cell Biol. 85:473-480
Lin CT, Sun D, Song GX, Wu JY (1986) Calmodulin: localization in plant tissues. J. Histochem. Cytochem. 34:561-567
Lo Schiavo F, Giuliano G, De Vries SC, Genga A, Bollini R, Pitto L, Cozzani G, Nuti-Ronchi V, Terzi M (1990) A carrot cell variant temperature sensitive for somatic embryogenesis reveals a defect in the glycosylation of extracellular proteins. Mol. Gen. Genet. 223:385-393

Marmé D (1989) The role of calcium and calmodulin in signal transduction. In: Boss WF, Morré DJ (eds) Second messengers in plant growth and development. Plant Biology vol. 6, Alan R Liss, New York, pp. 57-80

Marmé D, Dieter P (1983) Role of Ca^{2+} and calmodulin in plants. In: Cheung WY (ed) Calcium and cell function, vol. 4. Academic Press, New York, pp. 263-311

Mayer U, Torres Ruiz RA, Berleth T, Miséra S, Jürgens G (1991) Mutations affecting body organization in the *Arabidopsis* embryo. Nature 353:402-47

McCormack JG, Cobbold PH (1991) Cellular calcium. A practical approach. IRL Press, Oxford, New York, Tokyo

McGee-Russel SM (1958) Histochemical methods for calcium. J. Histochem. Cytochem. 6:22-42

McWilliam AA, Smith SM, Street HE (1974) The origin and development of embryoids in suspension cultures of carrot (*Daucus carota*). Ann. Bot. 38:243-250

Means AR, Tash JS, Chafouleas JG (1982) Physiological implications of the presence, distribution and regulation of calmodulin in eukaryotic cells. Physiol. Rev. 62:1-38

Melan MA, Sluder G (1992) Redistribution and differential extraction of soluble proteins in permeabilized cultured cells. Implications for immunofluorescence microscopy. J. Cell Sci. 101:731-743

Michaux-Ferriere N, Grout H, Carron MP (1992) Origin and ontogenesis of somatic embryos in *Hevea brasiliensis* (Euphorbiacea). Am. J. Bot. 79:174-180

Michler CH, Lineberger RD (1987) Effects of light on somatic embryo development and abscisic levels in carrot suspension cultures. Plant Cell Tissue Organ Cult. 11:189-207

Miller DD, Calaham DA, Gross DJ, Hepler PK (1992) Free Ca^{2+}-gradients in growing pollen tubes of *Lilium*. J. Cell Sci. 101:7-12

Minta A, Harootunian AT, Kao JPY, Tsien RY (1987) New fluorescent indicators for intracellular sodium and calcium. J. Cell Biol. 105:89A

Minta A, Kao JPY, Tsien RY (1989) Fluorescent indicators for cytosolic calcium based on rhodamine and fluorescein chromophores. J. Biol. Chem. 264:8171-8178

Mitsui T, Christeller JT, Hara-Nishimura I, Akazawa T (1984) Possible roles of calcium and calmodulin in the biosynthesis and secretion of α-amylase in rice seed scutellar epithelium. Plant Physiol. 75:21-25

Muto S, Hirosawa T (1987) Inhibition of adventitious root growth in *Tradescantia* by calmodulin antagonists and calcium inhibitors. Plant Cell Physiol. 28:1569-1574

Muto S, Miyachi S (1984) Production of antibody against spinach calmodulin and its application to radioimmunoassay for plant calmodulin. Z. Pflanzenphysiol. 114:421-431

Nielsen TB, Field JB, Dedman JR (1987) Association of calmodulin with lysosomes. J. Cell Sci. 87:327-336

Nishimura M (1982) pH in vacuoles isolated from castor bean endosperm. Plant Physiol. 70:742-746

Nomura K (1987) Mechanisms of somatic embryogenesis in carrot suspension cultures. PhD thesis. Univ. Tokyo, Japan

Nomura K, Komamine A (1985) Identification and isolation of single cells that produce somatic somatic embryos at a high frequency in a carrot suspension culture. Plant Physiol. 79:988-991

Nomura K, Komamine A (1986a) Molecular mechanisms of somatic embryogenesis. In: Miflin BJ (ed) Oxford surveys of plant molecular and cell biology, vol. 3. Oxford University Press, pp. 456-466

Nomura K, Komamine A (1986b) Polarized DNA synthesis and cell division in cell clusters during somatic embryogenesis from single carrot cells. New Phytol. 104:25-32

Norstog K (1972) Early development of the barley embryo: fine structure. Am. J. Bot. 59:123-132

Ogawa Y, Tanokura M (1984) Calcium binding to calmodulin: effects of ionic strength, Mg^{2+}, pH and temperature. J. Biochem. 95:19-28

Oparka KJ (1991) Uptake and compartmentation of fluorescent probes by plant cells. J. Exp. Bot. 42:565-579

Oparka KJ, Hawes C (1992) Vacuolar sequestration of fluorescent probes in plant cells: a review. J. Microsc. 166:15-27

Owen JH (1988) Role of abscisic acid in a Ca^{2+} second messenger system. Physiol. Plant. 72:637-

641
Owen JH, Hetherington AM, Wellburn AR (1987) Calcium, calmodulin and the control of respiration in protoplasts isolated from meristematic tissues by abscisic acid. J. Exp. Bot. 38:1356-1361
Padh H, Lavasa M, Steck TL (1989) Prelysosomal acidic vacuoles in *Dictyostelium discoideum*. J. Cell Biol. 108:865-874
Palmgren MG (1991) Acridine orange as a probe for measuring pH gradients across membranes: mechanism and limitations. Anal. Biochem. 192:316-321
Pedroso MC, Pais MS (1992) A scanning electron microscopy and X-ray microanalysis study during induction of morphogenesis in *Camellia japonica* L. Plant Sci. 87:99-108
Penel C, Castillo FJ, Kiefer S, Greppin H (1986) The regulation of plant peroxidases by calcium. In: Trewavas AJ (ed) Molecular and cellular aspects of calcium in plant development. Plenum Press, New York, London, pp. 365-366
Pitto L, Lo Schiavo F, Terzi M (1985) α-Amanitin resistance is developmentally regulated in carrot. Proc. Natl. Acad. Sci. 82:2799-2803
Poenie M, Alderton J, Steinhardt R, Tsien RY (1986) Calcium rises abruptly and briefly throughout the cell at the onset of anaphase. Science 233:886-889
Poenie M, Epel D (1987) Ultrastructural localization of intracellular calcium stores by a new cytochemical method. J. Histochem. Cytochem. 35:939-956
Poovaiah BW (1985) Role of calcium and calmodulin in plant growth and development. Hort Sci. 20:347-351
Poovaiah BW, McFadden JJ, Reddy ASN (1987) The role of calcium ions in gravity signal perception and transduction. Physiol. Plant. 71:401-407
Poovaiah BW, Veluthambi K (1986) The role of calcium and calmodulin in hormone action in plants: importance of protein phosphorylation. In: Trewavas AJ (ed) Molecular and cellular aspects of calcium in plant development. Plenum Press, New York, London, pp. 83-90
Pope AJ, Leigh RA (1988) Dissipation of pH gradients in tonoplast vesicles and liposomes by mixtures of acridine orange and anions. Plant Physiol. 86:1315-1322
Preusser E, Chudy M, Gründel M, Khalil FA (1988) Influence of Ca^{++} and other bivalent cations on the activity of granule-bound starch synthetase. Acta Physiol. Plant. 10:133-142
Prozialeck WC, Amino M, Weiss B (1981) Photoaffinity labeling of calmodulin by phenothiazine psychotics. Mol. Pharmacol. 19:264-269
Racusen RH, Schiavone FM (1988) Detection of spatially- and stage-specific proteins in extracts from single embryos of the domesticated carrot. Development 103:665-674
Raghavan V (1986) Embryogenesis in angiosperms. A developmental and experimental study. Cambridge University Press, New York
Ranjeva R, Boudet AM (1987) Phosphorylation of proteins in plants: regulatory effects and potential involvement in stimulus/response coupling. Ann. Rev. Plant Physiol. 38:73-93
Rasmussen H (1989) The cycling of calcium as an intracellular messenger. Scient. Amer. 260:44-51
Raven JA (1990) Sensing pH? Plant Cell Environm. 13:721-729
Read ND, Allan WTG, Knight H, Knight MR, Malhó R, Russel A, Shacklock PS, Trewavas AJ (1992) Imaging and measurement of cytosolic calcium in plant and fungal cells. J. Microsc. 166:57-86
Reinert J (1958) Morphogenese und ihre Kontrolle an Gewebekulturen aus Carotten. Naturwissenschaften 45:344-345
Reiss H-D, Herth W (1979) Calcium gradients in tip growing plant cells visualized by CTC-fluorescence. Planta 146:615-621
Robbins E, Marcus PI, Gonatas NK (1964) Dynamics of acridine orange-cell interaction. II. Dye-induced ultrastructural changes in multivesicular bodies (acridine orange particles). J. Cell Biol. 21:49-62
Roberts DM, Harmon AC (1992) Calcium-modulated proteins: targets of intracellular calcium signals in higher plants. Ann. Rev. Plant Physiol. Plant Mol. Biol. 43:375-414
Roberts DM, Lukas TJ, Watterson DM (1986) Structure, function and mechanism of action of calmodulin. Crit. Rev. Plant Sci. 4:311-339
Roe MW, Lemasters JJ, Herman B (1987) An assessment of the use of fura-2 for the determination of intracellular calcium concentrations. Fedn. Proc. Fedn. Am. Socs. Exp. Biol. 46:2277

Roux SJ, Wayne RO, Datta N (1986) Role of calcium ions in phytochrome response: un update. Physiol. Plant. 66:344-348

Russ U, Grolig F, Wagner G (1991) Changes of cytoplasmic free Ca^{2+} in the green alga *Mougeotia scalaris* as monitored with indo-1 and their effect on the velocity of chloroplast movement. Planta 184:105-112

Satter RL, Galston AW (1981) Mechanisms of control of leaf movements. Ann. Rev. Plant Physiol. 32:83-110

Saunders MJ (1992) Cytokinin signal transduction through Ca^{2+} in mosses. In: Karssen CM, Van Loon LC, Vreugdenhil D (eds) Progress in Plant Growth Regulation. Kluwer Academic Publishers, Dordrecht, Boston, London, pp. 65-72

Saunders MJ, Hepler PK (1981) Localization of membrane-associated calcium following cytokinin treatment in *Funaria* using chlorotetracycline. Planta 152:272-281

Scarpa A (1985) Measurements of intracellular calcium. Cell Calcium 6:1-3

Scheurlein R, Schmidt K, Poenie M, Roux SJ (1991) Determination of cytoplasmic calcium concentration in *Dryopteris* spores. A developmentally non-disruptive technique for loading of the calcium indicator fura-2. Planta 184:166-174

Schiavone RM, Cooke TJ (1985) A geometric analysis of somatic embryo formation in carrot cell cultures. Can. J. Bot. 63:1573-1578

Schiavone FM, Cooke TJ (1987) Unusual patterns of somatic embryogenesis in the domesticated carrot: developmental effects of exogenous auxins and auxin transport inhibitors. Cell Diff. 21:53-62

Schleicher M, Iverson DB, Van Eldik LJ, Watterson DM (1982) Calmodulin. In: Lloyd CW (ed) The cytoskeleton in plant growth and development. Academic Press, New York, pp. 85-106

Schnepf E (1986) Cellular polarity. Ann. Rev. Plant Physiol. 37:23-47

Schroeder JI, Thuleau P (1991) Ca^{2+} channels in higher plant cells. The Plant Cell 3:555-559

Seeman P, Cheng D, Iles GH (1973) Structure of membrane holes in osmotic and saponin hemolysis. J. Cell Biol. 56:519-527

Selzer PM, Webster P, Duszenko M (1991) Influence of Ca^{2+} depletion on cytoskeleton and nucleolus morphology in *Trypanosoma brucei*. Eur. J. Cell Biol. 56:104-112

Slay RM, Grimes HD, Hodges TK (1989) Plasma membrane proteins associated with undifferentiated and embryonic *Daucus carota* tissue. Protoplasma 150:139-149

Slocum RD, Roux SJ (1982) An improved method for the subcellular localization of calcium using a modification of the antimonate precipitation technique. J. Histochem. Cytochem. 30:617-629

Smith JA, Sung ZR (1985) Increase in regeneration of plant cells by cross feeding with regenerating *Daucus carota* cells. In: Terzi M, Pitto L, Sung ZR (eds) Somatic embryogenesis. IPRA, Roma, Italy

Smith DL, Krikorian AD (1988) Production of somatic embryos from carrot tissues in hormone-free medium. Plant Sci. 58:103-110

Smith DL, Krikorian AD (1990a) Somatic proembryo production from excised, wounded zygotic carrot embryos on hormone-free medium: evaluation of the effects of pH, ethylene and activated charcoal. Plant Cell Rep. 9:34-37

Smith DL, Krikorian AD (1990b) Low external pH replaces 2,4-D in maintaining and multiplying 2,4-D initiated embryogenic cells of carrot. Physiol. Plant. 80:329-336

Snowdowne KW, Borle AB (1985) Effects of low extracellular sodium on cytosolic ionized calcium. Na^+-Ca^{2+} exchange as a major calcium influx pathway in kidney cells. J. Biol. Chem. 260:14998-15007

Sobota A, Skoczylas B, Glowacka SK (1987) Analysis of cytochemical procedure of precipitation of calcium ions by N,N-Naphtaloylhydroxylamine (NHA) in *Acanthoameba* cells. Acta Protozool. 26:145-152

Somlyo AP (1984) Cellular site of calcium regulation. Nature 309:516-517

Somlyo AP (1985) Cell calcium measurement with electron probe and electron loss analysis. Cell Calcium 6:197-212

Steer MW (1988) The role of calcium in exocytosis and endocytosis in plant cells. Physiol. Plant. 72:213-220

Sterk P, Booij H, Schellekens GA, Van Kammen A, De Vries SC (1991) Cell-specific expression of the

carrot EP2 lipid transfer protein gene. The Plant Cell 3:907-921
Steward FC, Mapes MO, Mears K (1958) Growth and organized development of cultured cells. II. Organization in cultures grown from freely suspended cells. Am. J. Bot. 45:705-708
Sticher L, Penel C, Greppin H (1981) Calcium requirement for the secretion of peroxidase by plant cell suspensions. J. Cell Sci. 48:345-353
Stinemetz CL, Kuzmanoff KM, Evans ML, Jarret HW (1987) Correlation between calmodulin activity and gravitropic sensitivity in primary roots of maize. Plant Physiol. 84:1337-1342
Strack D, Sharma V, Felle H (1987) Vacuolar pH in radish cotyledon mesophyll cells. Planta 172:563-565
Street HE, Withers LA (1974) The anatomy of embryogenesis in culture. In: Street HE (ed) Tissue culture and plant science. Academic Press, London, New York, pp. 71-100
Sung ZR, Fienberg A, Chorneau R, Borkbird C, Furner I, Smith J, Terzi M, Lo Schiavo F, Giuliano G, Pitto L, Nuti-Ronchi V (1984) Developmental biology of embryogenesis from carrot cultures. Plant Mol. Biol. Rep. 2:3-14
Sung ZR, Okimoto R (1981) Embryogenic proteins in somatic embryos of carrot. Proc. Natl. Acad. Sci. 78:3683-3687
Tazawa M, Reinert J (1969) Extracellular and intracellular chemical environments in relation to embryogenesis *in vitro*. Protoplasma 68:157-173
Terzi M, Pitto L, Sung ZR (1985) Somatic embryogenesis. IPRA, Rome, Italy
Thomas MV (1986) The definition and measurement of intracellular free Ca^{2+}. In: Trewavas AJ (ed) Molecular and cellular aspects of calcium in plant development. Plenum Press, New York, London, pp. 141-147
Thomas A, Delaville F (1991) The use of fluorescent indicators for measurement of cytosolic free calcium concentration in cell populations and single cells. In: McCormack JG, Cobbold PH (eds) Cellular Calcium. A practical approach. IRL Press, Oxford, New York, Tokyo, pp. 1-54
Timmers ACJ (1990) Calcium and calmodulin during carrot somatic embryogenesis. In: Sangwan RS, Sangwan-Norreel BS (eds) The impact of biotechnology in agriculture. Kluwer Academic Publishers, Dordrecht, Boston, London, pp. 215-234
Timmers ACJ, De Vries SC, Schel JHN (1989) Distribution of membrane-bound calcium and activated calmodulin during somatic embryogenesis of carrot (*Daucus carota* L.). Protoplasma 153:24-29
Timmers ACJ, Reiss H-D, Schel JHN (1991) Digitonin-aided loading of fluo-3 into embryogenic plant cells. Cell Calcium 12:515-521
Timmers ACJ, Schel JHN (1990) Immunocytochemical localization of calmodulin during carrot somatic embryogenesis. In: Nijkamp HJJ, Van der Plas LHW, Van Aartrijk J (eds) Progress in plant cellular and molecular biology. Kluwer Academic Publishers, Dordrecht, pp. 443-448
Timmers ACJ, Schel JHN (1991) Localization of cytosolic Ca^{2+} during carrot somatic embryogenesis using confocal scanning laser microscopy. In: Karssen CM, Van Loon LC, Vreugdenhil D (eds) Progress in Plant Growth Regulation. Kluwer Academic Publishers, Dordrecht, Boston, London, pp. 347-353
Tisserat B, Esan EB, Murashige T (1979) Somatic embryogenesis in angiosperms. Hort. Rev. 1:1-78
Torii K, Satoh S, Fujii T (1991) Immunohistochemical localization of a glycoprotein, GP80, in the outermost layer of the developing endosperm of immature seeds of carrot. Planta 185:201-208
Traas JA, Renaudin JP, Teyssendier de la Serve B (1990) Changes in microtubular organization mark the transition to organized growth during organogenesis in *Petunia hybrida*. Plant Sci. 68:249-256
Tretyn A, Kopcewicz J (1988) Calcium localization in oat aleurone cells using chlorotetracycline and X-ray microanalysis. Planta 175:237-240
Tretyn A, Wagner G, Felle HH (1991) Signal transduction in *Sinapis alba* root hairs: auxins as external messengers. J. Plant Physiol. 139:187-193
Trewavas A (1991) How do plant growth substances work? II. Plant Cell Environm. 14:1-12
Tsien RY, Rink TJ, Poenie M (1985) Measurement of cytosolic free Ca^{2+} individual small cells using fluorescence microscopy with dual excitation wavelengths. Cell Calcium 6:145-157
Tucker EB (1990) Calcium-loaded 1,2-bis(2-aminophenoxy)ethane- N,N,N',N'-tetraacetic acid blocks

cell-to-cell diffusion of carboxyfluorescein in staminal hairs of *Setcreasea purpurea*. Planta 182:34-38.

Van Eldik LJ, Watterson DM (1985) Calmodulin structure and function. In: Marmé D (ed) Calcium and cell physiology. Springer-Verlag, Berlin, pp. 105-126

Van Lammeren AAM (1986) Developmental morphology and cytology of the young maize embryo (*Zea mays*) L. Acta Bot. Neerl. 35:169-188

Van Lammeren AAM, Kieft H, Provoost E, Schel JHN (1987) Immunogold labelling in ultrathin cryosections of cultured carrot cells. Acta Bot. Neerl. 36:125-132

Weiss B, Sellinger-Barnette M, Winkler JD, Schechter LE, Prozialeck WC (1985) Calmodulin antagonists: Structure-activity relationships. In: Hidaka H, Hartshorne DJ (eds) Calmodulin antagonists and cellular physiology. Academic Press, New York, pp. 45-62

Wetherell DF (1978) *In vitro* embryoid formation in cells derived from somatic plant tissues. In: Huges KW, Henke R, Constantin M (eds) Propagation of higher plants through tissue culture. A bridge between research and application. United States Department of Energy, Oak Ridge, Tennessee.

Wetherell DF (1984) Enhanced adventive embryogenesis resulting from plasmolysis of cultured wild carrot cells. Plant Cell Tissue Org. Cult. 3:221-227

Whitaker M, Patel R (1990) Calcium and cell cycle control. Development 108:525-542

Wick SM, Duniec J (1986) Effects of various fixatives on the reactivity of plant cell tubulin and calmodulin in immunofluorescence microscopy. Protoplasma 133:1-18

Wilde HD, Nelson WS, Booij H, De Vries SC, Thomas TL (1988) Gene-expression programs in embryogenic and non-embryogenic carrot cultures. Planta 176:205-211

Williams DA, Cody SH, Gehring CA, Parish RW, Harris PJ (1990) Confocal imaging of ionised calcium in living plant cells. Cell Calcium 11:291-297

Williams EG, Maheswaran G (1986) Somatic embryogenesis: factors influencing coordinated behaviour of cells as an embryogenic group. Ann. Bot. 57:443-462

Williamson RE, Ashley CC (1982) Free Ca^{2+} and cytoplasmic streaming in the alga *Chara*. Nature 296:647-651

Wilson HJ, Israel HW, Steward FC (1974) Morphogenesis and the fine structure of cultured carrot cells. J. Cell Sci. 15:57-73

Wochok ZS (1973) Microtubules and multivesicular bodies in cultured tissues of wild carrot: changes during transition from the undifferentiated to the embryogenic condition. Cytobios 7:87-95

Wurtele ES, Keller GL, Nikolau BJ, Ulrich TH (1988) Quantitation of starch and ADP-glucose pyrophosphorylase in non-embryogenic cells and embryonic cell clusters from carrot suspension cultures. J. Plant Physiol. 132:683-689

Xu N, Bewley JD (1992) Contrasting pattern of somatic and zygotic embryo development in alfalfa (*Medicago sativa* L.) as revealed by scanning electron microscopy. Plant Cell Rep. 11:279-284

Yamamoto A, Takeuchi I (1983) Vital staining of autophagic vacuoles in differentiating cells of *Dictyostelium discoideum*. Differentiation 24:83-87

You JS, Li SW, Wang DS, Zhang Y, Suen DY, Xue SB (1988) The distribution of calmodulin and the calmodulin antagonist TFP in cell cycle of the friend erythro-leukemia cells. In: Abstr. 4th Int. Congr. Cell Biol., Montreal, p 50

Zhu Q, Clarke M (1992) Association of calmodulin and an unconventional myosin with the contractile vacuole complex of *Dictyostelium discoideum*. J. Cell Biol. 118:347-358

Zimmerman JL, Apuya N, Darwish K, O'Carrol C (1989) Novel regulation of heat shock genes during carrot somatic embryo development. The Plant Cell 1:1137-1146

SUMMARY

In this thesis a study of the regulation of coordinated growth and the development of polarity during embryogenesis of carrot, *Daucus carota* L., is described. To this end, several microscopical techniques were used, such as light microscopy, fluorescence microscopy, confocal scanning laser microscopy and electron microscopy. Next to this, immunocytochemical methods were used frequently to localize proteins in plant tissue sections.

Plants are composed of several types of organs and tissues, each of them having a characteristic structure and function. For the development of a full-grown germling from one cell, the zygote, a tight regulation of growth and differentiation is required. During this process of embryogenesis, growth proceeds through a number of developmental stages which are described subsequently as globular, oblong, heart-shaped and torpedo-shaped.

Despite the large number of observations on embryogenesis, made in various plants, the molecular and cellular basis of this developmental pathway is still poorly understood. The divalent cation Ca^{2+} participates in the initiation and maintenance of a great variety of physiological processes, including the regulation of cell polarity, cell division, cell growth, cell volume, hormone action and distribution, and enzyme synthesis and activation. Considering the diversity of processes in which Ca^{2+} is involved, it is to be expected that an investigation of the distribution of Ca^{2+}, and Ca^{2+} binding proteins, during plant embryogenesis, will lead to a deeper understanding of the regulation of this process.

Studies on zygotic embryogenesis are hampered by the presence of surrounding maternal tissue. Therefore, somatic embryos of carrot are used often as experimental substitutes for zygotic embryos, since the discovery of *in vitro* embryogenesis in carrot cultures in 1958. Carrot somatic embryos can be obtained, relatively easily, in great amounts, essentially free of surrounding tissue, just by transferring cell clusters, designated as proembryogenic masses, from medium supplemented with the growth regulator 2,4-D to medium without 2,4-D. This feature makes carrot an ideal model system for the study of plant embryogenesis.

In Chapter 1, the general introduction, the zygotic and somatic embryogenesis of carrot is described structurally. Similarities and differences between both processes are mentioned. Many external factors, which are described extensively in the literature, influence the development of somatic embryos. For normal growth and development to occur, the presence of Ca^{2+} in the medium is absolutely required, and embryogenesis is enhanced specifically by a rise of $[Ca^{2+}]$. In this chapter, the role and distribution of Ca^{2+} in plants is briefly described.

The principal targets of calcium signals in eukaryotes are calcium-binding proteins of which calmodulin, a protein present in all plant cells, has been studied most extensively. The structure, activity and localization of this acidic, small and heat-resistant protein is described from the literature. Chapter 1 ends with a survey of techniques which are nowadays available for the localization of Ca^{2+} and calmodulin in plants.

In Chapter 2, chlorotetracycline and fluphenazine, two fluorescent indicators, are being used to localize Ca^{2+} and activated calmodulin respectively, during carrot somatic embryogenesis. Embryogenesis appears to coincide with a rise in $[Ca^{2+}]$ and activated calmodulin is mainly found in the future root side of the embryo. It is concluded, that the polarity in the distribution of calmodulin is already present before polarity is visible morphologically.

Fluphenazine visualizes only activated calmodulin. In Chapter 3, the distribution of both activated and non-activated calmodulin has been studied with the aid of antibodies. Besides the various developmental stages of somatic embryogenesis, also zygotic embryos and a number of stages of zygotic embryo germination have been studied in this chapter. The most striking observation is that the distribution of calmodulin in somatic embryos differs strongly from the distribution in zygotic embryos, but resembles the distribution during zygotic embryo germination. Both in somatic embryos and in germinated zygotic embryos, calmodulin appears to be present mainly in amyloplasts, while in zygotic embryos calmodulin predominantly was found to be localized in the cytoplasm.

For a detailed analysis of the distribution of Ca^{2+} in living, intact plant cells in tissues with fluorescent indicators, confocal laser scanning microscopy is the method of choice. A suitable indicator is fluo-3. Unfortunately, the plasma membrane is not permeable for this compound. Therefore, a method had to be developed with which fluo-3 could easily be loaded into plant cells. In Chapter 4, it is described that with the aid of digitonin fluo-3 can be used successfully for the localization of Ca^{2+} in embryogenic plant cells, in combination with confocal scanning laser microscopy.

As has already been noticed in Chapter 2, carrot somatic embryogenesis coincides with a rise in $[Ca^{2+}]$. In Chapter 5, a detailed analysis has been made of the distribution of free cytosolic Ca^{2+} during carrot somatic embryogenesis with the aid of the method described in Chapter 4. It appeared that $[Ca^{2+}]$ is especially high in the protoderm of the embryos, and gradients in $[Ca^{2+}]$ along the longitudinal axis of torpedo-shaped embryos were frequently observed. Very obvious was the high $[Ca^{2+}]$ in the nuclei of protoderm cells. This nuclear localization was confirmed by antimonate precipitation, by which Ca^{2+} is visualized as electron dense precipitates in the electron microscope.

The concentration of Ca^{2+} in the cytosol is not only linked with the concentration in the vacuole, but also with the pH of the cytosol and the vacuole. Since both pH and $[Ca^{2+}]$ are important factors during embryo-

genesis, in Chapter 6 a study is described of the distribution of pH in vacuoles during somatic and zygotic embryogenesis and during zygotic embryo germination of carrot. Neutral red and acridine orange were used as indicators of vacuolar pH and their distribution has been compared with the distribution of fluphenazine. Strikingly, major similarities were found between the distribution of the three probes used, and all three reacted similarly on treatments with A23187, EGTA or propionic acid. Confocal microscopy revealed a network of vesicles and tubules, predominantly present in the protoderm of somatic embryos and germinated zygotic embryos after incubation in acridine orange. Proposed is, that calmodulin is possibly involved in the digestion of cell material in autophagic vacuoles or is involved in the regulation of the movements of vacuolar tubules. However, additional research is necessary to explain the observed distribution patterns satisfactory.

From the previous chapters it appeared that noticeable differences exist between somatic and zygotic embryos in the distribution of anti-calmodulin, fluphenazine fluorescence, neutral red and acridine orange. In Chapter 7 a possible structural basis of these differences has been searched for. The distribution of anti-calmodulin, and perhaps also fluphenazine fluorescence, could be linked with the presence of amyloplasts, which were abundant in somatic and germinated zygotic embryos, but which were not found in zygotic embryos. Differences in the localization of neutral red and acridine orange are related to differences in vacuolation between somatic and zygotic embryos.

Chapter 8 is the general discussion. Here, somatic embryo initiation, its early development and the formation of polarity during somatic and zygotic embryogenesis of carrot are the main topics. It is concluded, that important differences exist between somatic and zygotic embryogenesis and that the process of somatic embryogenesis shows similarities with zygotic embryo germination. The chapter ends with some concluding remarks about the methods used for the localization of Ca^{2+} and calmodulin.

SAMENVATTING

In dit proefschrift is een onderzoek beschreven naar de regulatie van gecoördineerde groei en het ontstaan van polariteit tijdens de embryogenese van de wilde peen, *Daucus carota* L. Hiertoe is gebruik gemaakt van verscheidene microscopische technieken waaronder lichtmicroscopie, fluorescentiemicroscopie, confocale scanning laser microscopie en electronenmicroscopie. Daarnaast is veelvuldig gebruik gemaakt van immunocytochemische methoden voor de lokalisatie van eiwitten in coupes van planteweefsel.

Planten zijn opgebouwd uit diverse organen en weefsels met elk een eigen bouw en funktie. Om vanuit één cel, de zygote, te komen tot een volledig ontwikkeld kiemplantje is een strakke regulatie van groei en differentiatie een vereiste. Tijdens dit proces, de embryogenese, wordt door middel van gerichte celdeling en differentiatie een aantal ontwikkelingsstadia doorlopen die achtereenvolgens worden aangeduid met globulair, langwerpig, hartvormig en torpedovormig stadium.

Ondanks vele waarnemingen aan de embryogenese bij planten is de moleculaire en cellulaire basis van deze ontwikkelingsroute nog slecht begrepen. Het divalente kation Ca^{2+} participeert in de initiatie en in stand houding van een groot aantal fysiologische processen in planten waaronder de regulatie van celpolariteit, celdeling, celgroei, celvolume, hormoon werking en verdeling, en synthese en activiteit van enzymen. Gezien de diversiteit van processen waarbij Ca^{2+} is betrokken is te verwachten dat onderzoek naar de verdeling van Ca^{2+} en Ca^{2+}-bindende eiwitten tijdens de embryogenese van planten leidt tot een beter inzicht in de regulatie van dit proces.

Onderzoek aan zygotische embryo's wordt bemoeilijkt door de aanwezigheid van maternaal weefsel dat het embryo omhult. Derhalve worden, sinds de ontdekking van de *in vitro* embryogenese in cultures van de wilde peen in 1958, somatische embryo's van deze plant vaak gebruikt als experimentele vervangers van zygotische embryo's. Embryo's van de wilde peen kunnen relatief eenvoudig in grote hoeveelheden, vrij van enig omhullend weefsel, worden verkregen door celclusters, aangeduid met proembryogene massa's, over te brengen van medium met de groeiregulator 2,4-D naar medium zonder 2,4-D. Deze eigenschap maakt de wilde peen een ideaal modelsysteem voor de bestudering van de embryogenese van planten.

In hoofdstuk 1, de algemene inleiding, wordt een structurele beschrijving gegeven van de zygotische en somatische embryogenese van de wilde peen en er wordt kort ingegaan op overeenkomsten en verschillen tussen beide processen. De ontwikkeling van somatische embryo's wordt beïnvloed door vele externe factoren die uitvoerig in de literatuur zijn belicht. De aanwezigheid van Ca^{2+} in het medium is onontbeerlijk

voor normale groei en ontwikkeling van cellen, en tevens wordt door verhoging van de [Ca^{2+}] de embryogenese specifiek bevorderd. Kort wordt in dit hoofdstuk ingegaan op de rol en aanwezigheid van Ca^{2+} in planten.

De belangrijkste aangrijpingspunten van calciumsignalen in eukaryoten zijn Ca^{2+}-bindende eiwitten waarvan calmoduline, dat algemeen voorkomt in plantecellen, het best beschreven is. Vanuit literatuurgegevens wordt de struktuur, werking en lokalisatie van dit zure, kleine en hitte-resistente eiwit in planten beschreven. Het hoofdstuk eindigt met een overzicht van technieken die gebruikt kunnen worden voor de lokalisatie van Ca^{2+} en calmoduline in planten.

In hoofdstuk 2 worden twee fluorescerende indikatoren, chlorotetracycline en fluphenazine, gebruikt voor de lokalisatie van respectievelijk Ca^{2+} en geactiveerd calmoduline tijdens de somatische embryogenese van de wilde peen. Embryogenese blijkt samen te gaan met een stijging van de [Ca^{2+}] en geactiveerd calmoduline wordt voornamelijk waargenomen in de toekomstige wortelzijde van het embryo. Er wordt geconcludeerd dat een polariteit in de verdeling van calmoduline al aanwezig is voordat polariteit morfologisch zichtbaar is.

Fluphenazine is slechts een indikator voor geactiveerd calmoduline. Met behulp van antilichamen gericht tegen calmoduline wordt in hoofdstuk 3 de lokalisatie van zowel geactiveerd als niet geactiveerd calmoduline onderzocht. Tevens worden, naast diverse ontwikkelingsstadia van de somatische embryogenese, ook de zygotische embryogenese en diverse kiemingsstadia bij het onderzoek betrokken. De meest opvallende waarneming is dat de lokalisatie van calmoduline in somatische embryo's sterk verschilt van die in zygotische embryo's en dat er overeenkomsten bestaan tussen de verdeling van calmoduline in somatische embryo's en de verdeling tijdens kieming van zygotische embryo's. In somatische embryo's en tijdens kieming blijkt calmoduline vaak gebonden te zijn aan amyloplasten terwijl in zygotische embryo's calmoduline voornamelijk cytoplasmatisch gelokaliseerd is.

Voor een gedetailleerde analyse van de verdeling van Ca^{2+} met fluorescente indikatoren in levende, intakte plantecellen in weefselverband is het gebruik van confocale scanning laser microscopie een goede methode. Een geschikte indikator is fluo-3. Deze verbinding kan de plasmamembraan echter niet passeren. Daarom werd een methode ontwikkeld waarmee fluo-3 gemakkelijk kon worden ingebracht in embryogene plantecellen. In hoofdstuk 4 wordt beschreven dat met behulp van digitonine fluo-3 succesvol kan worden gebruikt voor de lokalisatie van Ca^{2+}, in combinatie met confocale scanning laser microscopy, in embryogene plantecellen.

Zoals al opgemerkt in hoofdstuk 2 gaat somatische embryogenese van de wilde peen samen met een stijging van de [Ca^{2+}]. In hoofdstuk 5 wordt, met behulp van de in hoofdstuk 4 beschreven methode, een gedetailleerde analyse gemaakt van de verdeling van vrij cytosolisch Ca^{2+} tijdens de somatische embryogenese.

[Ca^{2+}] bleek vooral hoog te zijn in het protoderm van de embryo's en vaak werden gradiënten in de [Ca^{2+}] waargenomen langs de longitudinale as van torpedovormige embryo's. Een in het oog springend hoge [Ca^{2+}] werd waargenomen in de kern van protodermcellen. Deze nucleaire lokalisatie werd bevestigd met behulp van antimonaatprecipitatie waarbij in de electronenmicroscoop Ca^{2+} zichtbaar wordt gemaakt als electronendichte precipitaten.

De concentratie van Ca^{2+} in de cytosol en de vacuole zijn met elkaar verbonden maar ook met de pH van de cytosol en de vacuole. Daar zowel pH als [Ca^{2+}] belangrijke factoren zijn tijdens embryogenese is in hoofdstuk 6 gekeken naar de verdeling van de pH in de vacuole tijdens somatische en zygotische embryogenese en tijdens kieming van de wilde peen. Neutraal rood en acridine oranje werden gebruikt als pH indikatoren van de vacuole en de verdeling werd vergeleken met de verdeling van het fluorescentiesignaal van fluphenazine. Opvallend was dat de verdeling van de drie indikatoren grote overeenkomsten vertoonde en dat ze alle drie hetzelfde reageerden op behandelingen met EGTA, A23187 en propionzuur. Confocale microscopie onthulde een netwerk van blaasjes en buizen, aanwezig in voornamelijk het protoderm van somatische embryo's en gekiemde zygotische embryo's na incubatie met acridine oranje. Er wordt verondersteld dat calmoduline mogelijk een rol vervult bij de vertering van celmateriaal in autofage vacuolen of betrokken is bij de regulatie van bewegingen van vacuolaire buizen. Aanvullend onderzoek is echter nodig om de verkregen verdelingspatronen bevredigend te kunnen verklaren.

Uit de voorgaande hoofdstukken is gebleken dat aanmerkelijke verschillen aanwezig zijn tussen somatische en zygotische embryo's ten aanzien van de verdeling van anti-calmoduline, fluphenazine fluorescentie, neutraal rood en acridine oranje. In hoofdstuk 7 wordt bekeken of deze verschillen een structurele basis bezitten. De verdeling van anti-calmoduline en mogelijk fluphenazine fluorescentie kon gekoppeld worden aan de aanwezigheid van amyloplasten, die voornamelijk voorkwamen in somatische embryo's en gekiemde zygotische embryo's maar niet werden aangetroffen in zygotische embryo's. Verschillen in de lokalisatie van neutraal rood en acridine oranje, en mogelijk ook van fluphenazine, zijn gerelateerd aan verschillen in vacuolisatie tussen somatische en zygotische embryo's.

Hoofdstuk 8 is de algemene discussie. Hier wordt ingegaan op de initiatie van somatische embryogenese, de vroege ontwikkeling van het embryo en het ontstaan van polariteit tijdens somatische en zygotische embryogenese. In dit hoofdstuk wordt geconcludeerd dat er belangrijke verschillen aanwezig zijn tussen somatische en zygotische embryo's en dat het proces van somatische embryogenese overeenkomsten vertoont met kieming van zygotische embryo's. Het hoofdstuk wordt afgesloten met enige opmerkingen omtrent de gebruikte methoden voor de lokalisatie van Ca^{2+} en calmoduline.

CURRICULUM VITAE

Antonius Cornelis Jozef Timmers werd geboren op 2 april 1962 te Oisterwijk. Na het behalen van het diploma voorbereidend wetenschappelijk onderwijs aan het Theresialyceum te Tilburg in 1980 vervulde hij zijn dienstplicht van juli 1980 tot september 1981. Hierna begon hij met de studie biologie aan de Katholieke Universiteit te Nijmegen. Afstudeervakken tijdens de doctoraalperiode lagen op het vlak van de dierfysiologie, algemene botanie en de fytopathologie. Het laatste werd uitgevoerd aan de vakgroep Fytopathologie van de Landbouwuniversiteit. Tevens behaalde hij tijdens deze periode de onderwijsbevoegdheid in de biologie. Het doctoraaldiploma werd hem uitgereikt op 29 maart 1988.

Het in dit proefschrift beschreven onderzoek werd uitgevoerd van 14 maart 1988 tot 10 april 1992 binnen de vakgroep Plantencytologie en -morfologie van de Landbouwuniversiteit te Wageningen. In deze periode werden enkele voordrachten gehouden tijdens internationale wetenschappelijke congressen te Amiens, Amsterdam en Praag. Een gedeelte van het onderzoek werd ondersteund door een beurs van NWO en vond plaats binnen de Universiteit van Heidelberg op de vakgroep Zellenlehre in samenwerking met dr. H.-D. Reiss. Op uitnodiging werd korte perioden gewerkt in het Biological Research Centre te Szeged in Hongarije in en het Institute of Plant Genetics te Nitra in Tsjecho-Slowakije. Tijdens zijn AIO-aanstelling volgde hij de cursussen methoden en technieken in de celbiologie, moleculaire biologie en recombinant-DNA technologie, veilig omgaan met radioaktieve stoffen en stralingsbronnen, ontwikkelingen in de plantenbiotechnologie, DNA *in situ* hybridisatie en engels in de werksituatie. Tevens werd een bijdrage geleverd aan diverse onderwijstaken van de vakgroep. Vanaf 1 september 1992 is hij in dienst als moleculair cytoloog binnen de vakgroep Biochemie en Moleculaire biologie van de Vrije Universiteit te Amsterdam.